Final Report

PERFORMANCE PREDICTION AND ANALYSIS OF THE LUNAR HEAT FLOW PROBES

By D. NATHANSON and R. MERRIAM

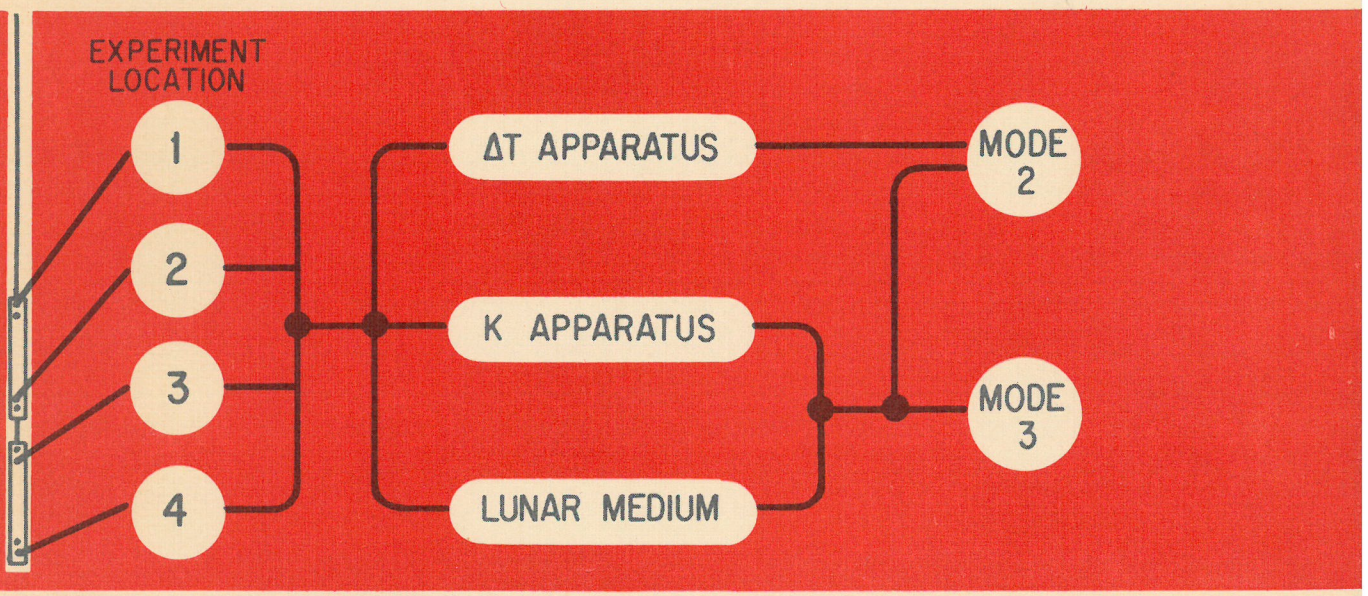

PREPARED FOR

LAMONT-DOHERTY GEOLOGICAL OBSERVATORY

JANUARY 1970

Arthur D. Little, Inc.

PERFORMANCE PREDICTION AND ANALYSIS OF THE LUNAR HEAT FLOW PROBES

by

D. Nathanson and R. Merriam

Final Report to

Lamont-Doherty Geological Observatory

Palisades, New York

Under

Subcontract No. 8 of

Prime Contract No. NAS 9-6037

with

Columbia University

Arthur D. Little, Inc.
Cambridge, Massachusetts 02140

January 1970

C-71424

Arthur D. Little, Inc.

TABLE OF CONTENTS

TABLE OF CONTENTS - Cont'd.

TABLE OF CONTENTS - Cont'd.

ACKNOWLEDGMENTS

The authors greatly appreciate the coordination and direction provided by the Principal Investigator, Dr. M. Langseth, and his associate, Dr. J. Chute, of Lamont-Doherty Geological Observatory. They value their many discussions with Dr. E. Drake, Dr. A. E. Wechsler and Mr. Frank Ruccia of Arthur D. Little, Inc., regarding the probe thermal tests. The authors also thank Mr. Edward Boudreau, who provided valuable information relating to the construction details and assembly procedures of the heat flow probes.

SUMMARY

The Heat Flow Experiment (HFE), part of the Apollo Lunar Scientific Experiment Package (ALSEP), when deployed on the moon, will provide in situ measurement of heat flow from the lunar interior. Each HFE, consisting of two heat flow probes emplaced by the astronaut at the bottom of a three-meter drilled hole, will measure the temperature gradient, the ambient temperature, and the thermal conductivity of the lunar surface layers--characteristics that in combination will provide a measure of the heat flow.

Thermal conductivity measurements will be made indirectly by monitoring the temperature response of sensors in the probes after appropriate heaters in the instrument are energized. Thermal conductivity data will be extracted from the temperature response of the sensors. The sensor response is related to the thermal conductivity of the lunar material surrounding the probe, the inherent thermal characteristics of the probe, the thermal interaction between the probe and the drill casing which will line the lunar bore hole, and the thermal characteristics of the interface between the drill casing and the surrounding lunar material. The interpretation of lunar temperature data and subsequent transformation of this data to conductivity predictions is influenced by these factors.

This report describes the mathematical modeling of the thermal behavior of the heat flow probes and surrounding medium. The computer models developed simulate the thermal performance of the conductivity experiments and will aid in the interpretation of lunar data. They provide a convenient means of examining experiment performance for any value of thermal conductivity or absolute temperature level existing in the lunar environment.

Predictions of probe performance in the lunar environment were made by the use of the mathematical models to aid the Principal Investigator of the HFE during a real-time data reduction, which is planned after emplacement of the experiment in the upcoming Apollo 13

lunar landing. The mathematical models will also be suitable as an aid to a refined data analysis during the post-flight period.

Other studies described in this report:

1) demonstrated that computer time was not excessive for solution of the finite-difference model of the probe and its surroundings;

2) led to an improved understanding of instrument performance during conductivity experiments; and

3) established the influence of certain environmental and physical uncertainties on probe thermal performance.

LIST OF FIGURES

LIST OF FIGURES - Cont'd.

LIST OF TABLES

LIST OF APPENDICES

I. INTRODUCTION

With the guidance of Dr. M. Langseth of Lamont-Doherty Geological Observatory, Columbia University, Arthur D. Little, Inc., designed, developed, fabricated and tested lunar heat flow probes for the ALSEP* Heat Flow Experiment.[1] The Lunar Heat Flow Experiment (HFE) is designed to measure both the temperature gradients in the subsurface of the moon and the thermal conductivity of the local lunar material. The purpose of the measurements is to provide a basis for calculating the heat flow from the lunar interior.

Thermal conductivity measurements are performed by energizing heaters in the probe and monitoring the temperature responses of two types of probe sensors. The relationship between the sensor responses and the thermal conductivity of the surrounding medium provides an indirect measurement of conductivity. Thermal responses of the probe sensors are also inherently related to the thermal properties of the probe and its structural elements, heat flow in the drill string which will line the lunar bore hole, the thermal coupling between the probe and the liner, the interface between the liner and the bore hole, and the absolute temperature level. These factors all complicate the calibration or interpretation of the experiment.

Subsequent to the construction and performance testing of the heat flow probes, an analysis of existing test data was conducted at Arthur D. Little, Inc., under Lamont-Doherty sponsorship. This work involved the use of simplified descriptions of the thermal behavior of the probe and lunar surroundings. The assumptions necessary to make the analytical solutions mathematically tractable limited the precision and generality of the results. One of the final recommendations of this work was the development of digital-computer thermal models which could include details of the heat flow probe and a comprehensive representation of the surrounding lunar material.

---

* Apollo Lunar Scientific Experiment Package.

[1] Superscript numerals refer to references listed in Section VII.

This report describes the development and use of computer mathematical models to describe the lunar probe and its surroundings. The main objectives of this work can be summarized as follows:

- Develop computer mathematical models capable of describing the details of heat flow in the probe and the lunar surroundings - and the interaction between them.
- Analyze the thermal performance of the heat flow probe in laboratory tests and investigate the relationship between sensor performance and experiment location.
- Predict the performance of the experiment after equilibration in the lunar environment (in an undisturbed medium), considering a drill string lining the lunar bore hole. The thermal response of the probe is to be related to the thermal conductivity of the surrounding lunar material as a function of time and absolute temperature.
- Provide information to the Principal Investigator of the HFE to aid in real-time data reduction of the experiment in the upcoming Apollo 13 lunar landing.
- Provide mathematical models of the probe and lunar surroundings for use in a refined data analysis during the post-flight period.

All the studies and predictions presented in this report relate to the performance of the heat flow probes in a homogeneous, thermally isotropic, and thermally equilibrated lunar environment. Analysis of diurnal variations in the lunar bore hole or of thermal perturbations and their effect on the conductivity experiments were beyond the scope of the subject work. The influence of diurnal variations and techniques

for correcting lunar data for their effects are being studied by Lamont-Doherty Geological Observatory for use during real-time data reduction and post-flight reduction of lunar data.

II. BRIEF REVIEW OF HEAT FLOW EXPERIMENT

A. Introduction

Detailed documentation on the heat flow probe is available in Reference 1, which contains a comprehensive description of the probe design, fabrication and tests performed. A brief review of the general probe configuration and thermal sensors is presented below, primarily to define important thermal components and serve as a suitable reference for discussion contained in other sections of this report.

Each lunar heat flow probe is approximately 100 cm long and is comprised of two 50 cm-long static sections or half-probes. The two half-probes are connected by electrical wiring and an extension spring, so that one is directly above the other after installation at the bottom of a 3-meter, lined bore hole (Figure 1).

Each 50 cm section consists of a filament-wound, epoxy-fiberglass structure which houses a "gradient"-sensor bridge, a "ring"-sensor bridge, and two heaters. The entire probe assembly contains four gradient sensors, four ring sensors and four heaters. It has been convenient to identify four experiment locations, each location comprising a heater winding, a gradient sensor, and a remote ring sensor approximately 10 cm from the heater. Experiment location number 1 is uppermost when the probe is emplaced inside the drill casing and number 4 is lowermost.

The gradient sensors shown in Figure 2a are platinum resistors. They are positioned concentric and internal to the heater windings at each of the four experiment locations. Each gradient sensor consists of a sealed enclosure formed by an outer platinum can and inner platinum mandrel. The enclosure is filled with helium. Lead wires from the sensor enclosure pass through an epoxy plug which is used to position the sensors.

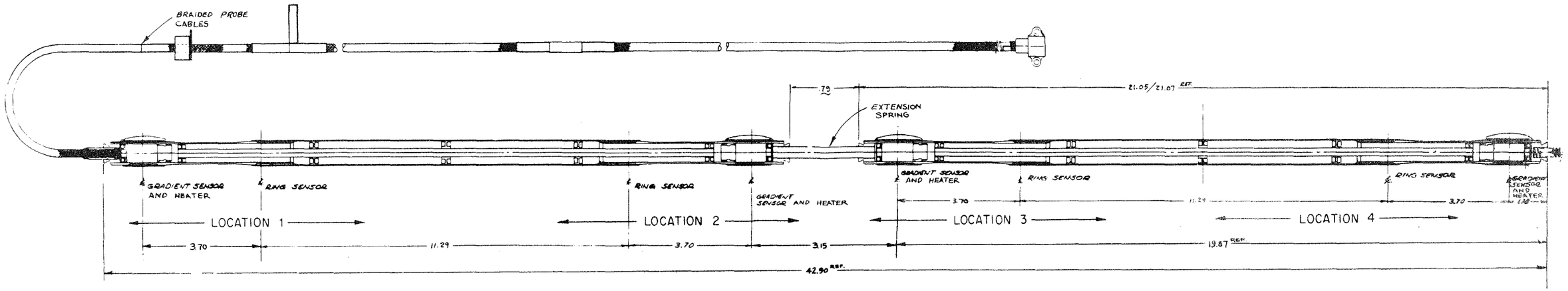

PROBE IN FULLY EXTENDED POSITION
FIGURE 1a

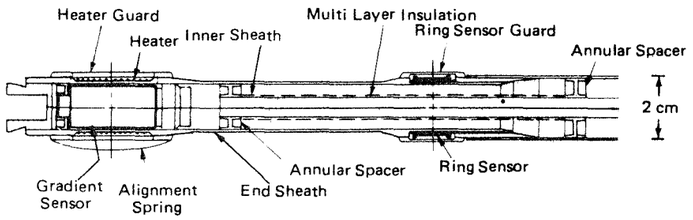

DETAIL OF TYPICAL EXPERIMENT LOCATION
(LEAD WIRES NOT SHOWN)
FIGURE 1b

FIGURE 1 LUNAR HEAT FLOW PROBE

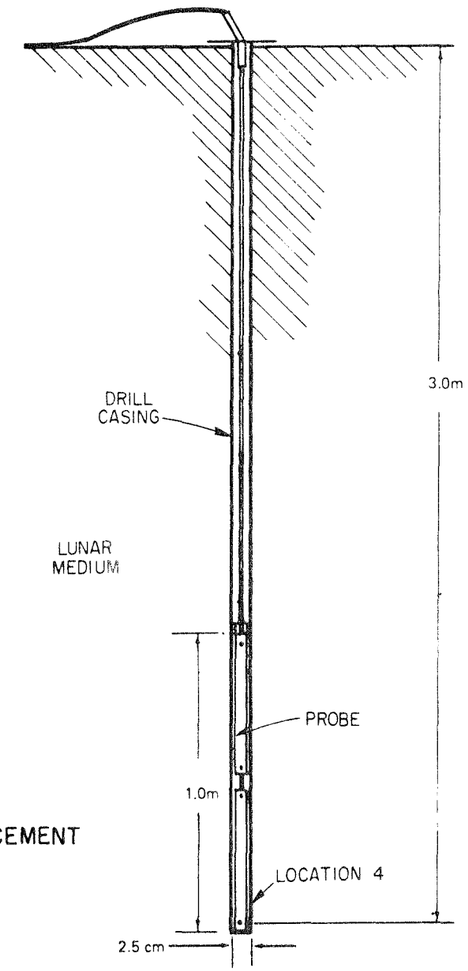

TYPICAL
PROBE EMPLACEMENT
FIGURE 1c

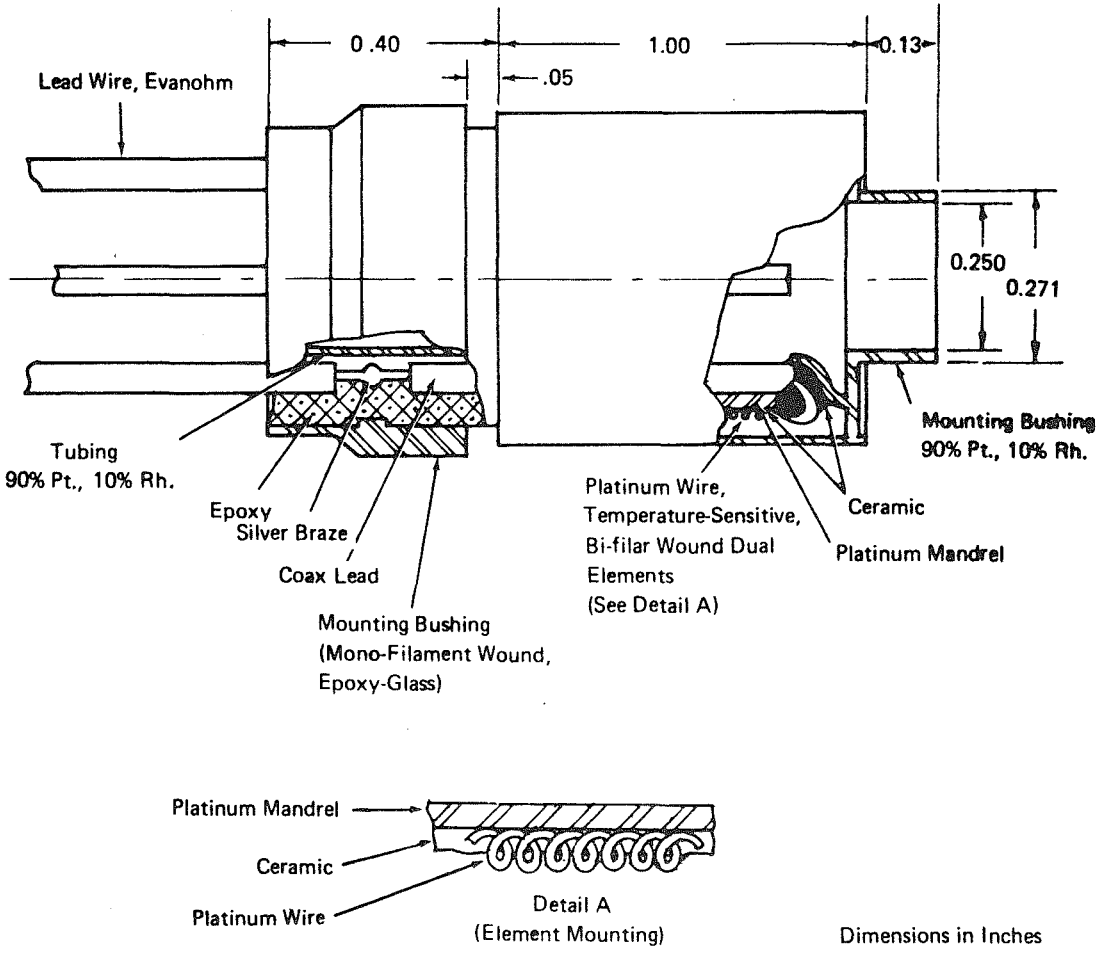

Detail A
(Element Mounting)

Dimensions in Inches

GRADIENT SENSOR
FIGURE 2a

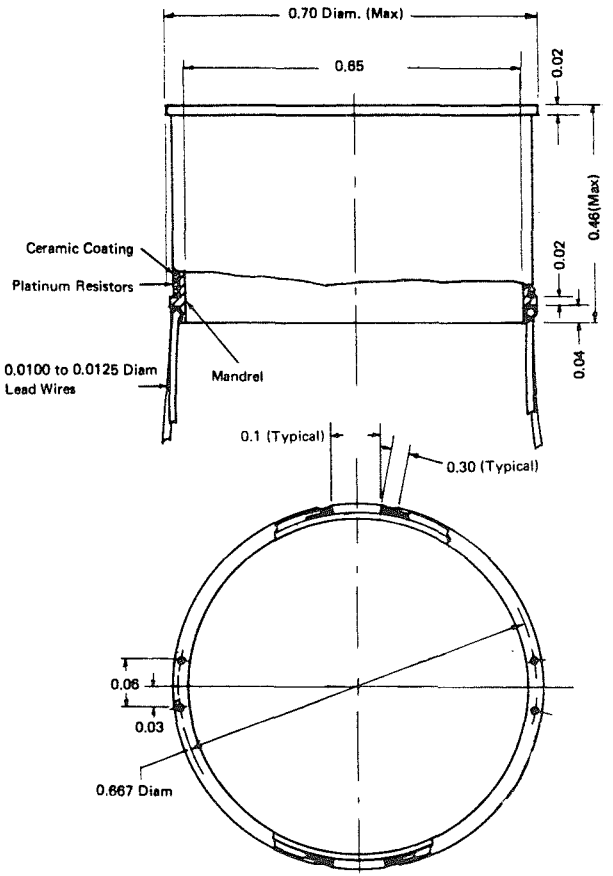

Dimensions in Inches

RING SENSOR
FIGURE 2b

FIGURE 2 PROBE TEMPERATURE SENSORS

The ring sensors illustrated in Figure 2b consist of thin platinum bands on which are wound two resistors. The resistors are embedded in a blue-glaze ceramic coating on the external surface. A portion of the internal surface of the platinum band is cemented to a filler sheath which supports it and is, in turn, cemented to the outer sheath of the probe structure.

B. Operating Modes for Thermal Conductivity Measurement

In situ thermal conductivity measurements are to be made by one of two methods, depending upon whether the material surrounding the probes is in the low or high range of anticipated thermal conductivity.[1] In either mode, a heater is activated and the temperature response of probe sensors provides an indication of thermal conductivity of the surroundings. Thermal transients propagating from the lunar surface or due to instrument emplacement may be present in the lunar medium. These effects must be evaluated and corrections applied to the instrument response to interpret the conductivity experiments.

1. Low-Conductivity Range ($K < 2 \times 10^{-4}$ w/cm °K)

The low-range conductivity experiment, identified as the Mode 2 experiment, can be performed at any of the four locations along a probe by energizing the appropriate heater at a power level of 2 milliwatts and subsequently monitoring the temperature rise of the gradient sensor. (The other gradient sensor associated with the resistance bridge is unaffected by the heater and serves as a reference temperature.) The temperature rise of the gradient sensor at the location of the energized heater is related to the thermal conductivity of the lunar surroundings, absolute temperature level, thermal characteristic of probe structure and drill casing, and the conductive heat flow paths presented by lead wires and cables.

The lead wires in each probe half play an important role in the Mode 2 operation. The physical arrangement of lead wires in the lower probe half is depicted schematically in Figure 3. The influence

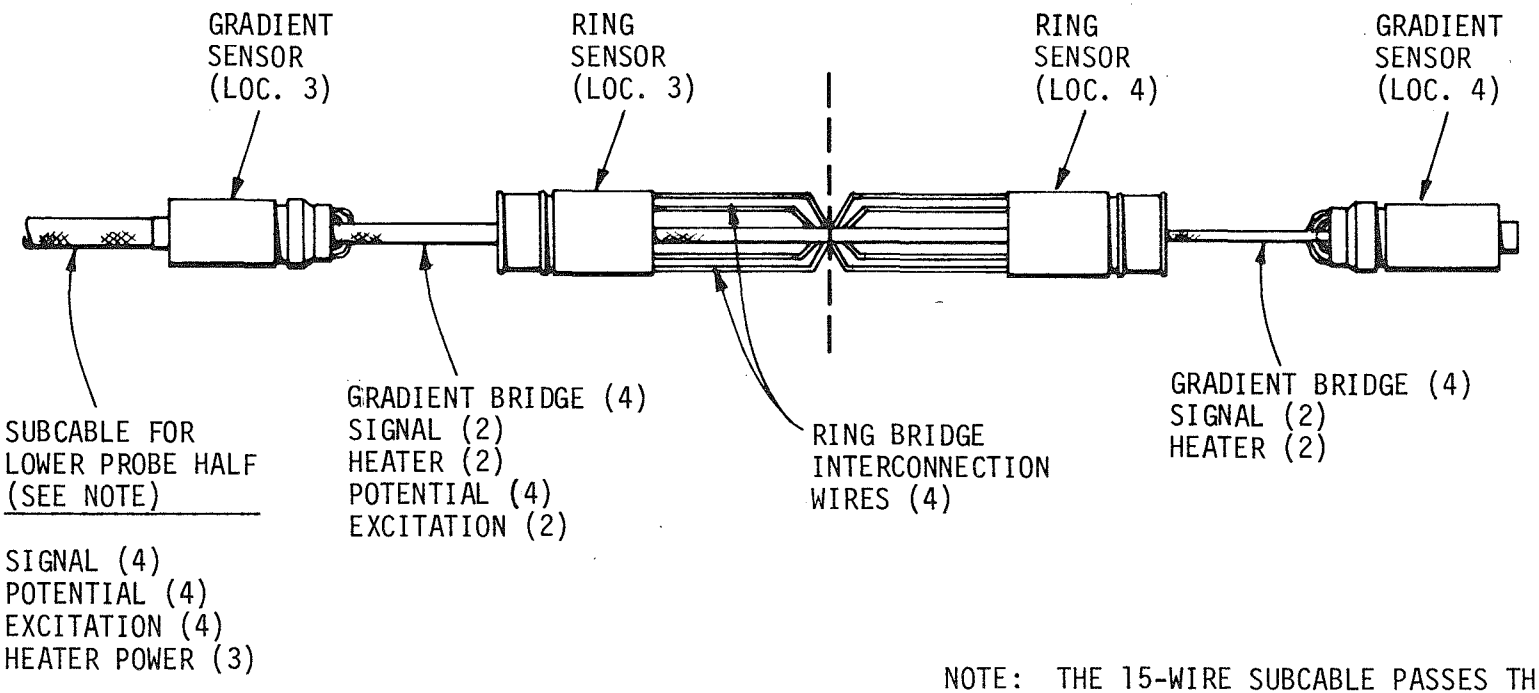

NOTE: THE 15-WIRE SUBCABLE PASSES THROUGH THE ENTIRE UPPER PROBE HALF, WHICH ALSO CONTAINS A WIRING CONFIGURATION IDENTICAL TO THAT SHOWN HERE.

FIGURE 3 SCHEMATIC ARRANGEMENT OF WIRING IN LOWER PROBE HALF

of lead wires on thermal performance is least at location 4 where the fewest wires (8) are thermally coupled to the gradient sensor. In comparison, at location 3 a total of 29 wires provides thermal couplings to the gradient sensor. Similarly, in the upper probe half, which is not shown in Figure 3, 38 wires are thermally coupled to the gradient sensor at location 2. For the gradient sensor at location 1, heat flows along two 15-conductor subcables which are in radiative communication with the probe surroundings, and along 29 other wires routed in the direction of location 2.

Heat flow along the wires depresses the temperature of the gradient sensor associated with the energized heater. Therefore, the temperature rise of the gradient sensor is highest at location 4 and lowest at location 1.

2. High-Conductivity Range ($K > 2 \times 10^{-4}$ w/cm °K)

The Mode 3 experiment is designed for measurements in the high range of possible lunar conductivities. One of the heater windings is energized at a 0.5-watt level, and the temperature rise of the ring sensor - approximately 10 cm from the heater - is monitored as a function of time. The temperature response of the ring sensor is also dependent on the thermal characteristics of the probe. However, transient effects primarily related to the probe characteristics and absolute temperature level have short time constants and become small after approximately a three-hour period. Thereafter, the time rate of change of ring-sensor temperature ("slope") is controlled by the thermal conductivity of the surrounding lunar material.

III. DESCRIPTION OF THERMAL MODELS

A. Introduction

A computerized thermal analysis of a physical system, involving finite-difference procedures, requires the following steps:

- Subdividing the physical system into thermal zones or nodes.
- Preparing input data, which describe the heat-balance equations, for a computer program.
- Solving for the temperatures on a digital computer.

When finite-difference techniques are used in thermal analysis, the geometrical subdivision of the system being analyzed is important from the standpoints of accuracy and cost. If the subdivision is too fine (or the number of subdivisions too large), a large amount of computer time is required to formulate and solve the thermal models; if it is too coarse, excessive error will result in the computations.

Stringent requirements must be observed for computer simulation and numerical predictions of performance of the HFE. For example, in the Mode 2 operation, the thermal conductivity of the surrounding lunar medium is related to a small temperature rise of the gradient sensor - between 0.3 and 2°K. A 10% change in the signal can correspond to a 50% change in thermal conductivity, for values in the range of 2×10^{-5} to 4×10^{-5} w/cm °K. Therefore, accurate modeling of the lunar medium and proper simulation of the interplay between the probe and the medium are of prime importance.

Prior to the development of detailed models for the lunar heat flow probe and surrounding lunar medium, preliminary studies were made for the following purposes:

1) determine the finite-difference subdivision in the low-conductance probe sheath necessary

to render an accurate description of the heat flow between sensor locations; and

2) develop finite-difference models and procedures for describing an infinite lunar medium.

A discussion of these studies and the models developed for the probe and lunar medium is given in the following section. An evaluation of the models, performed prior to performance predictions in the lunar environment, is described in Section IV.

The heat flow equations for the thermal models were written in finite-difference form using the Zone Method of Strong and Emslie.[4] Numerical solutions were obtained using an existing Arthur D. Little, Inc., Generalized-Thermal-Analyzer computer program (ADLGTA) discussed in Appendix I. Appendix II contains a complete input data listing for a typical thermal model of the probe and surroundings.

B. Modeling of Lunar Probe

1. Preliminary Study for Subdivision Requirements

Two thermal models, shown schematically in Figure 4, were used to examine the relationship between the number of subdivisions in the probe and the accuracy of the temperature predictions. Model A considers an epoxy-fiber-glass probe sheath 50-cm long, separated from a surrounding medium by a radiation gap. The surrounding medium has a specified temperature distribution which varies linearly from 240°K at the lower end to 238°K at the top end. The emittances of the outer surface of the probe sheath and the internal surface of the surrounding medium are taken as unity. Heat flow in the probe sheath is governed by radiation transfer at the outer surface and by conduction along the length. In this physical model, the internal and end boundaries are adiabatic. Model B considers a similar arrangement but with a drill casing (lunar drill string) between the probe sheath and the surrounding medium.

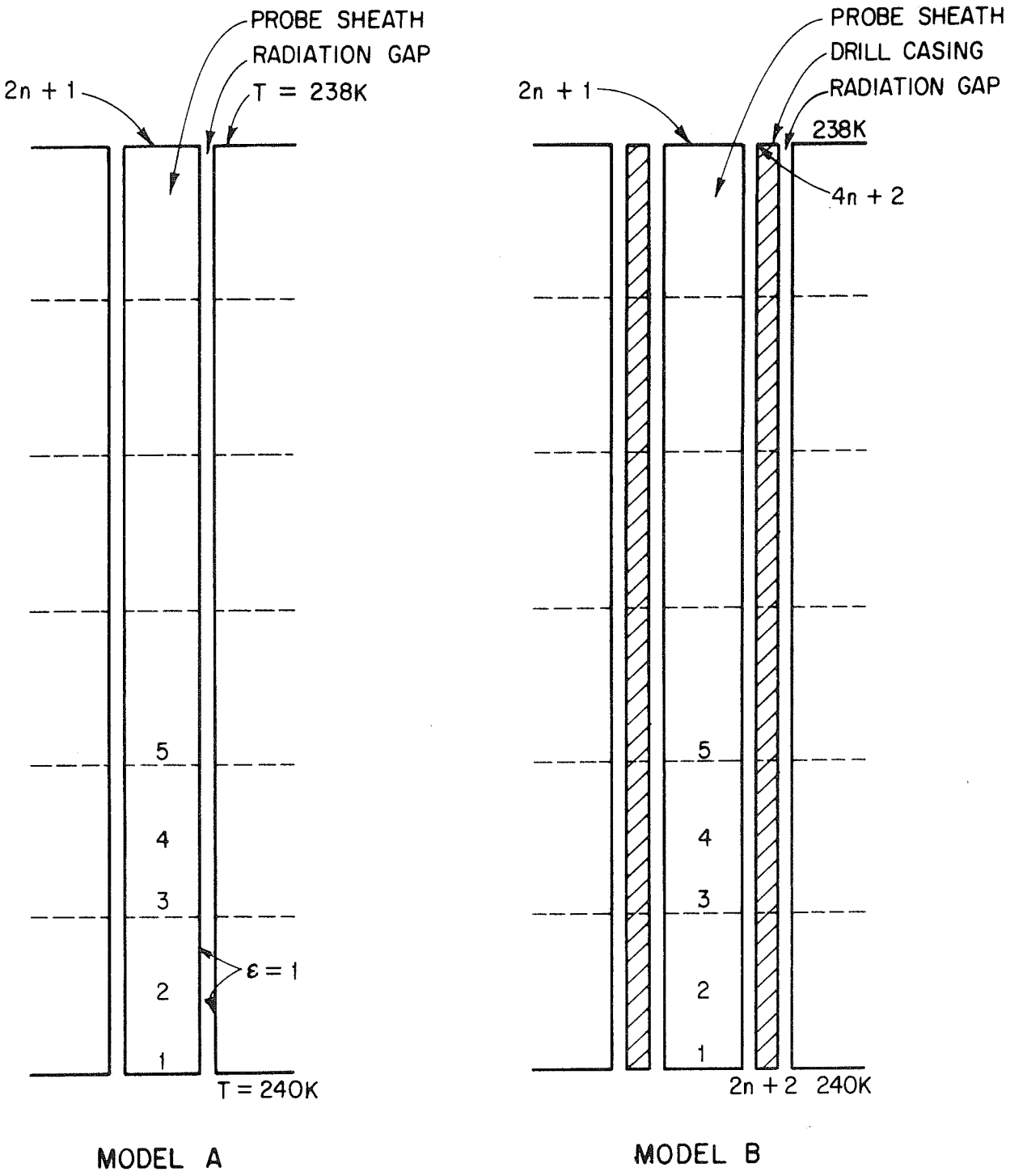

NOTE: DOTTED LINE DENOTES FINITE DIFFERENCE SUBDIVISION

$\Delta T_{probe} = T_1 - T_{2n+1}$

FIGURE 4 THERMAL MODELS FOR STUDY OF SUBDIVISION REQUIREMENTS IN LUNAR PROBE

The number of equal-length subdivisions in the probe sheath (and in both the probe sheath and drill casing for Model b) was varied from a minimum of 2 to a maximum of 40. The results of this study are shown in Figure 5 where the end-to-end ΔT in the probe is plotted as a function of the number of subdivisions (and subdivision size). The calculations show that a subdivision size of approximately 2.0 cm is adequate for an accurate description of both configurations. The calculations also demonstrate the possible influence of a conductive drill casing on the predicted temperature difference in the probe sheath. The 2°K temperature difference in the environment corresponded to a temperature difference along the probe of 1.94°K for Model A and 1.77°K for Model B.

Based on this work, the length of vertical subdivisions did not exceed 2 cm in thermal models of the lunar heat flow probe in the regions near the gradient and ring sensor. This requirement also applied to thermal models of the drill casing and lunar medium in the same region.

2. Models for Thermal Conductivity Experiments

Computer models were developed to describe the thermal performance of the heat flow probe at four experiment locations during the two modes of operation. These models were developed to enable simulation of the probe thermal performance during tests in the Temperature Gradient Apparatus and the Thermal Conductivity Test Apparatus[1,3] and during operation in the lunar environment.

Many of the construction details in the gradient and ring sensor regions are similar at all four locations. However, certain details are specific to each experiment location, the most important of these being the wire harnesses. As an example of the approach used to model the four experiment locations, the overall configuration of the thermal model for experiment location 1 is shown in Figure 6. Details of the gradient-sensor and ring-sensor regions, which apply to all experiment locations, are illustrated schematically in Figures 7

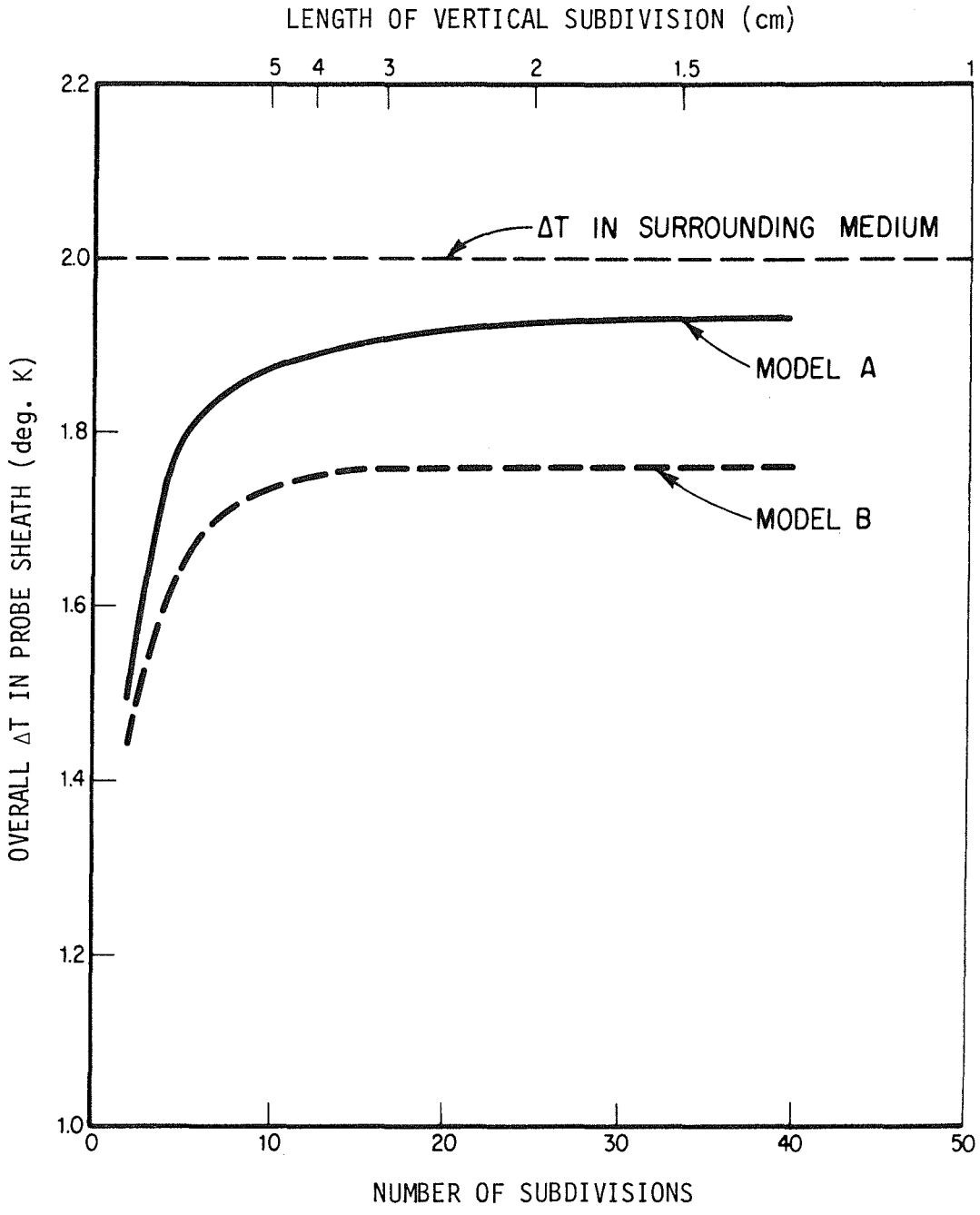

FIGURE 5 COMPUTED VERTICAL TEMPERATURE DIFFERENCE IN PROBE SHEATH VERSUS NUMBER OF SUBDIVISIONS

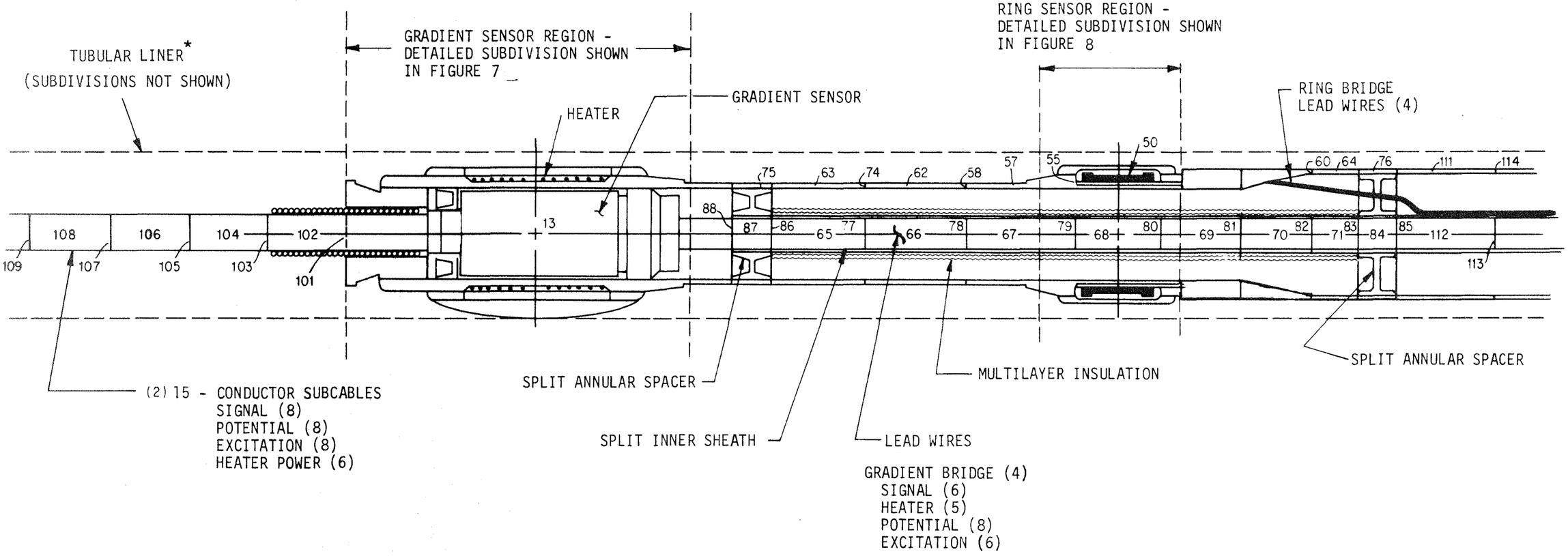

* ALUMINUM TUBE IN ΔT TEST APPARATUS
EPOXY-FIBER-GLASS TUBE IN K APPARATUS
BORON-REINFORCED DRILL CASING IN
LUNAR ENVIRONMENT.

FIGURE 6 OVERALL CONFIGURATION OF THERMAL MODEL FOR EXPERIMENT LOCATION 1

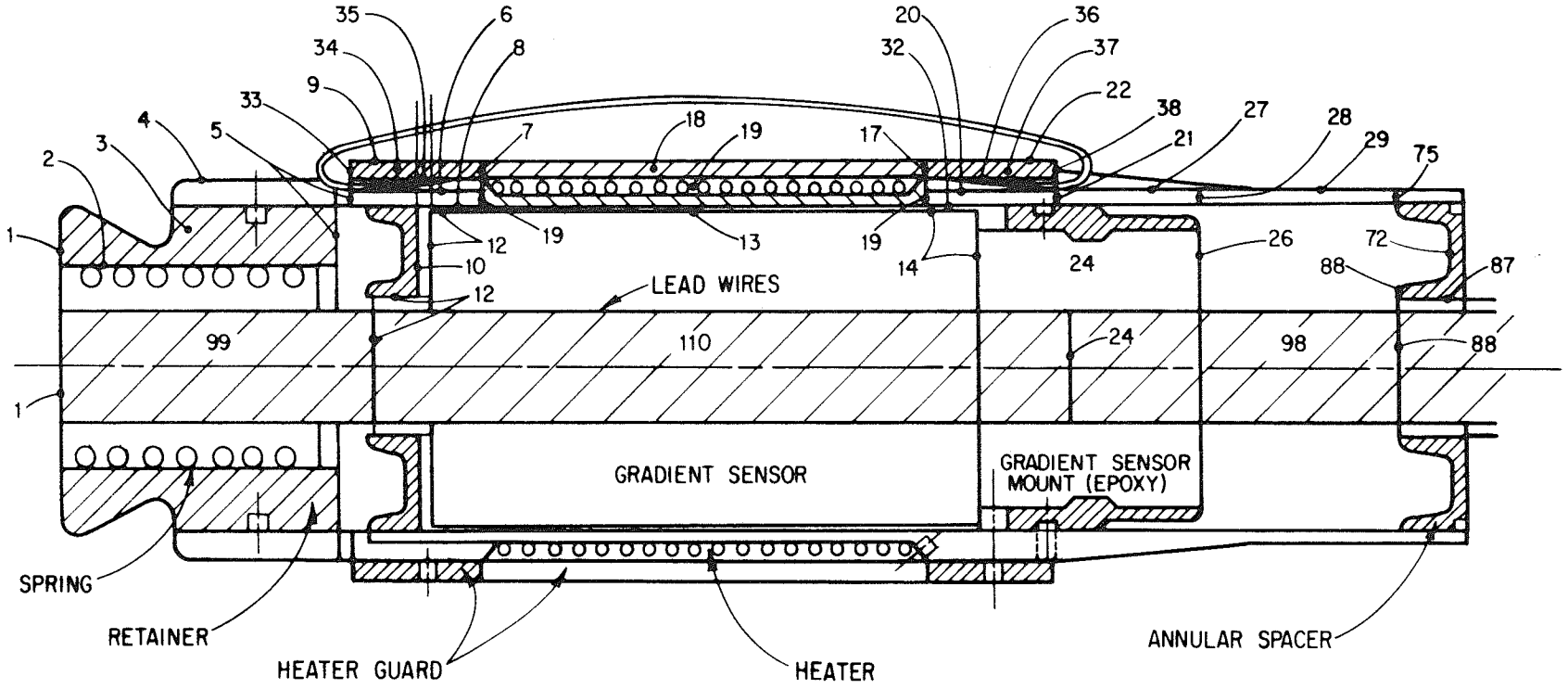

FIGURE 7 DETAIL OF GRADIENT SENSOR THERMAL MODEL

and 8. The numbers shown on Figures 6-8 are temperature subscripts identifying zones or boundaries in the thermal models of the probe. The dotted line shown in Figure 6 represents the environmental boundary which is in thermal communication with the external surface of the probe.

The arrangement of the thermal models for each of the experiment locations is shown schematically in Figure 9. Each model extends approximately 25 cm in length and includes the details of the gradient sensor, ring sensor, heater and thermal couplings at a given location. The subdivision in these models extends to regions which are essentially uninfluenced by the heater activation. The specification of boundary conditions at the ends of the models and the length of the probe chosen for modeling were checked out in early calculations.

a. Gradient Sensor

Approximately 40 equations were used to describe the heat flow in the region of a gradient sensor location (Figure 7). Most of the thermal conductances are well defined in terms of lengths and probe thermal properties. The most important parameters which determine the thermal behavior are the emittance of the heater wires, emittance of probe casing, thermal conductance of probe body, and conductance between lead wires and gradient sensor.

The model accounted for the following modes of energy interchange in the gradient sensor region:

- Conduction along epoxy probe casing -

  Because of the high conductance as compared to radiant interchange between the heater sections and the gradient sensor, the major portion of heat is conducted through Zones 6, 30, 34 and 37.

- Conduction along lead wires -

  Because of the snug fit between the lead wires and other elements in the gradient sensor

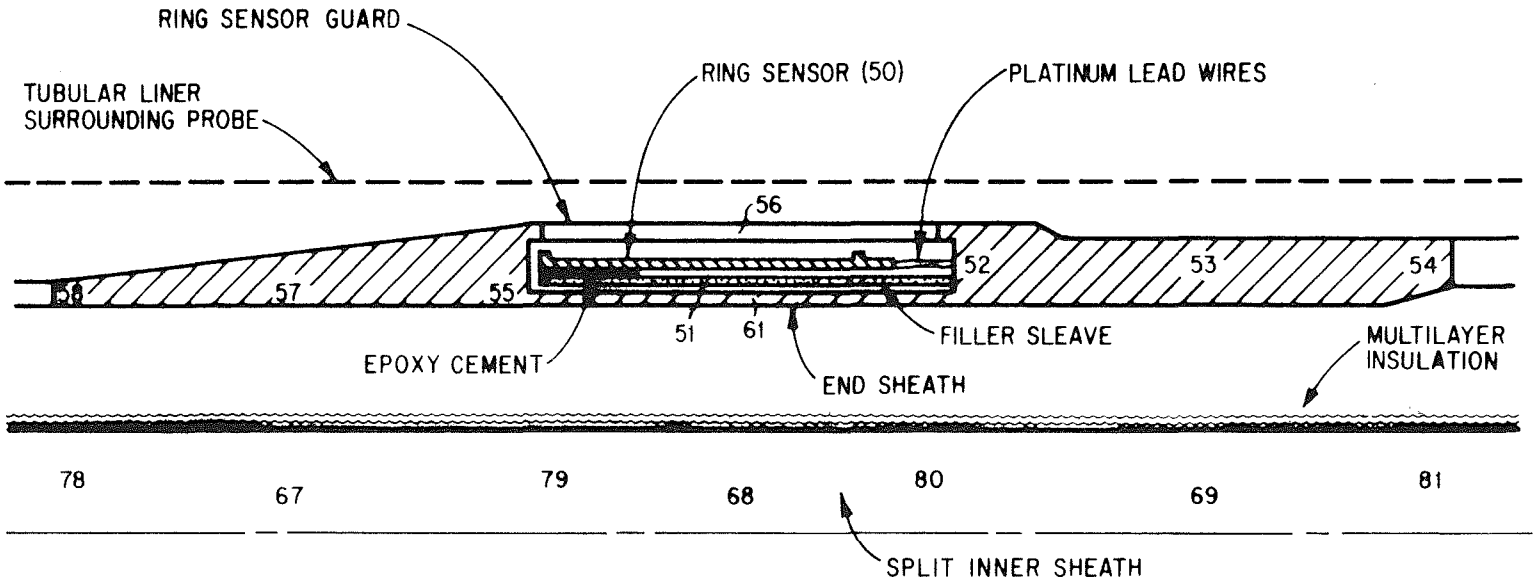

FIGURE 8 DETAIL OF RING SENSOR THERMAL MODEL

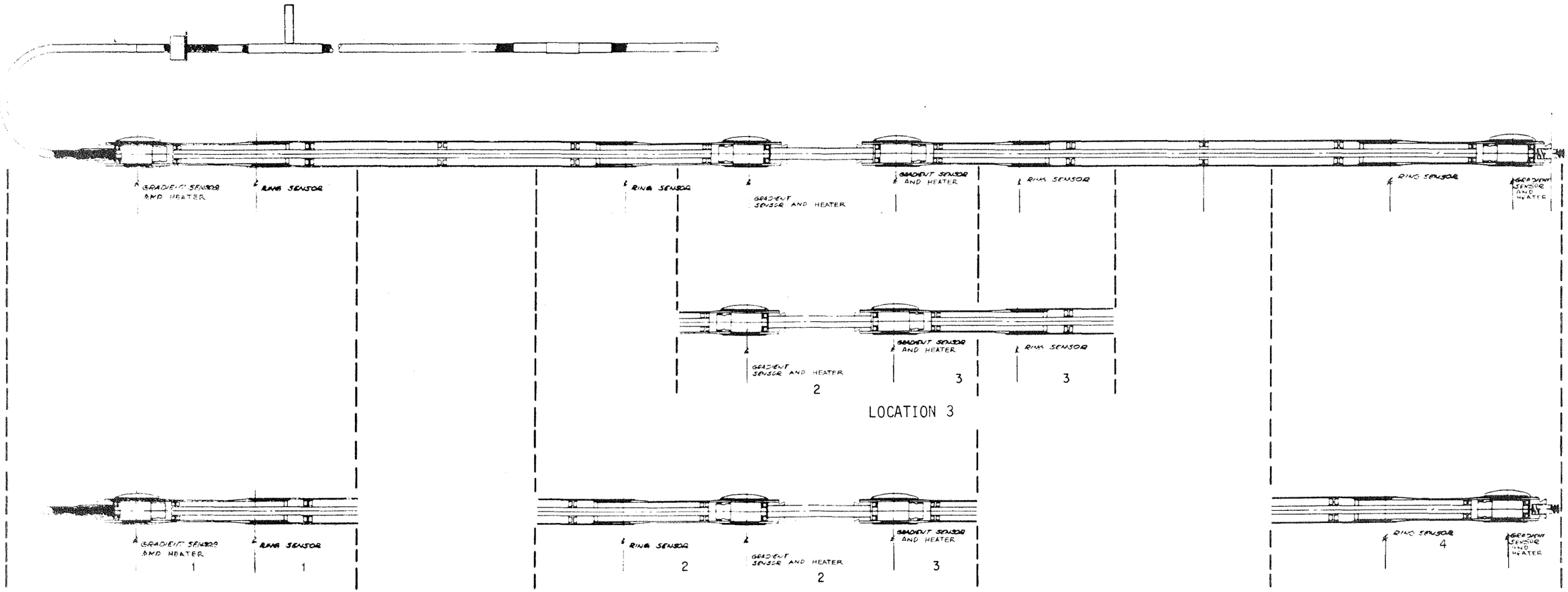

FIGURE 9 SCHEMATIC ARRANGEMENT OF THERMAL MODELS FOR THE FOUR EXPERIMENT LOCATIONS

region, the wires were considered to be heat stationed at several locations (1, 12, 24, 88). Lead wire conductance is most important in the region from the gradient sensor mount to the annular spacer.

- Radiation interchange within probe body

  Zones within the probe body exchange energy with each other and with the lead wires by radiation.

b. Ring Sensor

Approximately 50 heat-balance equations described the heat flow in the ring sensor region (see Figures 6 and 8). The model description accounted for the following important characteristics which govern the thermal performance of the ring sensor:

- Radiation heat transfer between the ring sensor and the ring sensor guard, drill casing, and filler sleeve.

  The ring sensor is radiatively coupled to the ring sensor guard. It is also radiatively coupled* and thermally coupled via four platinum lead wires to a filler sleeve which supports it.

- Radiant heat transfer between the filler sleeve and end sheath.

  The filler sleeve, in the region of the ring sensor, is radiatively coupled to the end sheath.*

* Across a 1 1/2 to 3 1/2-mil radial clearance.

- Radiant heat transmission along the annular space formed by the internal surface of the end sheath and the external surface of the insulated split inner tube.

- Conduction heat transfer along probe body and lead wires (not shown on Figure 8).

  Wire harnesses thermally coupled to the gradient sensor are routed inside and epoxied to the split inner tube. Bridge wires, spliced to the four platinum lead wires on the ring sensor, pass through the filler sleeve to the annular spacer beyond the ring sensor. The bridge wires continue along the outside surface of the split inner tube to another annular spacer midway between two heater locations on a half probe.

C. Modeling of Lunar Medium

Computer models were developed to represent the lunar medium surrounding the heat flow probe. The medium was constructed to be infinite in extent in all directions. The heat flow was assumed to be two-dimensional in the radial and vertical directions and to have radial symmetry, since the heat flow in the probe is radially symmetric.

The lunar medium surrounding the probe was modeled as many layers of concentric annuli of varying radial thickness and equal vertical length. Finite-difference equations written for the annular zones and the heat flow equations required at the boundaries of the medium are presented in Appendix III.

Figure 10 illustrates a typical annular element. The vertical height, ℓ, of each element was chosen to be a constant whose value depends on the thermal properties of the medium and the operating mode of the conductivity experiment. Studies showed that the accuracy of calculations could be enhanced if two separate models of the lunar medium were developed--one tailored for simulation of the Mode 2 experiment (low power, low conductivity) and the other for the Mode 3 experiment (high power, high conductivity).

Because of the rapid attenuation of a thermal wave within the medium, the thickness of each zone varies with the radial distance, r. The radial temperature distribution in a medium for analogous physical problems (point or spherical-surface heat sources in an infinite medium) varies approximately as 1/r. Hence, in the finite-difference models the ratio of outer-to-inner radii (b/a) of a typical annular element was chosen to vary as r:

$$b = c_2 a$$

where c_2 is a parameter.

Figure 11 shows the model of the lunar medium surrounding a probe experiment location. The intersection of the horizontal and vertical centerlines of the medium coincide with the center of the heater at the experiment location. The number of vertical subdivisions M, the number of concentric annuli, N, and values of the quantities c_2 and ℓ define the geometrical configuration of the medium and the number of locations or nodes that require descriptive heat flow equations. The values of these parameters which were used to define the surrounding medium are summarized in Table I.

To assist in the preparation of data cards describing the lunar medium heat flow, an automatic numbering system was adopted for identifying each zone. Figure 12 illustrates this system. Each zone is identified by the indices I and J where the maximum value of J is an odd number so that the innermost element of the central layer surrounds the gradient sensor. In Figure 12 the plus signs represent

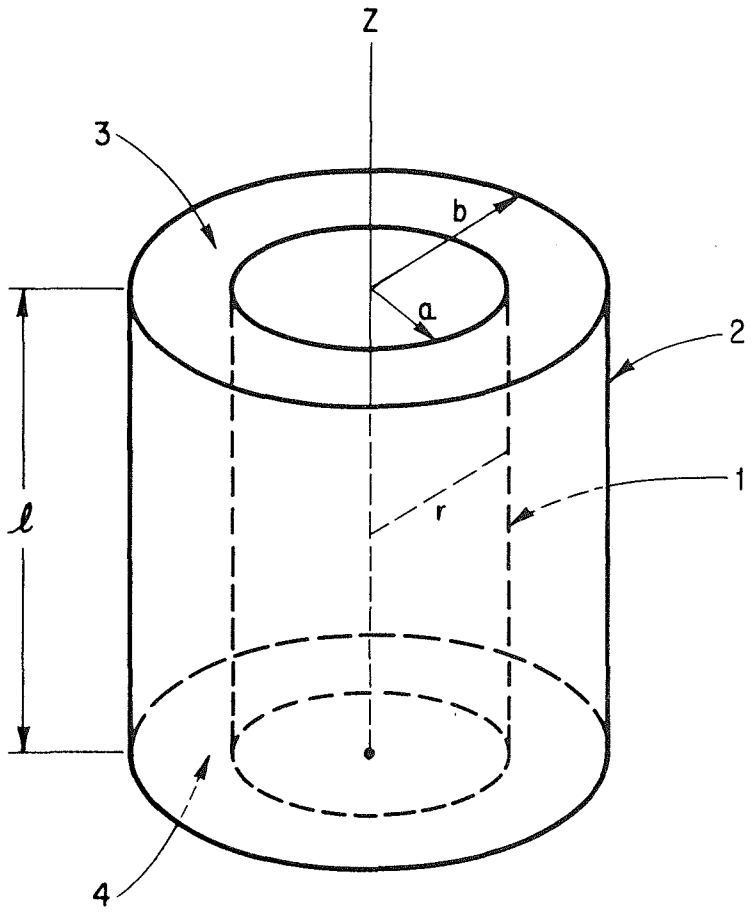

FIGURE 10 ANNULAR CYLINDER ELEMENT OF LUNAR MEDIUM

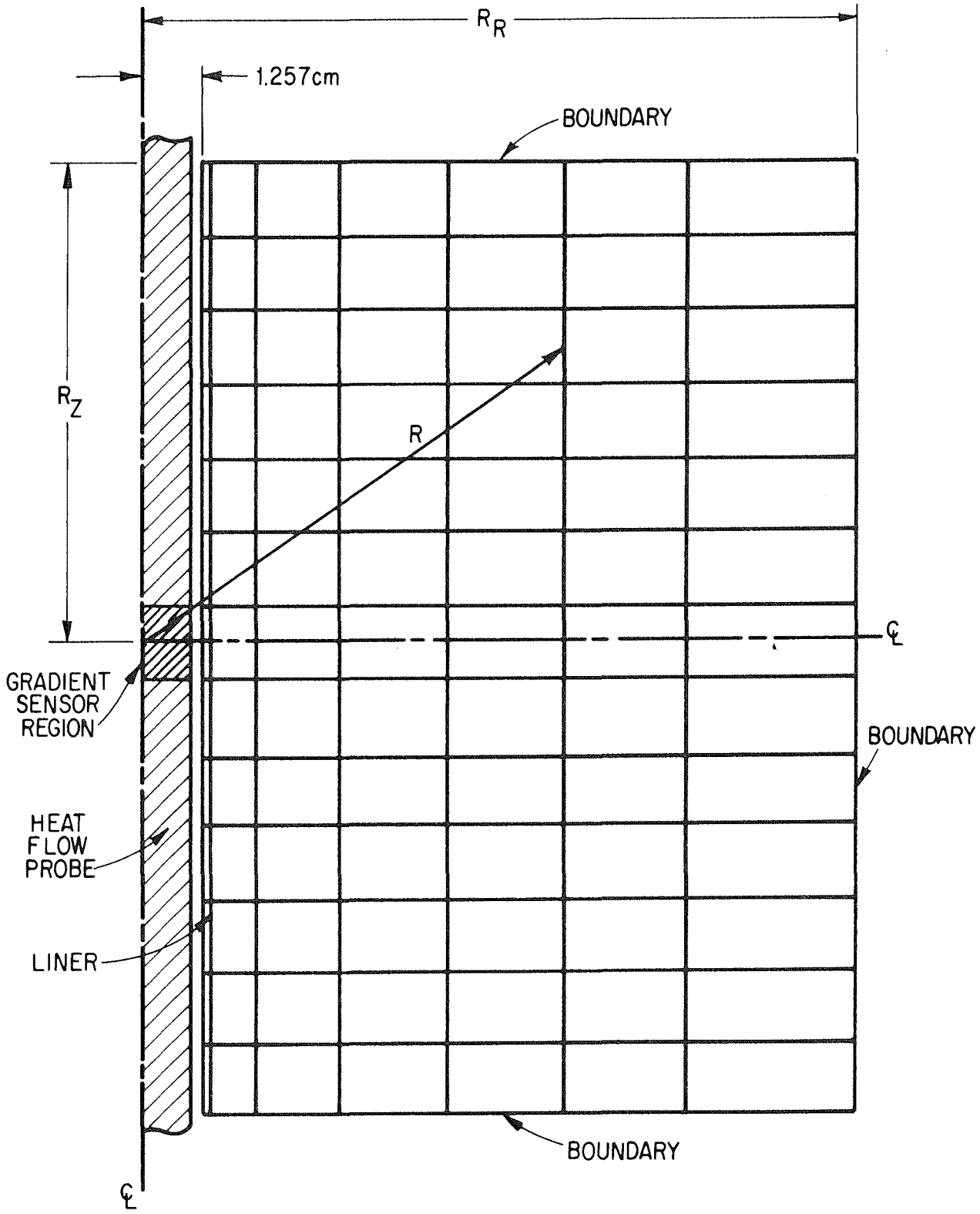

FIGURE 11 SCHEMATIC DIAGRAM OF FINITE-DIFFERENCE MODEL FOR 2-DIMENSIONAL MODEL OF LUNAR MEDIUM

TABLE I

SUMMARY OF PARAMETERS FOR

LUNAR SURROUNDINGS OF PROBE

Quantity	Mode 2	Mode 3
ℓ, length of vertical subdivision (cm)	1.091	1.846
M, number of vertical subdivisions	13	15
N, number of radial subdivisions	5	6
c_2, ratio of outer-to-inner radius of each annulus	1.367	1.512
Number of finite-difference heat flow equations describing lunar medium	213	291

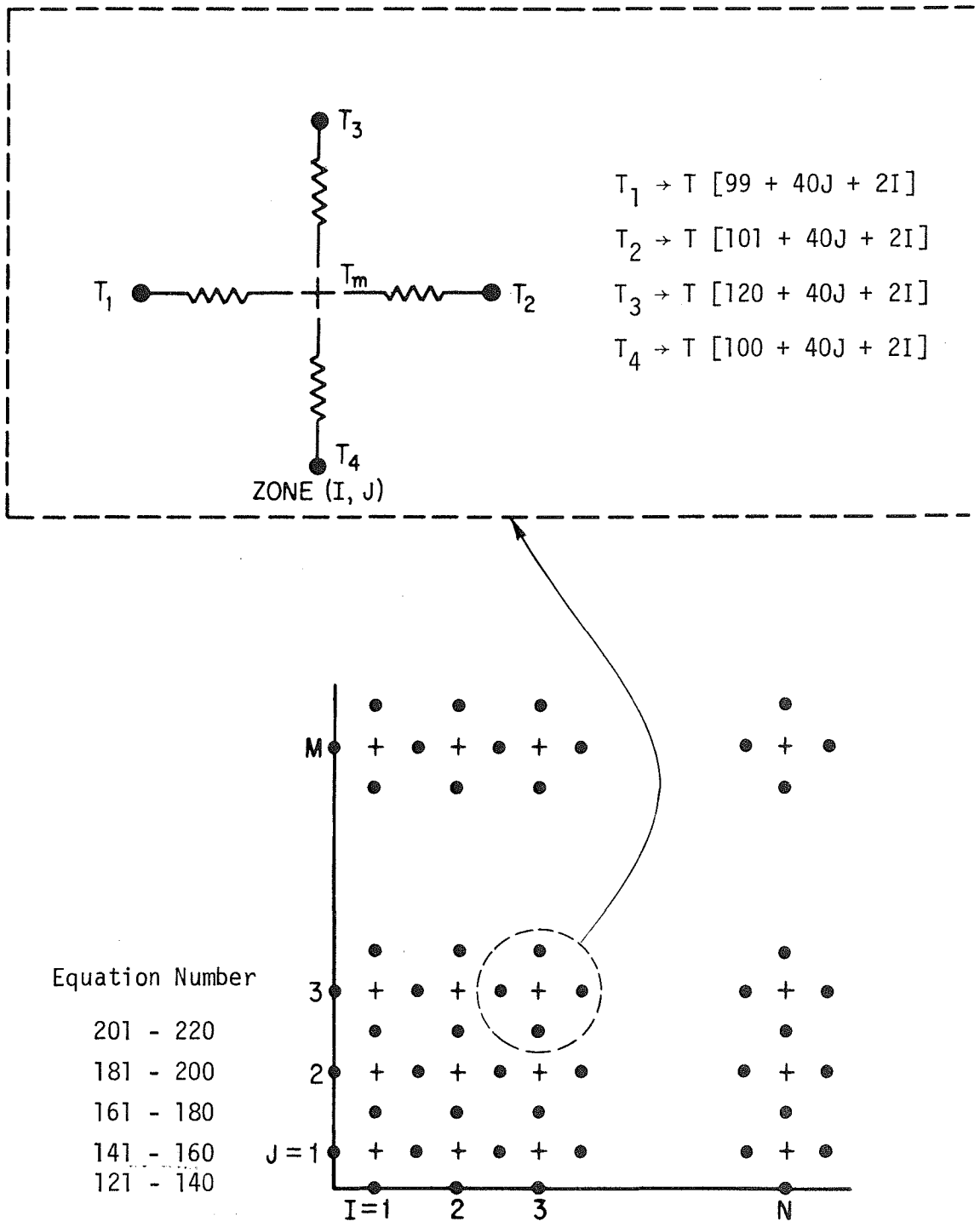

FIGURE 12 NUMBERING PATTERN FOR TEMPERATURE LOCATIONS (See Text)

the mean temperature node, while the dots represent the surfaces shown as 1 through 4 in Figure 10.

D. Tubular Liner

A description of the liner is required to complete the modeling of the conductivity experiments. The liner is important to the test performance of the probe and the performance in the lunar environment.

An epoxy-fiber-glass tube (called a bore tube in previous references) is imbedded in a medium of glass beads contained in the Thermal Conductivity Test Apparatus.[3] It was assumed that the thermal coupling between the probe and the bore tube was purely radiative. This is consistent with the original conceptual design of the probe and the clearance provided by the 1-inch inside diameter of the bore tube.* Also, since the glass beads in the K Apparatus were compacted, it was assumed that the external surface of the tube and the inner boundary of the medium were well coupled thermally and were equal in temperature. Heat flow equations were written to describe the longitudinal conduction of heat along the tube and its radiative interchange with the heat flow probe. The vertical subdivisions in the tube were the same as those in the lunar model. Parameters and zone identification numbers associated with the model for the liner are summarized in Table II.

Although the configuration of the experiment in the lunar medium is apparently similar to that in the K Apparatus, there are some basic differences associated with the lunar drill casing. The drill casing is approximately four times as conductive as the bore tube. In addition, the 7/8-inch inside diameter of the drill casing is

---

* The validity of the assumption was also confirmed by the agreement between computer-predicted and test results when the probe was inserted in a 1" ID tube which was temperature-controlled.

TABLE II

DESCRIPTION OF PARAMETERS FOR

THERMAL MODELS OF TUBULAR LINER

Parameter	Mode 2	Mode 3
Number of vertical subdivisions	13	15
Length of vertical subdivisions (cm)	1.091	1.846
Identification numbers for thermal zones	141, 181, ... 621	141, 181, ... 701
Identification numbers for zone boundaries	123, 163, ... 643	123, 163, ... 723
Zone on centerline of probe heater	381	421

smaller than the corresponding dimension for the bore tube. This smaller dimension introduces some uncertainty in contact conductance to the three alignment springs situated at each heater location (see Figure 6). The overall diameter of the circular envelope defined by the extension springs exceeds 7/8-inch.* Contacting between the springs and the inside of the drill casing could provide another path for transfer of heat from the probe heater to the drill casing. There is also some uncertainty as to the exact nature of the thermal coupling at the interface between the external surface of the drill casing and the lunar material.

For the performance predictions in the lunar medium prepared to facilitate real-time data reduction, it was decided that the drill casing would be modeled according to the same guidelines developed for the bore tube. A limited number of parametric calculations were made to investigate the effect of the above-mentioned uncertainties on the thermal performance of the probe.

---

* No flight-configuration casings, or tubular liners with a 7/8-inch inside diameter have been used in probe performance tests.

IV. EVALUATION OF COMPUTER MATHEMATICAL MODELS

A. Surrounding Lunar Medium

The finite-difference method of modeling the thermal resistance of the lunar medium was evaluated by comparing computer predictions with available exact solutions for the line heat source problem and the spherical surface source problem. The formulation of these problems, and the results will be discussed separately in the present section.

1. One-Dimensional (Line Source) Problem

Finite-difference models were formulated for the problem of a thin, cylindrical heat source surrounded by a medium composed of concentric annular rings. Numerical calculations were compared with exact solutions for the problem of a line heat source in an infinite medium. The motivation for this study was to determine the requirements of radial subdivision in the lunar medium appropriate for accurate temperature predictions at regions close to the source of heat. For this purpose, the one-dimensional problem is more meaningful for the spherical-source model.

Figure 13 illustrates the radial subdivisions in the finite-difference model. Due to the differences in heat source power, thermal conductivity levels and important locations in the lunar medium, two finite-difference models were selected--one appropriate to each operating mode of the conductivity experiments. In the Mode 2 experiment accurate temperature predictions at locations near the source (i.e., near the heater and gradient sensor) are important. In the Mode 3 experiment accurate temperature predictions at remote locations from the source (i.e., near a ring sensor location) are important. Consequently, in the following discussion comparisons between exact and numerical solutions will be important at a radius of approximately 1.27 cm for the Mode 2 operation and at a radius of approximately 10 cm for the Mode 3 operation.

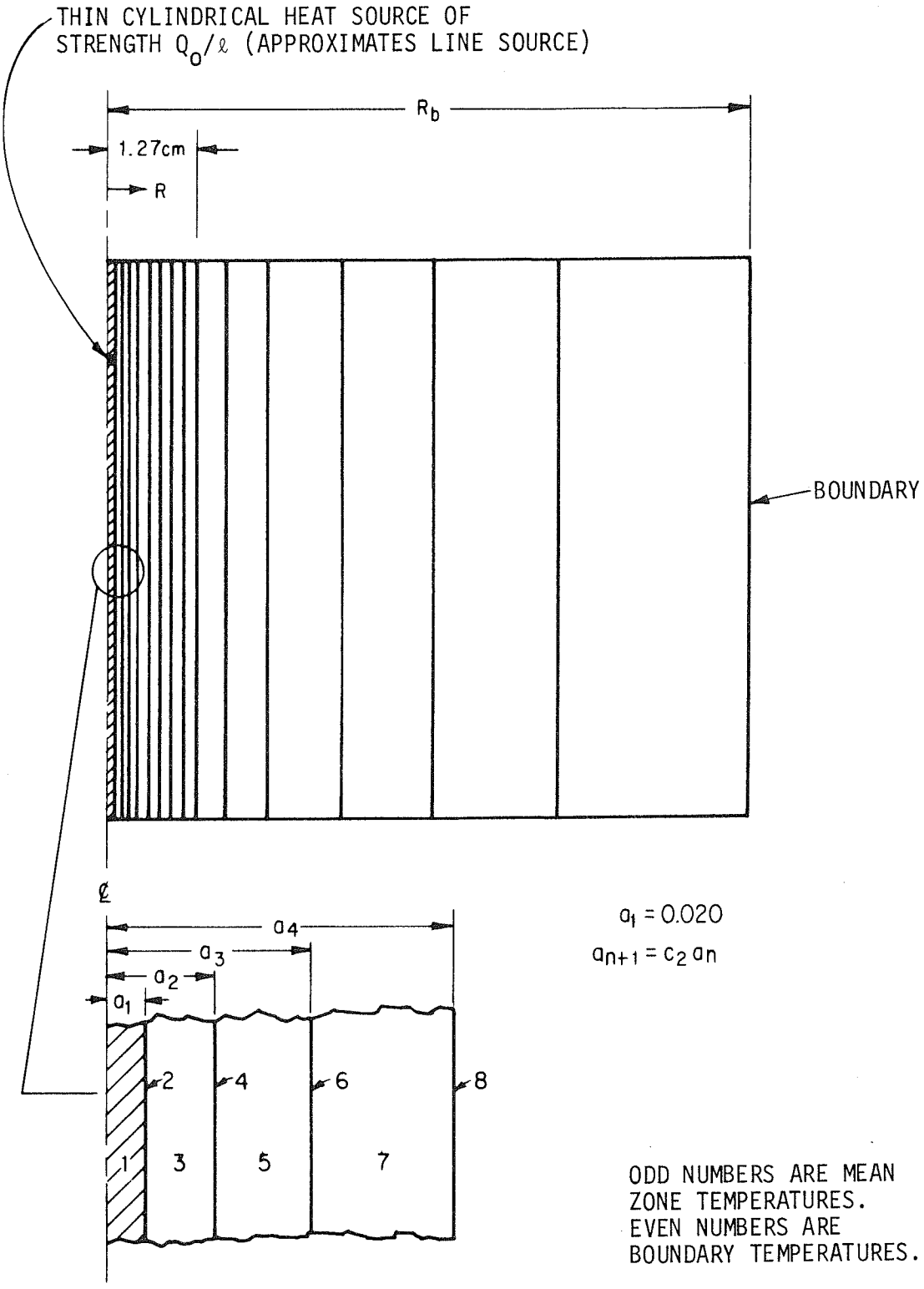

FIGURE 13 SCHEMATIC DIAGRAM OF FINITE-DIFFERENCE MODEL FOR LINE SOURCE PROBLEM

Figure 14 illustrates a comparison of temperature rise versus time for the Mode 2 finite-difference model and the exact model of the line source problem. The solid line corresponds to the exact solution at a radial location of 1.274 cm, and the circled symbols represent the values predicted with the computer program. The close agreement between exact and finite-difference models demonstrates that sufficient detail in the finite-difference model can be obtained using only five radial subdivisions.

Figure 15 illustrates exact and predicted values of temperature rise in the lunar medium at conditions corresponding to Mode 3 operation of the probe. The temperature rise at a distance of 10 cm from the heat source showed excellent agreement with the exact solution over the time span of solution. Six radial subdivisions were judged to give sufficient detail in the thermal model of the lunar medium.

2. Two-Dimensional Model of Lunar Medium

Two-dimensional, finite-difference representations of the lunar medium were made as described in Section (III-C). To evaluate these models, the lunar medium was considered to occupy the central core otherwise occupied by the heat flow probe and drill casing - see Figure 11 - with a cylindrical heat source located at the region corresponding to the gradient sensor. Calculations were performed for the temperature rise in an initially isothermal medium. These results were compared to analytical solutions for the spherical surface source.

In reviewing comparisons here between the computed results and the exact solution, it is important to consider the following:

1) In the finite-difference model, the heat source has the shape of a solid circular cylinder, while the exact solution applies to a spherical surface source. This difference should be most important at regions in the lunar medium close to the heat source. Checks on the

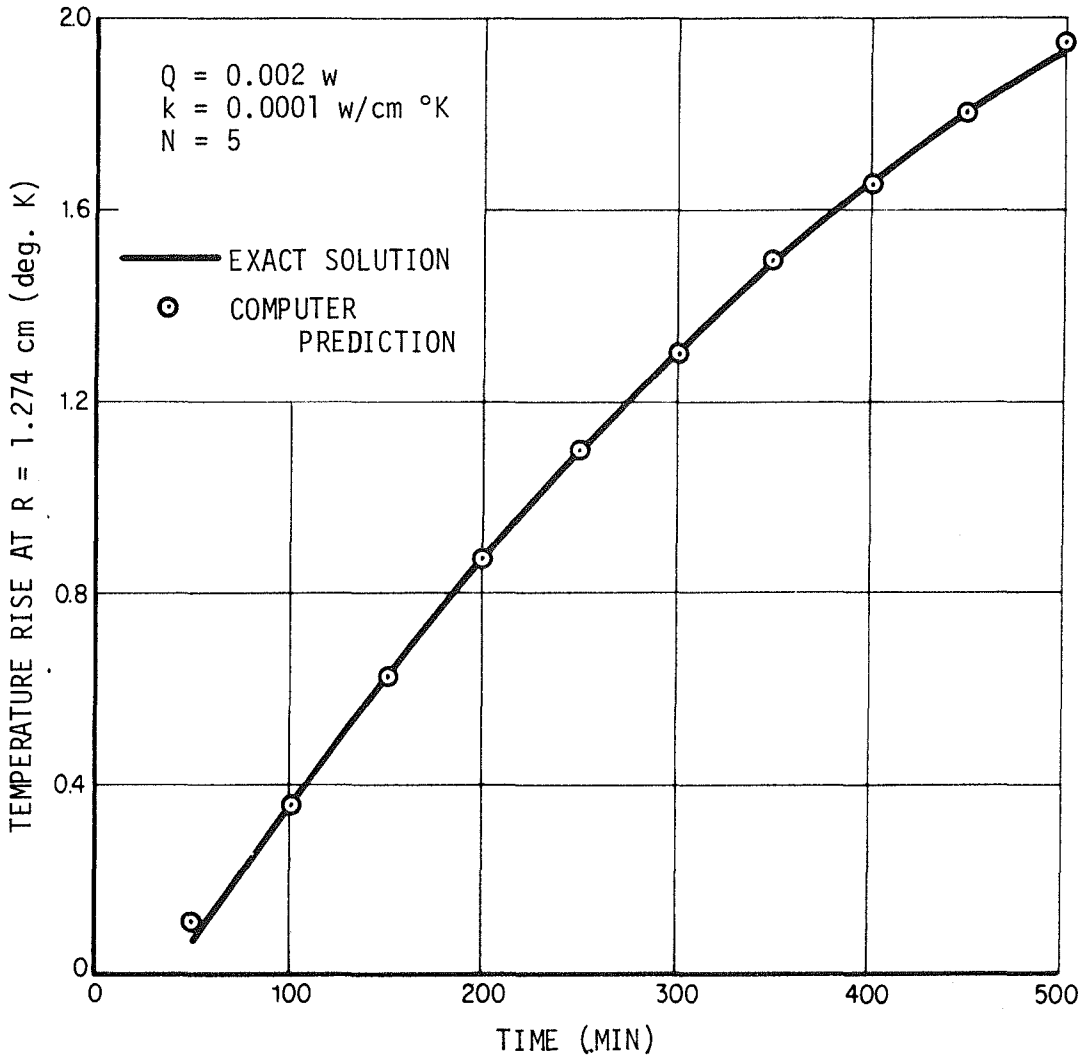

FIGURE 14 TEMPERATURE RISE VERSUS TIME FOR MODE 2 MODEL OF LINE SOURCE PROBLEM

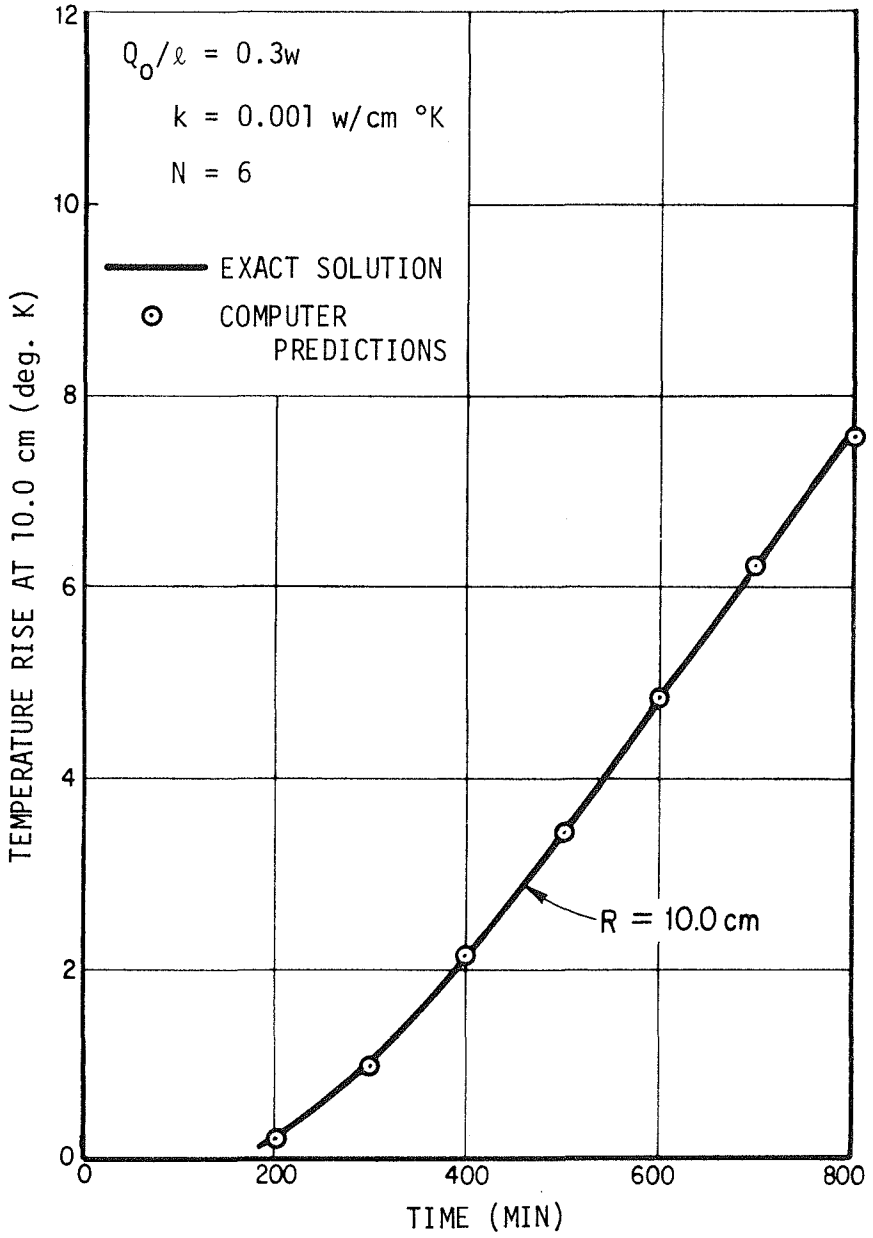

FIGURE 15 TEMPERATURE RISE VERSUS TIME FOR MODE 3 MODEL OF LINE SOURCE PROBLEM

subdivision close to the source were made in the work described above for a one-dimensional problem, where the geometrical difference between exact and finite-difference source is small.

2) Comparisons between exact and finite-difference models are made as a function of R, the distance from the center of the source to the location of interest in the lunar medium. We calculate R in the finite-difference model as the distance to the center of a radial boundary of an annular cylindrical zone. The computed temperature of this surface is the temperature averaged over the surface and is not necessarily equal to the center temperature of the surface.

Since the heat flows at the boundaries are determined as a function of the absolute distance from a spherical surface source, it is of interest to examine the computed results from the standpoint of radial symmetry. Figure 16 shows the radial temperature distribution in the lunar medium for a Mode 3 model at a time of 500 minutes. The solid curve corresponds to the values computed from the exact solution; the dotted symbols represent values computed using the finite-difference model. Values obtained from computer solution apply to position vectors extending in various angular directions to locations in the lunar medium. The close agreement between exact and computed values indicates that the Mode 3 model accurately predicts the radial temperature distribution in the lunar medium.

Figure 17 shows a comparison of exact and computed temperature rise at R = 8.811 cm, as a function of time up to 1,000 minutes. The computed values shown on this curve were obtained for several values of N, the number of radial subdivisions in the lunar medium, and α, an integration parameter used in the numerical solution of the

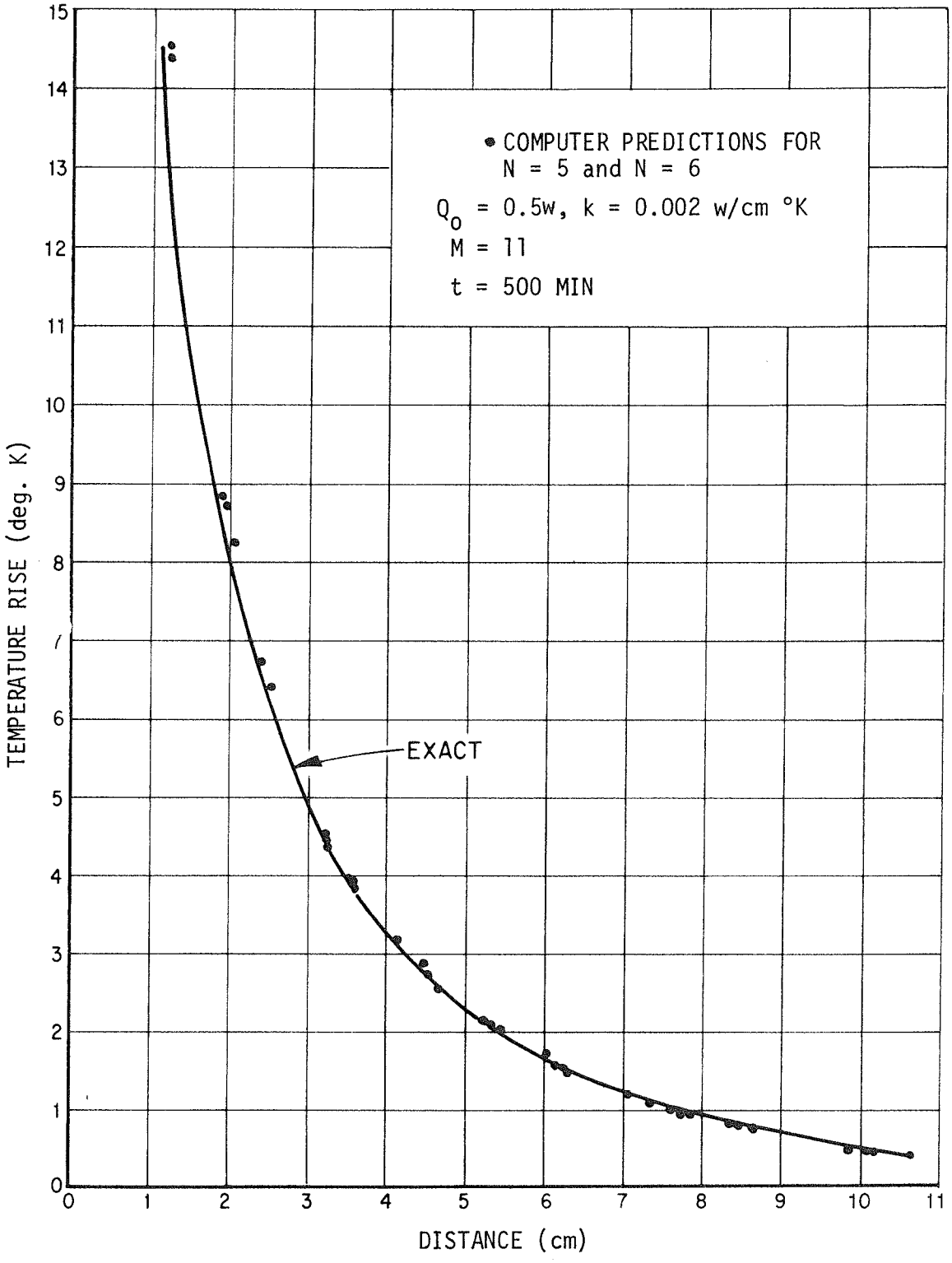

FIGURE 16 TEMPERATURE DISTRIBUTION IN MODE 3 MODEL OF LUNAR MEDIUM

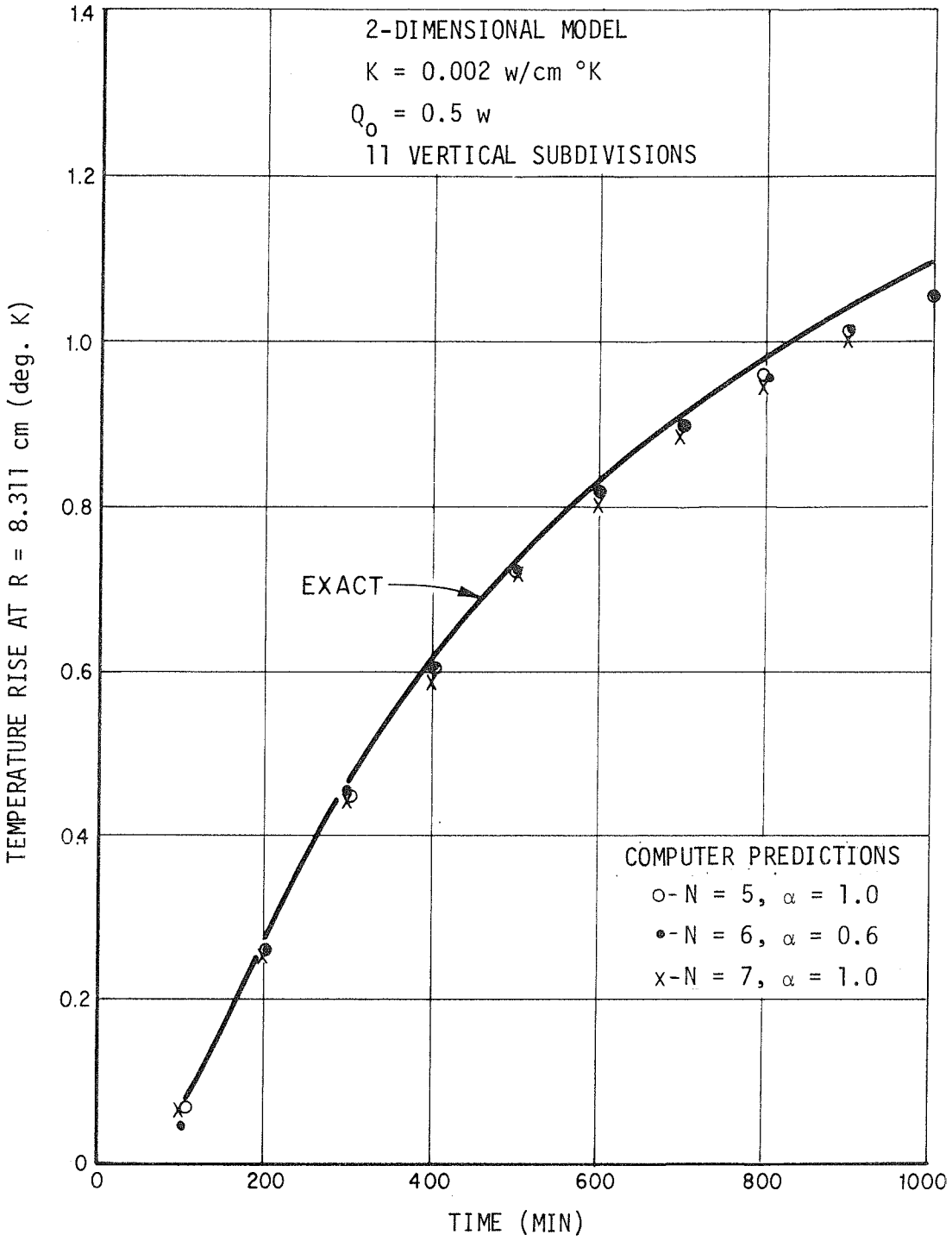

FIGURE 17 TEMPERATURE RISE VERSUS TIME FOR MODE 3 MODEL OF LUNAR MEDIUM

finite-difference equations by ADLGTA. (A discussion of the integration parameter α is included in Appendix I.)

The computed values of temperature rise show a slight but small dependence on the integration parameter. Results computed for other cases not shown here reveal that the most accurate solutions are obtained using large values of α. Subsequently, the calculations were performed using a value of $\alpha = 1.0$.

The agreement between exact and computed values of temperature rise is good up to times of 500 minutes. As time increases, the computed results begin to have a small deviation from the exact solution. It is believed that the deviation results from the difference in the source geometries discussed earlier. The uncertainties which arise because of this deviation are small compared to other uncertainties which can arise when analyzing the entire experiment.

B. Lunar Probe

The heat flow probes have built-in instrumentation for monitoring the temperature responses of gradient and ring sensors. Although tests were not designed or instrumented specifically for the purpose of providing detailed checks on the computer models, several tests were conducted for performance evaluation of the heat flow probes under other subcontracts.[1,3] Available data for the responses of gradient and ring sensors at particular locations during performance tests were used as a check on the probe computer models, prior to performance predictions in the lunar environment.

Two types of tests which were performed in the Arthur D. Little, Inc., HFE Thermal Test Facility[3] provided information useful for comparisons with predicted results. One series of tests was conducted in a Temperature Gradient Test Apparatus, where the probe was surrounded by a temperature-controlled, near-isothermal, aluminum tube. Another series of tests was performed in the Thermal Conductivity Apparatus where the probe was surrounded radially by a bore tube and a

medium comprising glass beads with interstitial gas. In this test procedure the pressure of the interstitial gas (helium or nitrogen) was varied between approximately 1μ and 1 atmosphere to simulate a range of thermal conductivity levels in the glass-beaded medium. An evacuated medium simulates a low thermal conductivity, in the range of Mode 2 operation, while a helium or nitrogen-filled medium simulates a high thermal conductivity, typical of the range for the Mode 3 operation of the experiment.

The tests in the ΔT apparatus provided a useful means for checking the ability of the computer models to predict Mode 2 performance of the probe. In these tests, one possible uncertainty was minimized--the thermal conductivity of the surrounding medium. The Mode 2 tests in the K Apparatus for low values of simulated conductivity provided only qualitative information and were not applicable for verification checks on the computer models. Interpretational difficulties with the Mode 2 tests in the K Apparatus are described in Reference 3.

Mode 3 tests in the K Apparatus for helium-filled and nitrogen-filled (at 1 atm) glass-bead beds were not subject to interpretational difficulties and were used for comparison with computer predictions.

1. Predicted Performance for Mode 2 Operation in the ΔT Apparatus

The computer model for the heat flow probe was evaluated by predicting gradient sensor temperature rises for Mode 2 operation in an isothermal environment and comparing them with corresponding measured values obtained from tests performed in the ΔT apparatus. Comparisons between experiment and theory were made for all six test conditions included in the Group I series of tests reported in Reference 3. The gradient sensor temperature rises were measured at all four experiment locations at one environmental temperature level; performance data for experiment location 2 was obtained at two additional temperature levels.

Table III presents test results and computer predictions for the gradient sensor temperature rise. At a temperature level of 224.4°K, the agreement between test and theory is within 4% for all locations. The maximum deviation between computer model predictions and experiments was obtained at the high temperature condition at location 2.

A comparison between predictions for the transient temperature response and test results from the ΔT apparatus is shown in Figures 18 and 19 for all four experiment locations and an environmental temperature level of 224.4°K. The agreement between experiment and theory is good over the total time to reach steady conditions.

Calculations were also made to evaluate the influences of uncertainties in probe thermal characteristics specified in the computer model. The influence of these uncertainties on the predicted gradient sensor temperature rise in an isothermal environment are summarized in Table IV.

The most important uncertainty affecting the computer predictions of probe performance is the radiation coupling between the probe body and the aluminum bore tube. A 1 percent uncertainty in the probe emittance corresponds to nearly a 1 percent change in steady-state temperature rise.

2. Predicted Performance for Mode 3 Operation in the K Apparatus

After the temperature calculations were performed for the Mode 3 experiment in the K Apparatus, slopes of the ring-sensor temperature were found using a simple curve-fitting technique. A parabolic equation was fitted to pass through the computed sensor temperature at a given time and through the temperatures computed in both the preceding and succeeding time intervals. The derivative of the curve then provided the slope of the temperature vs. time curve.

Figure 20 illustrates the predictions for rate of ring-sensor temperature rise versus time when the probe is surrounded by a

TABLE III

COMPARISON BETWEEN MEASURED AND PREDICTED

TEST PERFORMANCE IN ΔT APPARATUS

Experiment Location	Temperature Level °K	Temperature Rise of Gradient Sensor		Deviation %
		Test °K	Predicted °K	
1	224.4	0.1970	0.2004	1.7
2	205.4	0.2640	0.2663	0.9
	224.4	0.2055	0.2127	3.5
	244.5	0.1596	0.1702	6.6
3	224.4	0.2168	0.2159	- 0.4
4	224.4	0.2248	0.2226	- 1.0

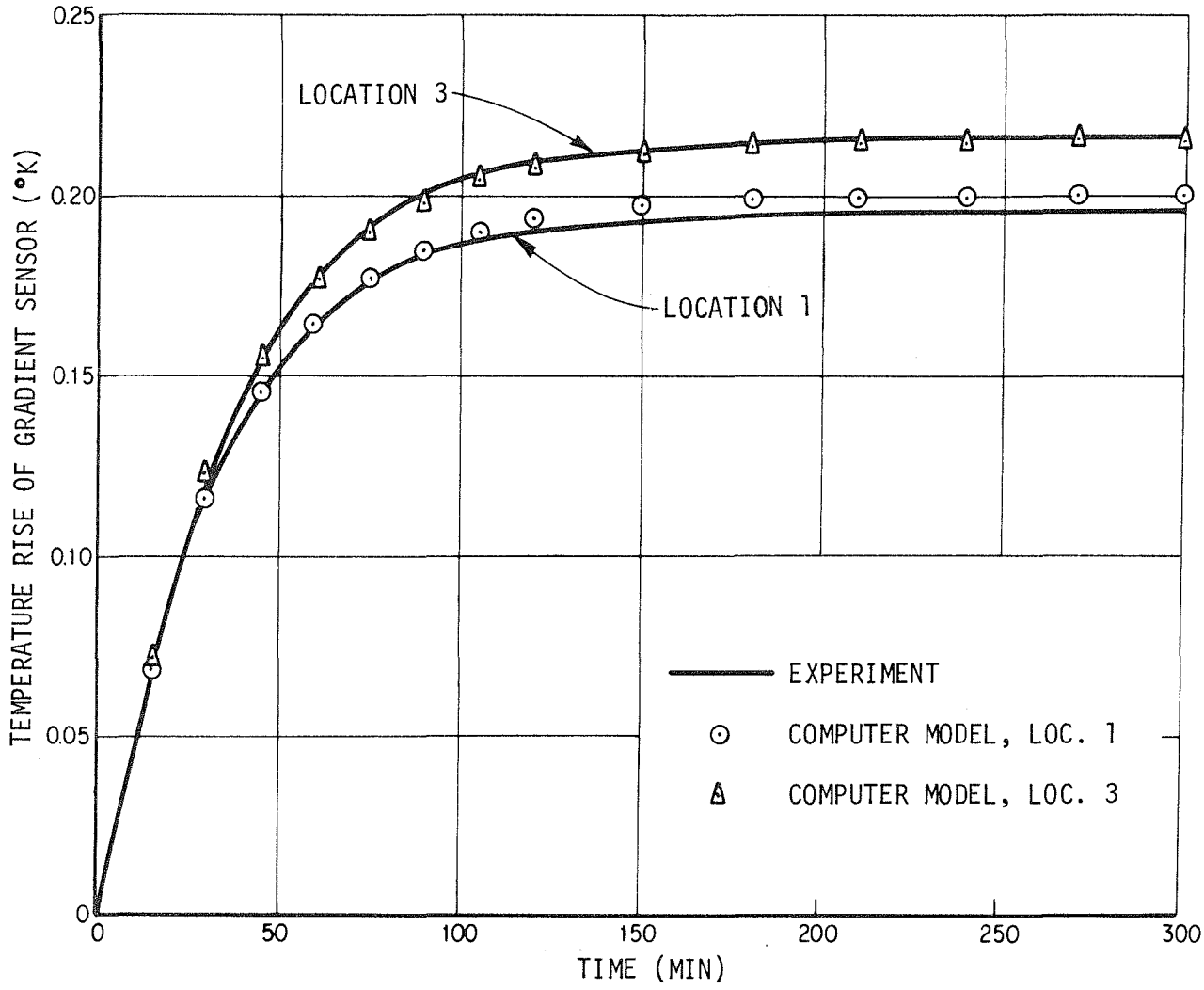

FIGURE 18 TRANSIENT TEMPERATURE RESPONSE FOR MODE 2 TESTS IN ΔT APPARATUS

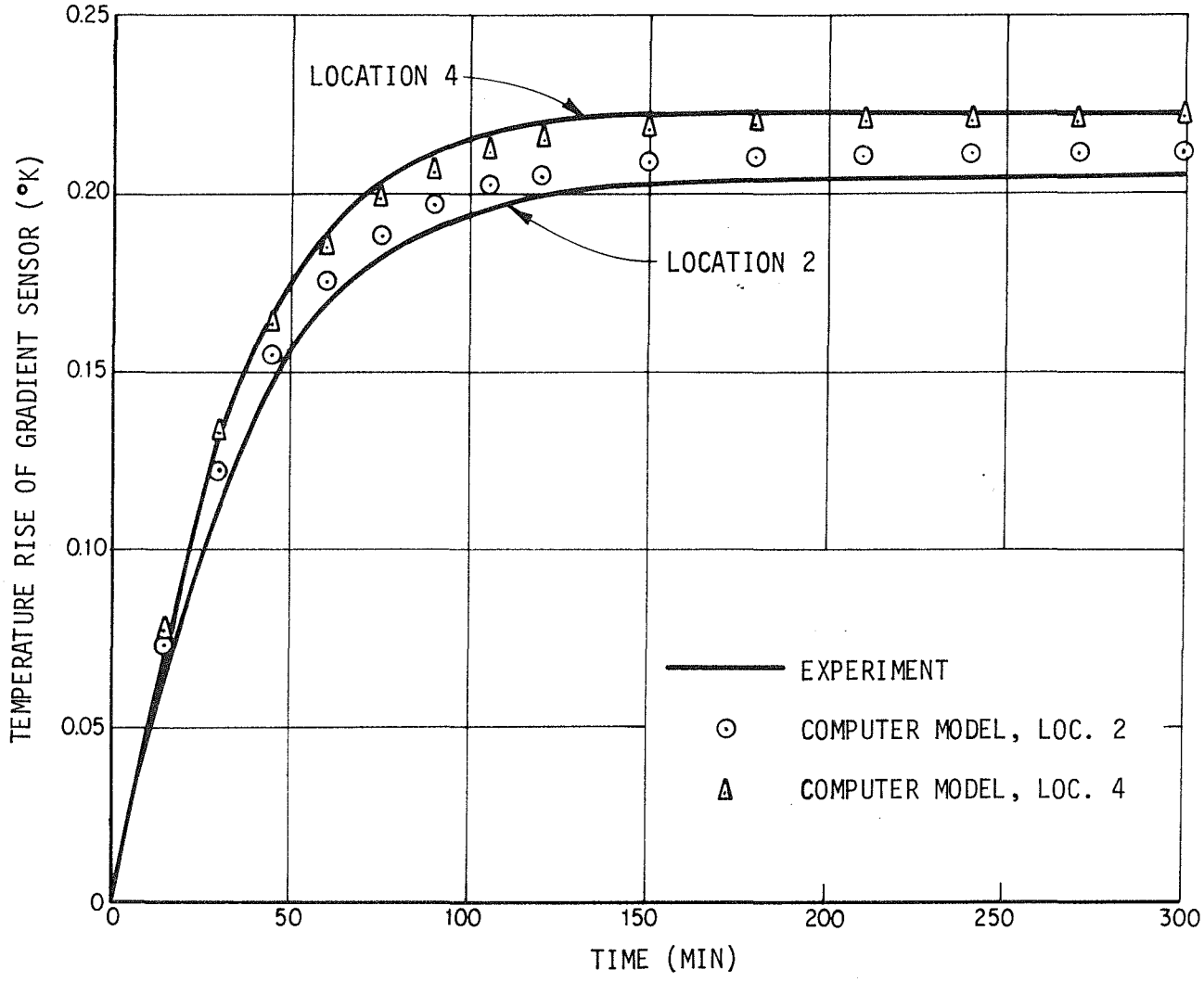

FIGURE 19 TRANSIENT TEMPERATURE RESPONSE FOR MODE 2 TESTS IN ΔT APPARATUS

TABLE IV

INFLUENCE OF UNCERTAINTIES ON PREDICTED TEMPERATURE RISES IN THE ΔT APPARATUS

	Parameter	Change	Change in ΔT(%)
1)	Thermal conductance of probe body	Increase 10%	- 0.7%
2)	Lead wire conductance	Decrease 21%	+ 0.7%
3)	View area from heater to space	Increase 5%	- 1.1%
4)	Emittance of sensor can	Decrease 43%	+ 0.2%
5)	Emittance of probe body	Decrease 6%	+ 5.0%

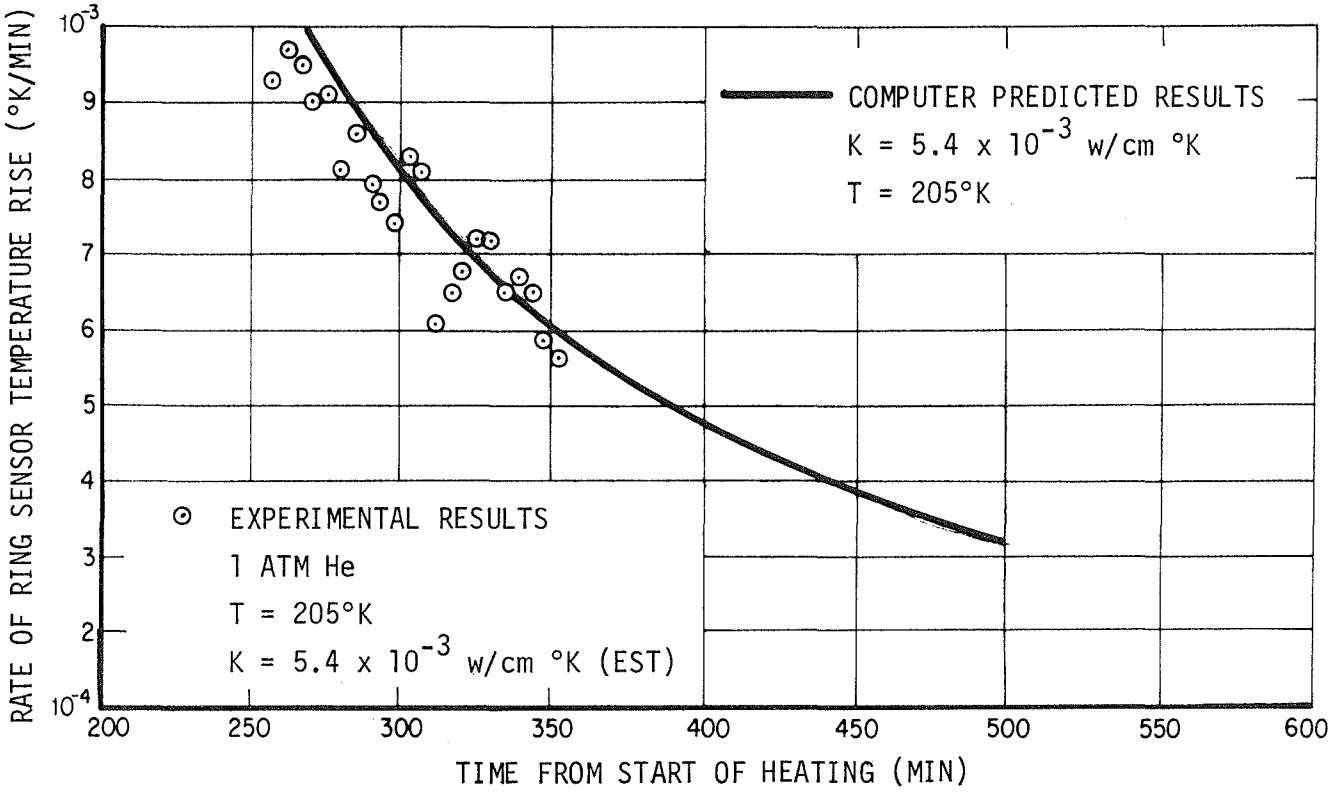

FIGURE 20 PREDICTED SLOPE OF RING-SENSOR TEMPERATURE DURING MODE 3 TEST IN K APPARATUS, K = 5.4 x 10^{-3} w/cm °K

medium having a thermal conductivity (K) of 5.4×10^{-3} w/cm °K. The rate of temperature rise is shown for times greater than 250 minutes; the values at earlier times are off-scale for the linear ordinate used. The circled points presented on Figure 20 represent test data for experiments performed in the K-1* Apparatus. Close agreement is shown between computer-predicted and test results.

Several interesting details concerning the probe operation in a Mode 3 experiment were revealed by the computer calculations. They will be discussed here prior to the presentation of another comparison between computer predictions and test performance.

In particular, there is a net transfer of heat from the ring sensor to the bore tube. This condition indicates that heat transfer along the probe elements, between the gradient and ring sensors, is appreciable. Important heat flow paths to the ring sensor are provided by the probe sheath, lead wires and ring-bridge wires (see Figures 6 and 8).

Also, during the Mode 3 experiments, the ring sensor is surrounded by elements of the probe at slightly higher temperatures. An illustration is presented with the aid of Figure 21. The temperature rises shown for the ring sensor and other elements (filler sleeve, ring sensor guard and the end sheath) lie in a range of 0.959 to 1.119°K. For the corresponding test in the K Apparatus, the measured temperature rise of the ring sensor was 1.04°K. The radial clearance between the filler sleeve and the warmer end sheath is very small (1 1/2 to 3 1/2 mils). Contacting surfaces could provide conductive heat transfer across this apparent clearance and slightly raise the temperature of both the filler sleeve and the ring sensor.

In Figure 22 the predicted transient response of the ring sensor and the end sheath are shown in comparison with test points for the ring sensor. The test conditions ($K = 1.7 \times 10^{-3}$ w/cm °K, T = 225°K) are the same as those referenced in Figure 21. The upper curve

* The Thermal Conductivity Apparatus having a 1-inch ID by 0.025-inch wall bore tube.

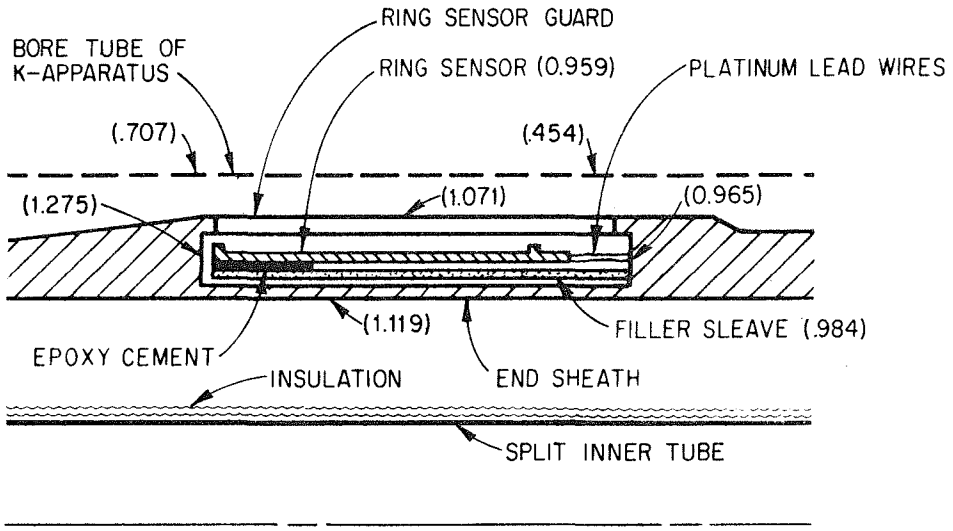

NOTE: NUMBERS IN PARENTHESES ARE COMPUTER-PREDICTED VALUES OF TEMPERATURE RISE FOR THE FOLLOWING CONDITIONS:

MODE 3, LOCATION 2 IN K APPARATUS

$K = 1.7 \times 10^{-3}$ w/cm °K

$T_{INITIAL} = 225°K$

TIME AFTER START OF HEATING = 350 MIN

FIGURE 21 SCHEMATIC SKETCH OF RING SENSOR DETAIL

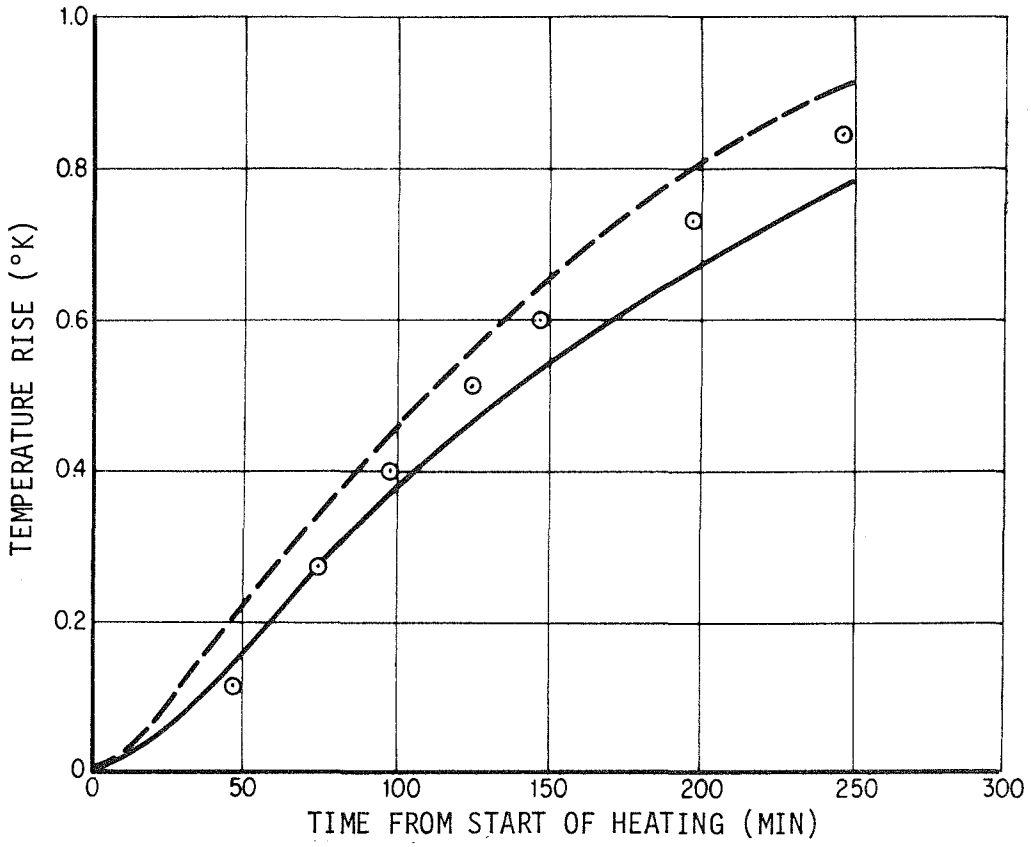

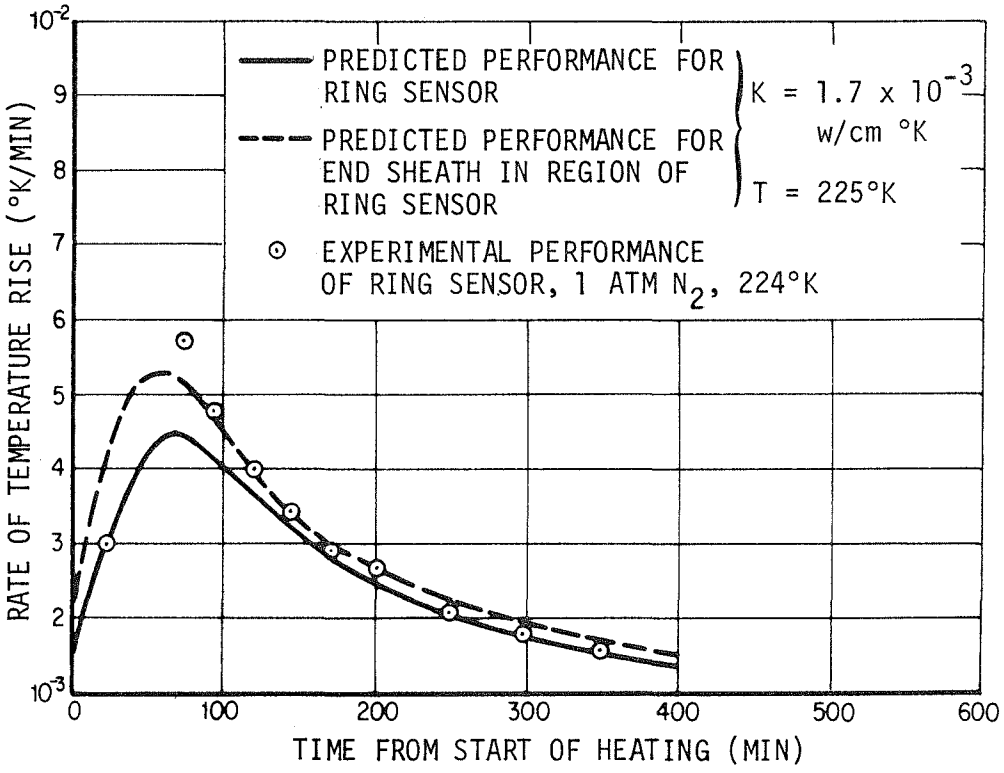

FIGURE 22 COMPARISON OF PREDICTED AND TEST RESULTS FOR MODE 3 EXPERIMENT IN K APPARATUS

in Figure 22 shows that the predicted temperature rises for the ring sensor and the end sheath bracket the ring sensor test results.

The rate of temperature rise for both the end sheath and the ring sensor are plotted in the lower curve and show close agreement with the test results.

The predictions for the Mode 3 operation of the probe indicate that the rate of ring-sensor temperature rise provides a good indication of thermal conductivity of the surrounding medium at times greater than three hours after the start of heating. At earlier times, the slope is sensitive to the thermal characteristics of the heat flow probes. A similar conclusion was drawn from results of performance tests of the probe.[3]

The predictions also show that the Mode 3 models of the probe and surroundings are accurate and agree with test results well within the limits of experimental accuracy. If contacting between the end sheath and filler sleeve occurs across the narrow clearance separating the two elements, it should not significantly affect the performance of the Mode 3 conductivity experiments.

V. PREDICTED PERFORMANCE IN THE LUNAR ENVIRONMENT

A. Introduction

An important objective of the performance predictions in the lunar environment was to prepare information for use as an aid to the Principal Investigator during the real-time data reduction of the Heat Flow Experiment. It was also of interest to compare the performance of conductivity experiments in the K Apparatus and the same experiment in the lunar medium.

As directed by the Principal Investigator, thermal performance was predicted at two experiment locations for the Mode 2 experiment - locations 2 and 4 - and at location 3 for the Mode 3 experiment. Gradient sensor temperature rise was computed as a function of time, thermal conductivity, and absolute temperature level for Mode 2 operation. In Mode 3 studies, both the temperature rise and rate of temperature rise (slope) of the ring sensor were computed as a function of time and thermal conductivity. The effect of temperature level and variations in several other parameters were investigated with the aid of the computer models. Runs were also made to investigate the decay behavior of the ring sensor and gradient sensor at location 2 after heater turn-off in a Mode 3 experiment.

All predicted data is presented in tabular form in Appendix IV to facilitate subsequent data processing by Lamont-Doherty Geological Observatory.

B. Mode 2 Experiment

Predicted data for gradient sensor temperature rise versus time is plotted in Figures 23 through 25 for experiment location 2. The predicted performance data for the gradient sensor at experiment location 4 (tabulated in Appendix IV) is similar, except that the temperature rises are approximately 10 to 20% higher at long times. As described earlier, the temperature rises of the gradient sensor at location 4 are higher than those at location 2 because of locational variations in the number of lead wires and their associated conductances.

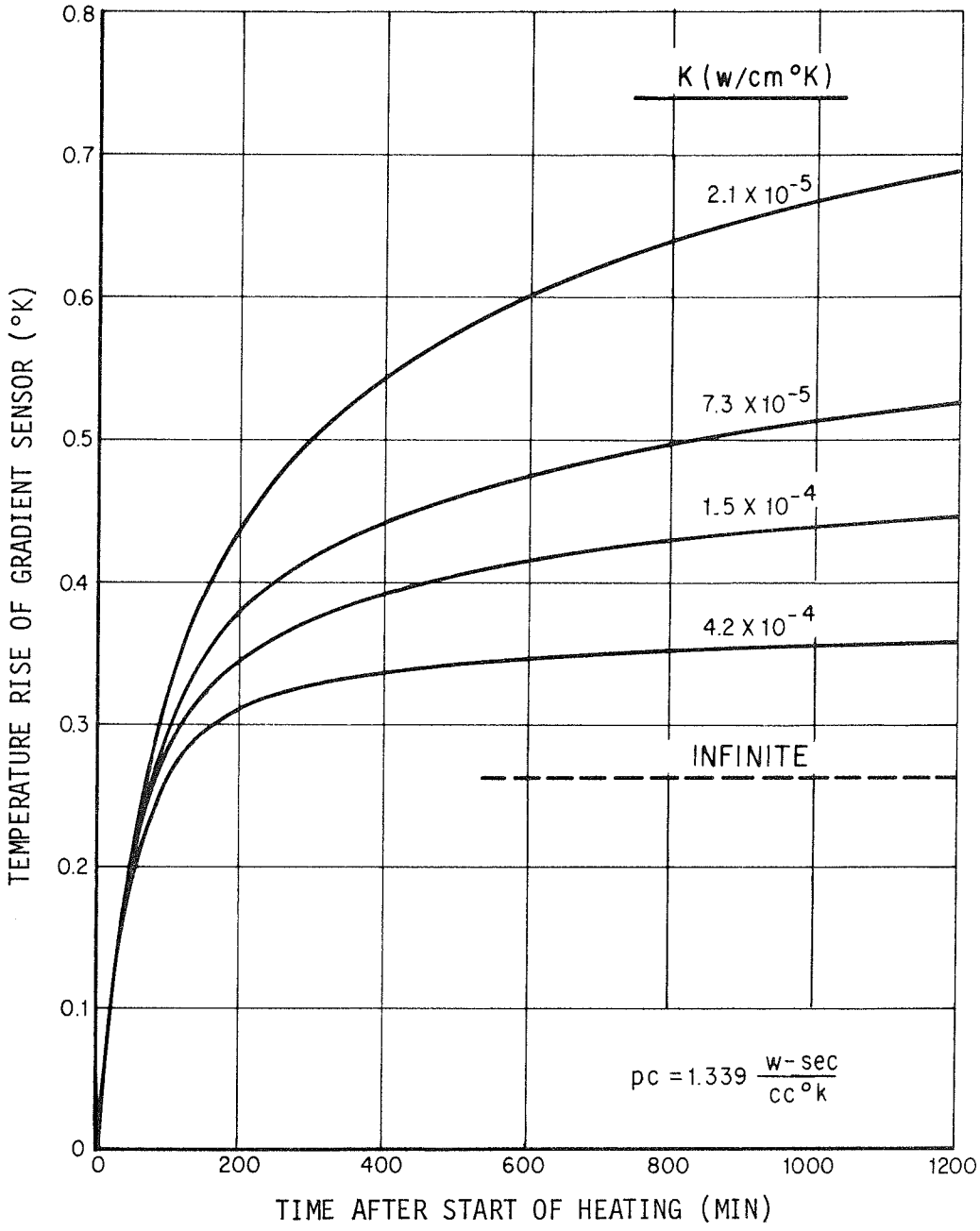

FIGURE 23 PREDICTED PERFORMANCE OF MODE 2 EXPERIMENT - LOCATION 2, T = 205°K

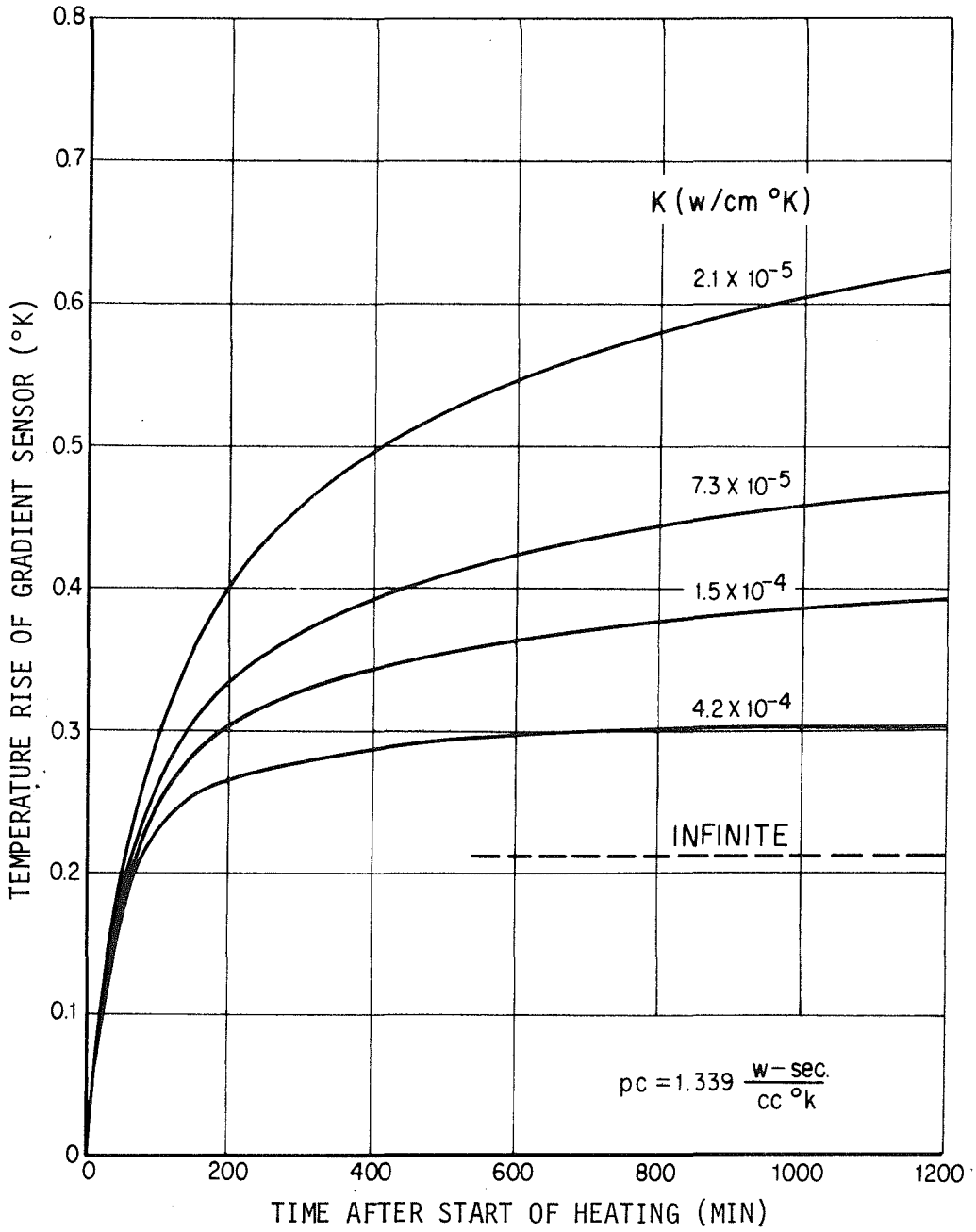

FIGURE 24 PREDICTED PERFORMANCE OF MODE 2 EXPERIMENT - LOCATION 2, T = 225°K

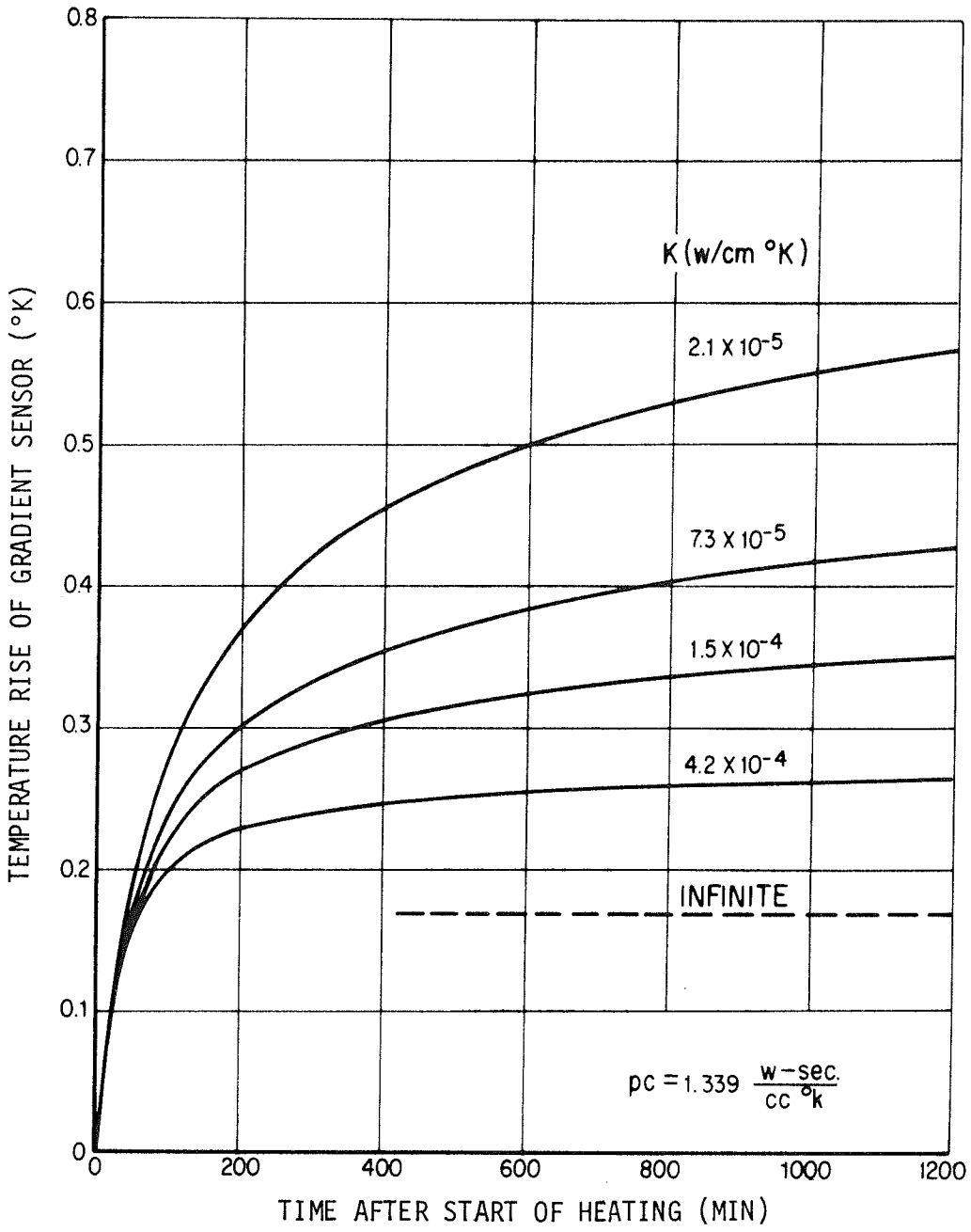

FIGURE 25 PREDICTED PERFORMANCE OF MODE 2 EXPERIMENT - LOCATION 2, T = 245°K

Several trends are obvious from an examination of the plots.

1) The temperature rise of the gradient is inversely proportional to both thermal conductivity and absolute temperature level;

2) The sensitivity of the Mode 2 experiment to changes in thermal conductivity decreases as thermal conductivity increases.

When the probe is surrounded by a medium having a near-infinite conductivity, the temperature rise is primarily governed by the inherent thermal resistance provided by the radiation gap between the probe and the drill casing. As the thermal conductivity of the medium decreases, the temperature rise of the gradient sensor increases. At low values of lunar conductivity the resistance provided by the medium becomes a major contributor to the temperature rise.

1. The Use of Slope Data to Supplement Evaluation of Mode 2 Data

Although not originally intended as a method of data interpretation, the use of the rate of change of gradient sensor temperature with time ("slope data") to determine the conductivity of the lunar medium surrounding the probe was investigated. This brief look was motivated by the successful use of slope data for interpreting Mode 3 data. In addition, a simple point-heat-source model[6] suggests that the slope may be a more sensitive indication of the thermal conductivity than is the value of the temperature rise. For a point source, the steady-state temperature rise varies inversely with the thermal conductivity; whereas, the time rate of change (slope) varies inversely with the conductivity raised to the three-halves' power.

Table V provides a comparison between the two methods of interpreting Mode 2 data over a wide range of thermal conductivities. The calculations were made for experiment location 2 assuming an initial temperature of 225°K. Shown in the table are predicted values of

TABLE V

COMPARISON OF SENSITIVITIES OF TEMPERATURE RISE AND SLOPE OF GRADIENT SENSOR, MODE 2 EXPERIMENT

Thermal Conductivity of Medium w/cm °K	Gradient Sensor* Temperature Rise (°K)	Gradient Sensor* Slope °K/min	Percentage Change in Conductivity (%)	Percentage Change in Temperature Rise (%)	Percentage Change in Slope (%)	% Change in Slope / % Change in ΔT
2.1×10^{-5}	0.547	0.000203	+248	-23	-40	1.7
7.3×10^{-5}	0.423	0.000121	+105	-14	-32	2.3
1.5×10^{-4}	0.364	0.000082	+180	-19	-61	3.2
4.2×10^{-4}	0.295	0.000032				

* Experiment Location 2
T = 225
ρc = 1.339 w-sec/cc °K
Time = 10 hours after start of heating

temperature rise and rate of temperature rise after 10 hours from start of experiment. From these values, the percent changes in temperature rise and in slope were determined as a function of the percent change in thermal conductivity. The results confirm that the slope data is two to three times more sensitive to the lunar thermal conductivity than is the temperature rise.

Figure 26 shows a plot of slope data versus time on log-log paper. For the case considered, the data very nearly fits a straight line after a heating time of only 50 minutes. The slope of the plot reveals a power law dependence on time of -1.35. Corresponding values for the point-source and line-source models are -1.5 and -1, respectively.

The behavior illustrated may be used to estimate the steady-state temperature rise and the time required to reach a given percentage of this value--on the basis of the temperature-time history at early times. The results may be fitted to the following simple model for the rate of change of temperature, T, with time, t:

$$\frac{\partial T}{\partial t} = \alpha t^{-\beta}$$

Once the parameters α and β are found from the data, the steady-state temperature rise can be estimated from:

$$T_{ss} = T_\tau + \int_\tau^\infty \frac{\partial T}{\partial t}\, dt$$

$$= T_\tau + \frac{\alpha \tau^{(1 - \beta)}}{\beta - 1}$$

where

T_τ = temperature rise after some time τ.

Using the data shown in Figure 26, a steady-state temperature rise of 0.507 is estimated compared to a computed value of 0.481.

The model may also be used to predict the time required to reach X% of steady-state temperature rise:

$$t_{X\%} = \frac{T_{ss}\ (1\text{-}0.01X)\ (\beta - 1)}{\alpha}^{\frac{1}{1-\beta}}$$

For the results illustrated, the times to reach 80% and 90% of the final value of temperature rise are estimated to be 61.6 hours and 459.5 hours, respectively.

The simple extrapolation model presented here is speculative since it has not been thoroughly investigated in the present work. It is offered here as a potential means of supplementing the interpretation of Mode 2 data, and as an aid in planning the experiments to be performed.

C. Mode 3 Experiment

For the Mode 3 experiment, computations of ring sensor temperature rise and slope were performed during a six-hour heating period for the following thermal conductivities: 1.5×10^{-4}, 6×10^{-4}, 1×10^{-3}, 1.7×10^{-3} and 5.4×10^{-3} w/cm °K. As directed by the Principal Investigator, the absolute temperature level was 225°K and the density, ρ, and specific heat, c, were specified at 1.6 gm/cm^3 and 0.2 cal/gm °C, respectively (ρc = 1.339 w-sec/cc °K). At the end of the six-hour heating period, the heater was turned off and the temperatures of the ring sensor and the gradient sensor at location 2 were computed as a function of time during a decay period of approximately 18 hours.

The computer-predicted results for the temperature rise and slope of the ring sensor during the six-hour heating period and the temperature decay of the ring sensor and gradient sensor during the decay period are tabulated in Appendix IV.

Before discussing the Mode 3 results, it is appropriate to state the measurement ranges of the gradient and ring bridges. The gradient bridges are designed to operate over the range of 200 to 250°K and measure differential temperature within two distinct ranges:

1) $\pm$ 2°K, and 2) $\pm$ 20°K. The ring bridges are designed to operate over the same temperature range but measure differential temperature within one range: $\pm$ 2°K. This means that the slope of the ring sensor during a Mode 3 experiment cannot be used to measure a thermal conductivity which is sufficiently low to cause the ring-sensor temperature to rise more than 2°K. Similarly, the decay data of the gradient sensor can only be obtained when the temperature rise of the ring sensor is less than 20°K.

The predicted temperature rise of the ring sensor is shown in Figure 27 for a heating period of 6 hours and a decay period of 18 hours. The performance data for a conductivity of 1.5×10^{-4} is not plotted since the predicted temperature rise of the ring sensor exceeded the measurable maximum of 2°K during the early transient.

The relationship between ring sensor slope and time is presented in Figure 28 for all five values of thermal conductivity. The predicted slope for a conductivity of 1.5×10^{-4} is described by a dotted line for times greater than 120 minutes where the temperature rise lies outside of the measuring range of the ring bridge.

Referring to Figure 29, it is evident that the cooling behavior of the gradient sensor at location 2 is also related to the thermal conductivity of the surrounding lunar material. This behavior can serve several purposes. It can be used to provide an experimental check on the conductivity measurement indicated by the ring sensor response. The decay behavior can also be used to measure conductivities lying in the transition between the Mode 2 and Mode 3 ranges, where conductivities may be too low to be measured by a Mode 3 experiment, and where a Mode 2 experiment may be resolution-limited. For example, in the range of 6.0×10^{-4} to 1.5×10^{-4} w/cm °K, the cooling behavior of the gradient sensor is quite sensitive to the thermal conductivity of the lunar medium.

The range limitations of the Mode 3 conductivity experiments are dependent upon the absolute temperature level of the moon, and the

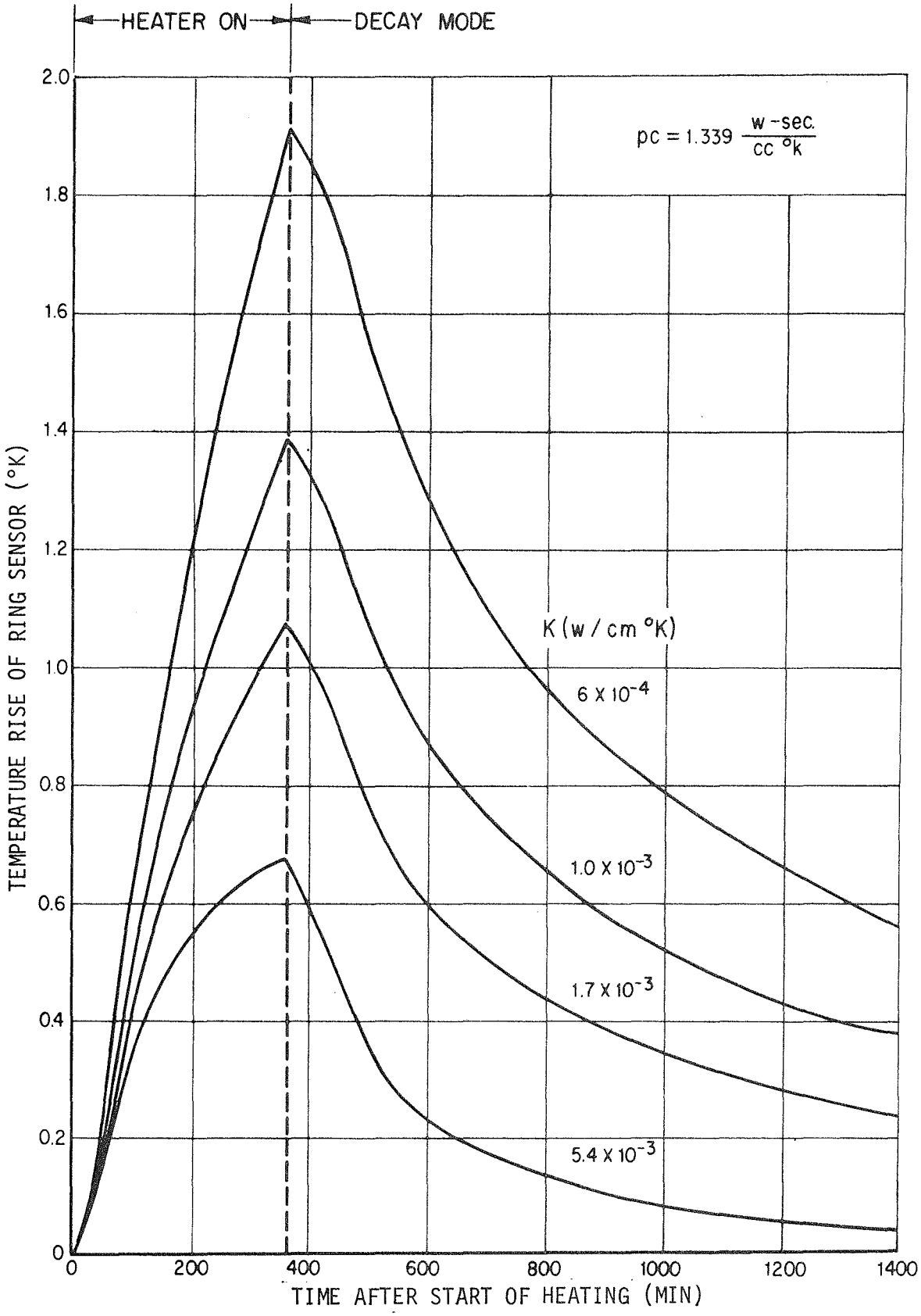

FIGURE 27 TEMPERATURE RISE OF RING SENSOR DURING HEATING AND DECAY PERIODS OF MODE 3 EXPERIMENT, LOCATION 2, T = 225°K

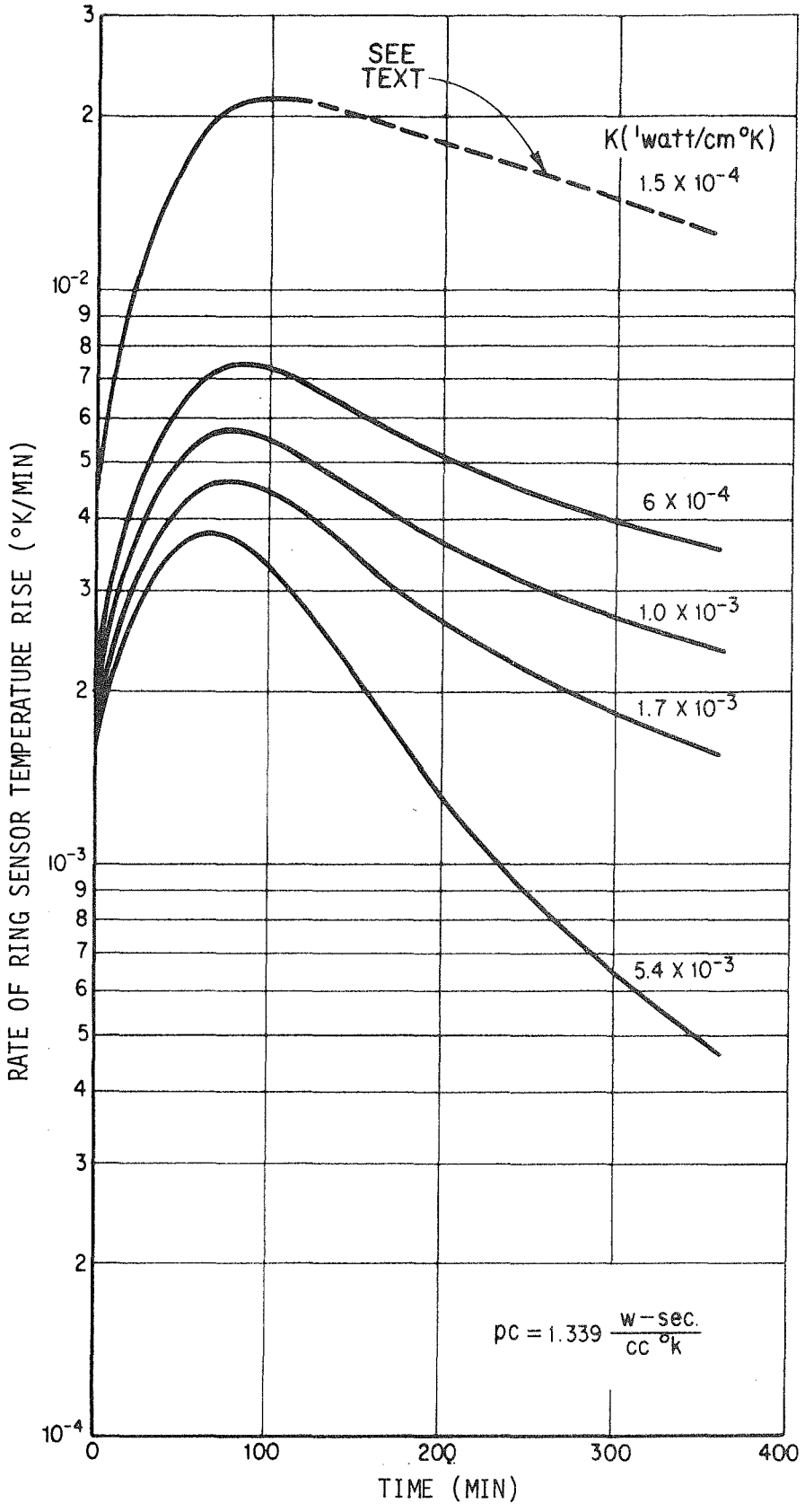

FIGURE 28 SLOPE OF RING-SENSOR TEMPERATURE DURING MODE 3 EXPERIMENT - LOCATION 2, T = 225°K

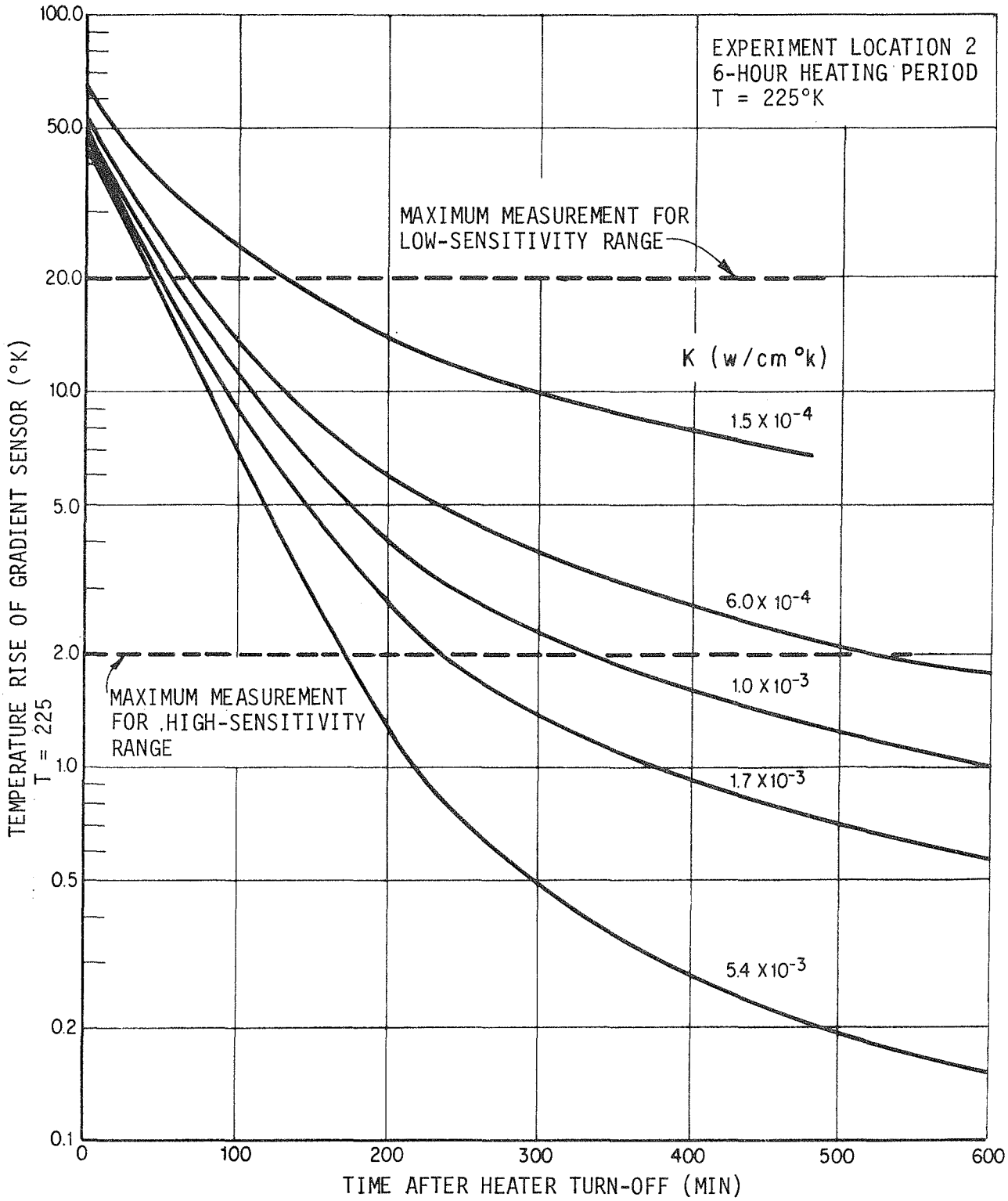

FIGURE 29 TEMPERATURE DECAY OF GRADIENT SENSOR AFTER MODE 3 EXPERIMENT

duration of the heating period necessary to minimize the effect of probe-related transients. It is presently planned to operate the Mode 3 experiments for a minimum of five or six hours. Parametric computer predictions could be used to evaluate and define experimental limitations. An example is presented below.

D. Typical Performance of Conductivity Experiments in the Lunar Environment

Figure 30 summarizes the predicted performance of the heat flow probes for lunar conductivities ranging from 2×10^{-5} to 5.4×10^{-3} w/cm °K. The performance capabilities shown are for several specified conditions:

- Experiment location 2
- An absolute temperature of 225°K
- A Mode 2 heating period of at least 16 hours
- A Mode 3 heating period of at least 6 hours

For the Mode 2 performance, both the temperature rise and the slope of the gradient sensor are shown at a time of 16 hours. It is interesting to note that the slope of the gradient sensor is significantly more sensitive to thermal conductivity than is the temperature rise. Over the range of 2.1×10^{-5} to 4.2×10^{-4} w/cm °K, the slope changes by almost an order of magnitude. In contrast, the temperature rise varies between 0.6 at $K = 2.1 \times 10^{-5}$ and 0.3°K at $K = 4.2 \times 10^{-4}$. The limited resolution of the temperature rise at $K = 4.2 \times 10^{-4}$ is apparent, since 90 millidegrees, a 30% change in signal, separates a low and near-infinite prediction of thermal conductivity.

The data show that the Mode 3 experiment is limited to measuring a thermal conductivity of approximately 5.5×10^{-4}, which is sufficiently low to cause the ring sensor to rise 2°K. The decay behavior of the gradient and ring sensors can be used in the range of 1.5×10^{-4} to 5.5×10^{-3} w/cm °K to supplement the Mode 2 and Mode 3 experiments.

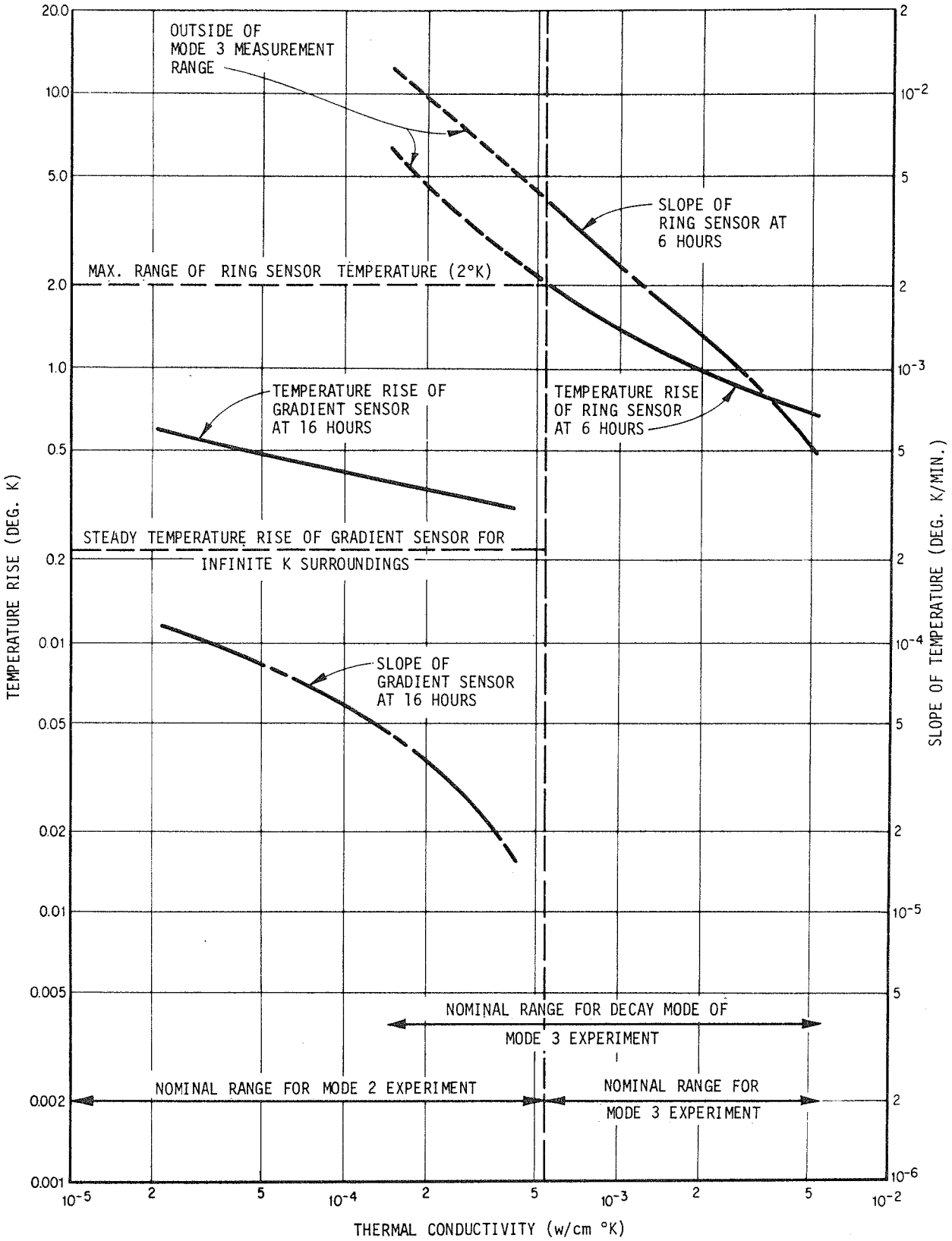

FIGURE 30 PREDICTED THERMAL PERFORMANCE OF EXPERIMENT LOCATION 2 AT A TEMPERATURE OF 225°K

It is important to note that these data are quite specific and apply to the conditions previously stated. Performance ranges will be different at other experiment locations and for other values of absolute temperature level. For example, calculations indicate that experiment location 4 will experience a smaller temperature rise at its ring sensor at given value of conductivity, although the slope behavior will be consistent with that of location 2. Therefore, the Mode 3 experiment at location 4 should be capable of measuring conductivities less than 5.5×10^{-4} w/cm °K. When the absolute temperature of the medium is less than 225°K (resulting in an increased temperature rise for the ring sensor), the Mode 3 limitation for location 2 will apply to thermal conductivities slightly higher than 5.5×10^{-4}.

E. Comparison of Experiment Performance in the K Apparatus and Lunar Environment

The physical differences between the bore tube in the K Apparatus and the lunar drill casing were discussed in Section III-D. The drill casing is approximately four times as conductive as the bore tube. Consequently, as shown in Table VI, probe performance in the K Apparatus and in the lunar environment differs for the same environmental conductivity.

For the Mode 2 experiments performed in the K Apparatus, the low-conductance bore tube permits less longitudinal heat transfer than the drill casing, resulting in a higher gradient sensor temperature rise. Therefore, the probe performs as if it were in a lunar environment having a conductivity 27 to 37% lower. The bore tube has the opposite effect on the response of the Mode 3 experiment. The low-conductance bore tube provides less longitudinal heat flow to the region of the bore tube near the ring sensor. In the Mode 3 test, the probe performed as if it were in a lunar medium having a conductivity 9% higher than the conductivity of the medium in the K Apparatus.

TABLE VI

COMPARISON OF EXPERIMENT PERFORMANCE IN THE K APPARATUS AND LUNAR MEDIUM*

	Lunar Environment (with boron-reinforced, epoxy fiber-glass, drill casing)	K Apparatus (with epoxy-fiber-glass bore tube)	% Deviation	Approximate Error in Conductivity Simulated by test (%)
Mode 2 experiment at 1200 minutes				
Temperature rise of ring sensor (°K)				
@ $K = 1.5 \times 10^{-4}$ w/cm °K	0.393	0.427	+ 8.6	-27
@ $K = 7.3 \times 10^{-5}$ w/cm °K	0.470	0.531	+13.0	-37
Mode 3 experiment at 301 minutes				
$K = 1.7 \times 10^{-3}$ w/cm °K				
Temperature rise of ring sensor (°K)	0.969	0.877	- 9.5	
Slope of ring sensor (°K/min)	0.00185	0.00175	- 5.4	+ 9

* Experiment location 2; absolute temperature = 225°K

F. Parametric Studies of Experiment Performance

1. Parametric Studies for Mode 3 Experiment

The Mode 3 performance predictions already described are based upon nominal values of parameters which were included in the computer model description of experiment location 2. The computer model description was specifically related to the following operational conditions:

Experiment location:	2
Absolute temperature:	225°K
Density of lunar material:	1.6 gm/cm^3
Specific heat of lunar material: (i.e., ρc = 1.339 w-sec/cc °K)	0.2 cal/gm °K

Suppose the density or specific heat of the lunar material were not previously known at the time of the measurements, or that the data correlations were made on performance data at 225°K while the measured environmental temperature was 205°K: What uncertainty would be involved if predicted data for experiment location 2 were used to evaluate the performance at experiment location 4?

It is first of interest to examine the relationship between changes in thermal conductivity and changes in slope of the ring sensor. This relationship is indicated in the following tabulation considering the slope at a time of five hours after the start of heating. Changes in conductivity were made from a base value of 1.7×10^{-3} w/cm °K.

Percent Change in Lunar Conductivity	Percent Change in Slope of Ring Sensor
-41	45
+20	-13
+218	-65

The results of examining the influence of various uncertainties on the Mode 3 experiment are presented in Table VII. Also shown is a column for the estimated error in a conductivity prediction, since this is a more meaningful quantity than the percentage change in slope. It is assumed that: 1) the thermal conductivity in the surrounding lunar material, which is to be evaluated by the measurement, is 1.7×10^{-3} w/cm °K, and 2) an estimate of the lunar conductivity is made by correlating the slopes of the ring sensor with the data for experiment location 2 and the conditions already described.

The estimates for errors in conductivity predictions are approximate, and the relationships described in Table VII specifically relate to a lunar conductivity value of 1.7×10^{-3} w/cm °K. A comprehensive uncertainty analysis would involve computations at other values of conductivity and consideration of other potential uncertainties not described here.

Computer models of the lunar probe were developed describing the Mode 2 and Mode 3 performance at all four experiment locations. Therefore, uncertainties associated with the effect of absolute temperature level and experiment location can be minimized in a refined data analysis.

Detailed listings of ring sensor response versus time for the parametric studies described above are presented in Appendix IV.

2. Possible Uncertainties Associated with the Experiment Configuration

Two other conditions which relate to uncertainties in the experiment configuration were examined with the aid of the computer models. The purpose of these calculations was to estimate the maximum possible influence of these uncertainties on experiment performance. While it is not suggested that the uncertainty intervals examined actually exist, it is believed that an examination of their possible influence is appropriate.

TABLE VII

INFLUENCE OF UNCERTAINTIES ON MODE 3 PERFORMANCE AT A THERMAL CONDUCTIVITY OF 1.7×10^{-3} w/cm °K

Time = 5 hours after start of heating

Parameter	Uncertainty Interval on Change	Influence on Response of Ring Sensor: % Change in Temperature Rise	Influence on Response of Ring Sensor: % Change in Slope	Approximate* Error in Conductivity Prediction (%)
Thermal Mass of Lunar Material (ρc)	+ 20%	- 7.6	- 7.6	+ 8
Absolute Temperature	- 20°K (T = 205°K)	+ 27.0	+ 4.9	- 6
	+ 20°K (T = 245°K)	- 14.6	- 2.7	+ 3
Thermal Conductance of Drill Casing	+ 20%	+ 2.8	+ 1.7	- 2
Experiment Location	Location 1	- 1.5	- 2.2	+ 3
	Location 3	- 10.6	- 1.6	+ 2
	Location 4	- 10.7	- 0.5	less than 1

* Based on estimating conductivity by correlating the predicted slopes with the performance of experiment location 2 listed in Table VIII.

a. Interface between Probe Alignment Springs and Drill Casing

As previously mentioned in Section III.D, the fact that the 7/8-inch inside diameter of the drill casing lining the lunar bore hole is smaller than the corresponding 1-inch dimension for the bore tube in the K Apparatus could introduce some uncertainty in predicting experiment performance. Heat flow to the casing via the alignment springs at the heater locations, apparently insignificant in a 1" ID surrounding, could become important in a 7/8" ID surrounding environment because of contacting between the alignment springs and the drill casing.

The magnitude of the thermal coupling or contact conductance is not known at this time. The approach used here was to select a condition which would surely bound the effect of heat flow between the alignment springs and the drill casing. The interfacial surfaces of the three equally spaced alignment springs and the drill casing were assumed to be in good thermal contact, i.e., negligible contact resistance. A well-coupled condition was also assumed at the ends of the springs which are positioned between the heater guard and the probe sheath. Conductance couplings between the probe and the drill casing were then evaluated on the basis of the thermal conductivity and cross-sectional area of the beryllium-copper springs and the effective thermal path between the probe and the drill casing.

The results of the study for the Mode 2 experiment are tabulated below.

Mode 2 Experiment

(Location 4)

(T = 225°K, time = 20 hrs. after start of heating)

Interface Condition	K (w/cm °K)	Temperature Rise of Gradient Sensor (°K)
Thermally isolated	4.2×10^{-4}	0.333
Well-coupled	4.2×10^{-4}	0.193
Thermally isolated	Infinite	0.223

The results show that the interfacial thermal coupling between the alignment springs and the drill casing is important and could significantly influence the performance of the Mode 2 experiment. Understandably, there is a non-zero contact resistance between the alignment springs and the drill casing, and between the springs and the probe, which would tend to diminish the trend noted here. Further investigations would be required to evaluate the effect on performance of other assumptions for the contacting interface, and the potential of alternate modes of interpreting experiment performance.

A similar calculation for the Mode 3 experiment indicated that even the worst-case assumption for the spring coupling could be tolerated and would not seriously influence experiment performance. This calculation was performed at experiment location 2 at a conductivity of 1.7×10^{-3} w/cm °K. The results are summarized below:

Mode 3 Experiment

($K = 1.7 \times 10^{-3}$ w/cm °K, T = 225, Location 2,
Time = 6 hrs. after the start of heating)

Interface Condition	Temperature Rise of Ring Sensor (°C)	Slope of Ring Sensor Temperature (°K/MIN)
Thermally isolated	1.071	0.00157
Well-coupled	0.760	0.00149

The estimated error in the conductivity prediction, if it were based on predicted slope data for thermally isolated interfaces, is only +6%. However, further studies at other values of thermal conductivity would be appropriate before concern for the Mode 3 experiment could be dismissed entirely.

b. Radiation Coupling between the Drill Casing and the Moon

For performance predictions in the lunar environment, the drill casing was modeled according to the same guidelines developed

for the bore tube in the K Apparatus. That is, the external surface of the drill casing was treated to be in intimate thermal contact with the lunar medium. A computation was also made under the assumption of a pure radiative coupling between the drill casing and the surrounding lunar material. A Mode 3 experiment was chosen for study since this assumption is more reasonable in a high-conductivity or rock moon than in a low-conductivity, powder-type material. Computations were made for experiment location 2 considering a conductivity of 5.4×10^{-3} w/cm °K; results are summarized below at a time of 6 hours after the start of heating.

INFLUENCE OF DRILL CASING - MOON INTERFACE ON MODE 3 PERFORMANCE

($K = 5.4 \times 10^{-3}$ w/cm °K)

	Interface between Drill Casing and Lunar Material	Temperature Rise of Ring Sensor (°K)	Slope of Ring Sensor °K/MIN
1)	Well-coupled	0.676	0.00047
2)	Radiatively coupled	3.368	0.00066

For the radiatively coupled interface the predicted temperature rise of the ring sensor exceeds the maximum measurement range of the Mode 3 experiment. Consequently, the slope at six hours could not be obtained experimentally. Since the temperature rise of the ring sensor is inversely proportional to thermal conductivity of the moon, the limitation on temperature measurement would be more prevalent at lower values of conductivity.

For a conductivity of 5.4×10^{-3}, the temperature rise reaches 2°K approximately two hours after the start of heating, a time not favorable to the evaluation of the Mode 3 experiment. At this time, the transient response of the ring sensor is strongly influenced by transient responses in the probe. However, the decay

behavior of the ring and gradient sensors after heater turn-off could possibly be used in conjunction with the computer models to determine the lunar conductivity.

VI. CONCLUSIONS AND RECOMMENDATIONS

The results of this work showed that the thermal behavior of the lunar medium could be accurately simulated by a detailed finite-difference model.

The detailed mathematical model of the thermal characteristics of the probe was extremely accurate. The accuracy was determined by comparing computer prediction to certain probe test results when the test boundary conditions were well defined.* The accuracy of the computer predictions demonstrated that the extension of the predictions to a probe in a lunar environment is appropriate.

A source of locational variations in sensor response, particularly significant to the interpretation of the Mode 2 experiment, was shown to be due to the conductive effects of lead wires passing through the entire probe. The total number of lead wires for instrumentation, resistance-bridge measurements and heaters vary along the length of the probe and thereby induce a spatial variation of thermal conductance in the probe.

The bore tube which contains the glass-beaded medium in the Thermal Conductivity Apparatus has dimensions and thermal characteristics different from the boron-reinforced, epoxy-fiber-glass drill casing which will line the bore hole in the lunar environment. Computer predictions were made to compare the Mode 2 and Mode 3 performance in the moon and in the Thermal Conductivity Apparatus for the same specified values of thermal conductivity. The comparisons indicated that precise calibration of the experiment performance in the laboratory (relating temperature responses and thermal conductivity) and performance check-out could best be accomplished if the emplaced experiment configuration and the test simulation had the same tubular liners (or liners with the same thermal conductance and internal dimensions).

---

* All experimental data used in the evaluation of the computer models were obtained from test programs sponsored under other subcontracts.

The analytical results showed that the interfacial thermal coupling between the probe alignment springs (at the heater locations) and the internal surface of the drill casing is important and could influence the accuracy of the Mode 2 experiment. The magnitude of this thermal coupling is unknown at this time since no flight-configuration casings, or tubular liners with the same internal dimensions were used in performance tests. Further study is recommended to investigate the nature of the thermal coupling at the spring-casing interface. Additionally, in the lunar environment, there are uncertainties in the thermal coupling at the interface between the external surface of the drill casing and the surrounding lunar material. Additional computer studies are recommended to assure that Mode 3 conductivity data can be interpreted with existing data reduction procedures if this interfacial coupling is radiation dominated.

Other parametric studies indicated that the computer models developed in this work could be used to establish potential ranges of limitations of certain conductivity-experiment modes and the suitability of others. Interpretation of the conductivity data in the range of transition between the Mode 2 and Mode 3 experiments can be enhanced by the use of a decay mode. Computer studies and previous test work demonstrated that additional information about the thermal conductivity of the surroundings can be obtained after a Mode 3 experiment by turning off the heater and monitoring the temperatures of gradient and ring sensors. The computation of slopes from temperature data for the gradient sensor during a Mode 2 experiment also shows promise of aiding in the interpretation of data.

The computer modeling and related studies provided information leading to a better understanding of instrument performance and limitations. Consequently, it is recommended that investigative work with computer models be incorporated into the early phases of a program involving similar experiments (design definition, instrument design, design of test equipment, etc.).

VII. REFERENCES

1. Arthur D. Little, Inc., "Lunar Heat Flow Probes for the ALSEP Heat Flow Experiment," Final Report prepared for Aerospace Systems Division, The Bendix Corporation, under Subcontract SC 0242 of Prime Contract NAS 9-5829, 30 April 1969.

2. Arthur D. Little, Inc., "Analytical Evaluation of Lunar Heat Flow Probe Thermal Conductivity Experiments," Final Report prepared for Lamont-Doherty Geological Observatory, Columbia University under Subcontract 3 of NAS 9-6037, 31 May 1968.

3. Arthur D. Little, Inc., "Lunar Heat Flow Probes - Experimental Characterization of Probe Thermal Conductivity Measurements," Final Report prepared for Lamont-Doherty Geological Observatory, Columbia University under Subcontract 8 of NAS 9-6037 (January 1970).

4. Strong, P. F., and Emslie, A. E., "The Method of Zones for the Calculation of Temperature Distribution," Paper 65 WA/HT-47, 1968, American Society of Mechanical Engineers.

5. Langseth, M., Jr., Simmons, G., Clark, S., Wechsler, A., and Drake, E., "The Apollo 13 Lunar Heat Flow Experiment," to be published.

6. Carslaw, H. S., and Jaeger, J. C., "Conduction of Heat in Solids," Oxford University Press, London, 1959.

APPENDIX I

COMPUTER SOLUTION OF HEAT FLOW MODELS

I. FINITE-DIFFERENCE EQUATIONS

Within this section we will discuss the form in which the finite-difference equations--governing the system thermal behavior--must appear in order to be solved using the Generalized Thermal Analysis Program (ADLGTA). The purpose is twofold: to present the format of the difference equations written to describe the probe and surrounding lunar medium; and to describe a disk or tape-oriented procedure for modifying the original input data for a problem. Methods of modifying input data will be described in a later section of this appendix. It is useful to introduce here the concept of a system. Nodes (or zones and their boundaries in the Method of Zones technique) whose temperatures are unknown and are to be calculated are taken to comprise a thermal system. On the other hand, nodes where the temperature is known are considered outside the system. During solution, energy balances are performed on the system to allow checks on the accuracy of the solution.

The basic form of the heat-balance equations for the system nodes is:

$$\sum_j Q_{ij} + P_i(t) + M_i \frac{dT_i}{dt} = 0 \qquad \text{(I-1)}$$

where

Q_{ij} = outward heat flow from node i in direction j (watts)
$P_i(t)$ = negative of power into node i (watts)
M_i = thermal mass of node i (Joule/°K)

The power term $P_i(t)$ may represent heat generated within the volume element represented by node i or may represent power into the volume element from some external source.

The outward heat flows Q_{ij} may be related to conductive and radiative interchange with other nodes in the system. In this case, the basic form of the energy equation becomes:

$$\sum_j C_{ij} T_j + \sum_j A_{ij} \sigma T_j^4 + P_i(t) + M_i \frac{dT_i}{dt} = 0 \qquad \text{(I-2)}$$

where

C_{ij} = thermal conductance between nodes i and j (watts/°K)
A_{ij} = radiative view area between nodes i and j (cm^2)

The energy Equation (I-2) relates the time rate of change in temperature at node i to the net energy transfer with surrounding nodal elements. An equation of the same form is written for each node within the system. The thermal mass M_i may be zero for any or all of the nodes in the system.

Similar equations can be written for the constant temperature nodes outside the system boundaries:

$$\frac{dT_i}{dt} = 0 \qquad \text{(I-3)}$$

By convention, the thermal mass of such a node is taken to be unity, although any non-zero value will suffice. The solution to Equation (I-3) is that the temperature T_i is a constant.

To obtain a heat balance on the entire system, an equation can be written for the total heat flow across the system boundaries:

$$Q_{out} = \sum_i C_i T_i + \sum_i A_i \sigma T_i^4 \qquad \text{(I-4)}$$

where

C_i = thermal conductance from node i to elements outside system boundary (watts/°K)

A_i = radiative view area from node i to elements outside system boundary (cm^2)

and where the summation over index i includes the nodes outside the system boundary. The appropriate energy balance on the system may then be written:

$$\sum_i M_i \frac{dT_i}{dt} + \sum_i P_i(t) + Q_{out} = 0 \qquad \text{(I-5)}$$

or, from Equation (I-4),

$$\sum_i M_i \frac{dT_i}{dt} + \sum_i C_i T_i + \sum_i A_i \sigma T_i^4$$

$$+ \sum_i P_i(t) = 0 \ . \qquad \text{(I-6)}$$

A sample problem illustrating the formulation of heat flow equations according to the format described above is given in Section VI of the Appendix.

II. INPUT DATA

A. Original Data

The input data consist mainly of a sequence of card images on magnetic tape. The data for several problems may be placed in succession on a single tape and followed by an end-of-file record. For the purpose of this description, we shall assume all data to be on cards as they might be before card-to-tape conversion.

A single problem consists of the following:

A. A heading card. This is an alphanumeric title to be printed on each sheet of output for identification and description.

B. A series of cards containing numerical information describing the differential equations to be solved. This series of cards is divided into sets, each of which describes a single equation. The format for all of these cards is the same, and in FORTRAN notation is I5, F20.9,

F20.9, I5, I5. A decimal point is customarily used in the two F-type fields so as to permit full flexibility. The first three fields contain the information needed to solve the problem, and the last two fields contain identification numbers. The identification in the fourth field is the equation number, and the identification in the fifth field is a serial number within the set of cards describing an equation. The information in the first three fields in a single set of cards is described below.

1. The first card contains the equation number i in the first field, the quantities A_i and C_i in the second and third fields, respectively, as required for use in Equation (I-4).

2. A series of cards comes next to give view areas, weighted conductances, and power inputs which determine A_{ij}, C_{ij}, and P_i for a single value of i in Equation (I-2). These cards are of two types:

a. The first type of card contains the quantities j, A_{ij}, and C_{ij} in the first three fields. The indices j may be in any order, and a single index may be repeated more than once if desired. If an index is repeated, the view areas and conductances given will be summed by the computer.

b. The second type of card is used when a power input is to be specified. A power input may be either constant or vary periodically. In the case of a constant power, a single card is needed: the first two fields are zero, and the third field contains the power. In all equations which contain input powers, it is required that the diagonal elements A_{ii} and C_{ii} be positive; otherwise, the conservation of energy check will fail. In case the power varies periodically, the power must be tabulated as a function of time over the period. The cards used for describing a periodic power are:

- A card which contains a zero in the first field, the period in suitable units of time in the second field, and the average power in the third field. The average power given will be used as a check when the data are read into the machine.

• A series of cards which tabulate the power as a function of time. The first field is zero, the second field contains the time, and the third field contains the power. The first time given must be zero, and the last time must be equal to the specified period. In case a discontinuity in power occurs, the time at which it occurs must be repeated, and the two values of power given.

3. The last card of each equation contains the negative of the equation number in the first field, the thermal mass M_i in the next field, and the starting temperature in the last field. The starting temperature may also be supplied in another way, and may be omitted in this card. This will be fully discussed later.

C. A blank card to terminate the data on the zones.

D. One or more control cards. The control cards contain ten fields whose format is, in FORTRAN notation, F5.2, E10.1, F10.3, I5, I5, F10.3, F10.3, I5, F5.2, I5. Decimal points are customarily used in all F-type and E-type fields.

The first field, F5.2, contains the acceleration factor used in solving the systems of simultaneous equations.

The second field, E10.1, contains a tolerance which determines when the iterations for solving the system of simultaneous equations are to be terminated.

The third field, F10.3, contains the time increment to be used in solving the differential equations.

The fourth field, I5, contains an integer which specifies the frequency of off-line print-out; the fifth field information is not used.

The sixth field, F10.3, contains the maximum value of time for which the problem is to be run before reading another control card.

The seventh field contains a starting temperature or zero. If a starting temperature is specified (and it must be on the first control card), this starting temperature will be used for all zones except for those which have already had a starting temperature specified under B-3

above. If the starting temperature punched in the second or later control card is zero, the computation will continue with the most recent temperatures as starting values but with any new parameters (e.g., time interval, acceleration factor, etc.) as specified by the new control card. If, on a second or later control card, the starting temperature is not zero, the computation will be restarted from time zero with the new parameters specified by the control card.

The eighth field, I5, specifies the largest value of the index i. Since some indices may be omitted, the number in the eighth field will be greater than or equal to the number of equations to be solved.

The ninth field, F5.2, contains the integration parameter α.

The tenth field, I5, contains a zero if the input data is expressed in watt, deg. K, cm., units, the integer 1 if the units are Btu, deg. R, ft., hr., or the integer 2 if the units are Btu, deg. R, ft., min.

E. The last card is a blank card which, when read in place of a normal control card, causes the computer to proceed to read in data for the next problem.

The data cards just described are read as card images from magnetic tape.

A sample problem with an illustration of the input data is presented in Section VI of this Appendix.

B. Data Modification Procedure

A problem description on magnetic tape can be used to generate a new tape which contains a modified version of the data on the original tape. This procedure could be used, for example, in a case where the geometrical subdivision and heat-balance equations for two problems are similar, but the boundary condition or surface properties are different. (A problem can be modified by changing the punched data cards which were described above. However, the tape modification procedure minimizes the chances of error inherent in manipulating large numbers of data cards.)

The input data for the modification procedure involves coded instructions for controlling logical units and instructions for storing the original data with modifications on another tape. The form of the data cards for these instructions are presented in Table I-1, and the general arrangement of the input data is described below.

The general arrangement of the input data to instruct the computer on generating a data tape from a problem using an original data tape is as follows:

F. A card or series of cards commanding tape maneuvers required to start the data modification.

G. A heading card. This is an alphanumeric title card to be printed on each sheet of output for identification and description.

H. A series of cards containing numerical information describing the modifications to be made to the data on the original tape in generating the modified tape. The format for all these cards is the same; and in FORTRAN notation is I5, F20.9, F20.9, I5, I5, I5. A decimal point is customarily used in the two F-type fields to permit full flexibility. The first three fields contain information needed to solve the problem. The identification in the fourth field is the equation number, and the identification in the fifth field is a serial number within a set of cards describing an equation. The fifth field contains an integer which specifies the modification to be made.

I. A card with the integer 9 in column 60 follows the last correction card and instructs the computer to copy the remainder of the reference tape without modification.

J. A blank card.

K. One or more control cards as described in II-D above.

L. A card with instructions to rewind and end file on the generated tape.

TABLE I-1

CODED INSTRUCTIONS FOR DATA INSERTION AND MODIFICATION

Card Column						Operation Description	
1 5	25	45	50	55	60		
			A	B	1	Copy through Equation A, Card B without correction.	Instructions Referenced to Data Cards or Card Images on Tape
			A	B	2	Skip through Equation A, Card B.	
A	B	C	D	E	3	Insert this card which describes Equation D, Card E.	
A	B	C	D	E	4	Copy to Equation D, Card E and substitute this card for Equation D, Card E.	
			A	B	10	Multiply through Equation A, Card B by the terms on the following card.	
	a	b				a multiplies radiation term, b multiplies conduction term (Note: If a radiation or conduction term is to remain unchanged, a or b, respectively, must be 1.0.)	
			A	B	0	Begin to copy problem to be modified from Tape A to Tape B.	Instructions Referenced to Tape Drive Units
			A	B	5	Rewind Tape A and/or Tape B.	
			A	B	6	End of file on Tape A and/or B, then rewind same.	
			A	B	7	Copy problem from Tape A to Tape B without corrections. (If B = 0, skip problem on Tape A.)	
					8	End of copy program.	

M. A card with the integer 8 in column 60 signifying that the copying procedure is completed.

III. DATA CHECK PROCEDURES

It is a laborious task to set up all of the numerical coefficients used in the equations describing the heat-balance conditions in a complicated problem, so that errors may frequently arise. Many of these errors can be detected by checks based on the principles of reciprocity and the conservation of energy. In general, the rows and columns of the matrices of conductances and view areas should add up to zero. This will be so if the equations are written in full exactly as prescribed by the method outlined in Section I with all diagonal elements positive. While it would make no difference to the final answer if various equations were multiplied by different constants, such manipulation would make it impossible to use the column sums to check the input data.

To test the consistency of the input data, row and column sum checks are made on the matrices $\left\{A_{ij}\right\}$ and $\left\{C_{ij}\right\}$. The row sums

$$S_R = \sum_j A_{ij} - A_i \tag{I-7}$$

$$S_c = \sum_j C_{ij} \tag{I-8}$$

are calculated for all values of i and tested to be small in magnitude. Any sums over tolerance (10^{-5}) are printed out. Also, the column sums

$$_cS_R = \sum_i \pm A_{ij} - A_j \tag{I-9}$$

$$_cS_C = \sum_i \pm C_{ij} - C_j \tag{I-10}$$

are calculated for each value of j and tested to be small in magnitude. Any column sums over tolerance are also printed. The signs in the

summations of Equations (I-9) and (I-10) are the same as the signs of the diagonal elements, A_{ii} or C_{ii}.

Certain complications may arise. When any part of the system (e.g., a boundary) has a fixed, preassigned temperature T, the equation for this temperature is simply

$$\frac{dT}{dt} = 0$$

The conductances and view areas of the rest of the system to this part are omitted, but not conversely, so that non-zero column sums will occur. As long as all the omitted conductances and areas are known, however, the non-zero sums can be checked.

It is to be noted that the method of solving the difference equations corresponding to the differential equation (I-2) requires that a diagonal element be in every row of the matrix $\left\{|A_{ij}| + |C_{ij}|\right\}$, or if $\left\{A_{ij}\right\}$ and $\left\{C_{ij}\right\}$ have only zeros in a certain row, that the corresponding M_i be non-zero. The program checks to make sure that this requirement is satisfied and automatically omits the solution of the equations if the requirement is not satisfied.

The average power into each zone, $\overline{P_i}$, is also calculated and printed. In the case of periodically varying power inputs, the average power over a period is part of the input data, so that $\overline{P_i}$ can be automatically checked. The total average power input is also calculated and printed.

IV. METHOD OF SOLUTION

A. Integration Scheme

The basic energy Equation (I-2) may be integrated with respect to time from t to t + h where h is a small increment in time:

$$\sum_j C_{ij} \int_t^{t+h} T_j \, dt + \sum_j A_{ij} \sigma \int_t^{t+h} T_j^4 \, dt + \int_t^{t+h} P_i(t) \, dt$$

$$+ M_i T_i(t + h) - M_i T_i(t) = 0 \qquad \text{(I-11)}$$

Where P_i is a constant, the integral term appearing in Equation (I-11) is simply $h P_i$. Where P_i is a function of time, $P_i = P_i(t)$, the integral is evaluated using the Trapezoidal rule:

$$\int_t^{t+h} P_i(t)\, dt \approx \frac{h}{2} [P_i (t + h) + P_i(t)] \qquad \text{(I-12)}$$

where the values $P_i(t)$ are found from input data by linear interpolation. Note that where the time span t to t + h encompasses a step change in power level P_i, the integral is evaluated in parts on either side of the discontinuity.

In order to obtain approximate expressions for the integrals of T_j and T_j^4, we use the general linear two-point integration formula:

$$\int_t^{t+h} f(t)\, dt = h [(1 - \alpha) f(t) + \alpha f(t + h)] \qquad \text{(I-13)}$$

where f is a function of time and α is any number between zero and one. It can be shown that the quadrature given by Equation (I-13) is of order h^2--that is, the error in Equation (I-13) is proportional to h^2 as h approaches zero. Hence, the integration scheme is most accurate for small values of h.

The choice of the quantity α, which we call the integration parameter, influences the accuracy and stability of the numerical solution of the set of difference equations that has been derived.

Using the integration formula, the heat-balance equations become:

$$h\left\{\sum_j C_{ij} [(1 - \alpha)T_j(t) + \alpha T_j(t + h)] + \sum_j A_{ij}\, \alpha[(1 - \alpha)T_j^4(t) + \alpha T_j^4(t + h)]\right\}$$

$$+ \int_t^{t+h} P_i(t)\, dt + M_i [T_i(t + h) - T_i(t)] = 0 \qquad \text{(I-14)}$$

Equation (I-14) is one of a set of non-linear simultaneous difference equations. This set of equations can be solved for $T_i(t + h)$ when the values $T_i(t)$ are given.

1. Stability of Integration Scheme

In order to investigate the factors which determine the optimum value of the integration parameter α, we will compare solutions of Equation (I-14) with solutions of Equation (I-2). In order to present this analysis as simply as possible, we investigate the conductive cooling of a lumped thermal mass M with an initial temperature T_o connected by a conductance C to a sink at zero degrees. If the temperature is T at time t, Equation (I-2) becomes

$$CT + M \frac{dT}{dt} = 0 \qquad \text{(I-15)}$$

with exact solution

$$T = T_o \, d^{-t/\tau} \qquad \text{(I-16)}$$

where

$$\tau = \frac{M}{C} . \qquad \text{(I-17)}$$

The corresponding difference equation is

$$hC \, [(1 - \alpha) \, T(t) + \alpha T(t + h)] + M[T(t + h) - T(t)] = 0 \qquad \text{(I-18)}$$

The solution to Equation (I-18) is

$$T(nh) = T_o \left(\frac{1 - (1 - \alpha) \frac{h}{\tau}}{I + \alpha \frac{h}{\tau}} \right)^n \qquad \text{(I-19)}$$

The maximum discrepancy between the values of T calculated from (I-16) and (I-19) is dependent on α and the ratio h/τ as shown in Figures (I-1) and (I-2). The error is given as a percentage of T_o. The time at which the maximum error occurs is

$$t = h \quad \text{for} \quad h > \tau$$

$$t \doteq \tau \quad \text{for} \quad h < \tau$$

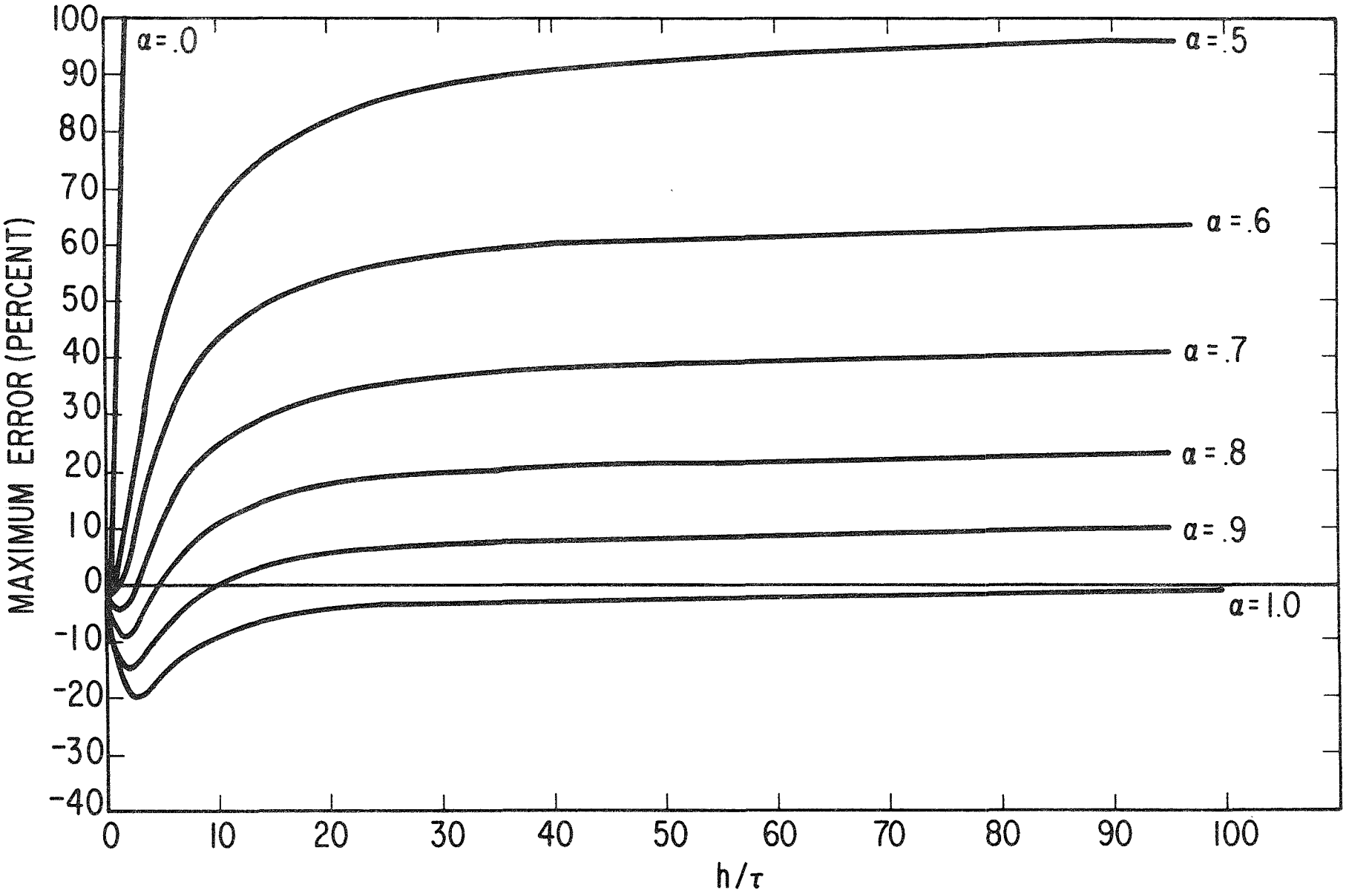

FIGURE I-1 MAXIMUM PERCENTAGE ERROR IN TEMPERATURE AS A FUNCTION OF THE RATIO OF TIME INCREMENT TO TIME CONSTANT FOR VARIOUS VALUES OF THE INTEGRATION PARAMETER α.

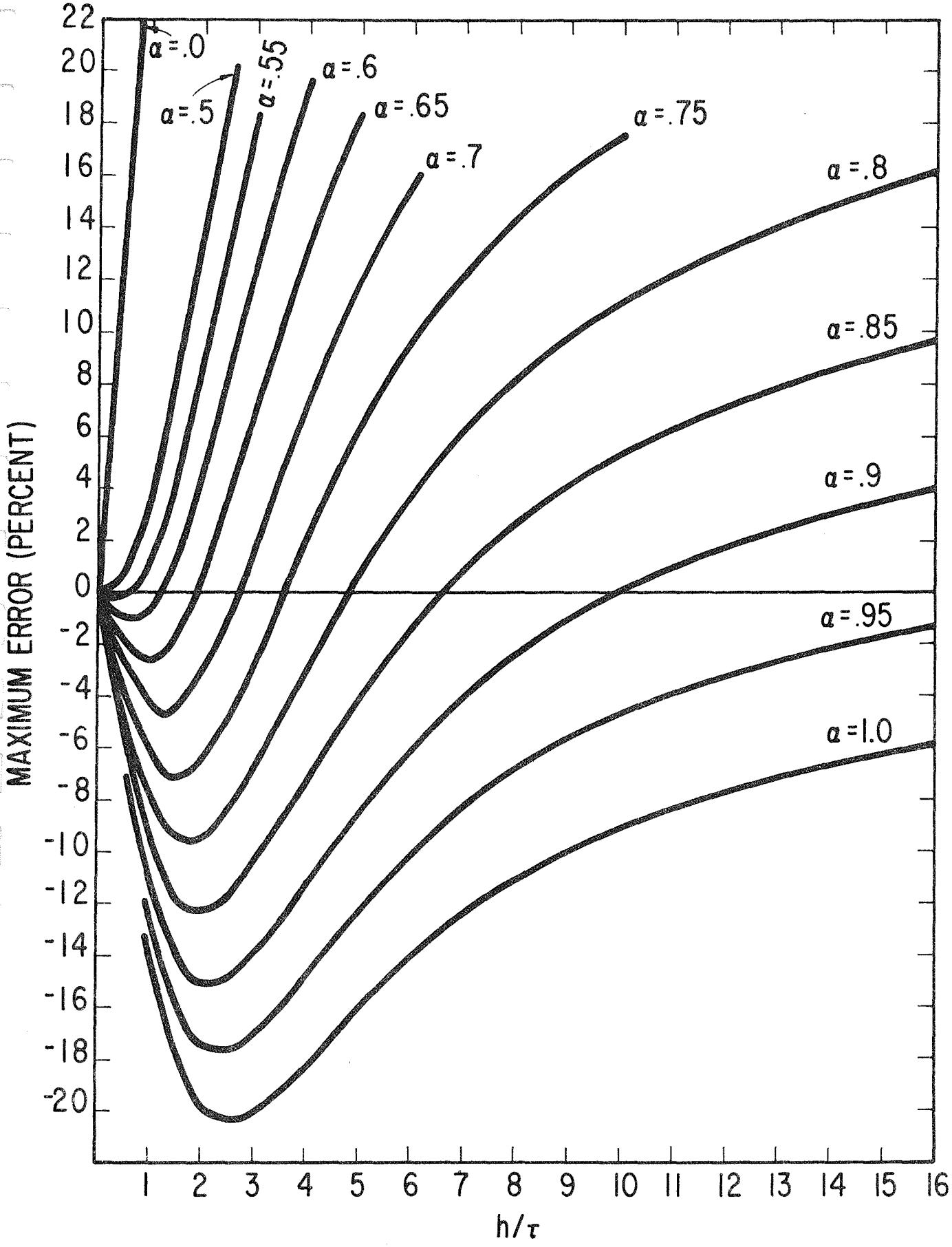

FIGURE I-2 DETAILS IN THE NEIGHBORHOOD OF THE ORIGIN OF FIGURE I-1

It will be seen From Equation (I-19) that if the quantity

$$\beta = \frac{1 - (1 - \alpha)\frac{h}{\tau}}{1 + \alpha \frac{h}{\tau}} \qquad \text{(I-20)}$$

becomes greater than unity in absolute value, the temperature T(nh) will tend to infinity instead of zero. This happens when

$$\frac{h}{\tau} > \frac{2}{1 - 2\alpha}, \quad \alpha < \frac{1}{2} \qquad \text{(I-21)}$$

and never for $\alpha > \frac{1}{2}$. Thus, values of α greater than $\frac{1}{2}$ always lead to stable solutions.

2. Selection of the Integration Parameter

In order to simplify the discussion of problems involving many zones, we assume the terms in T_j^4 can be linearized. Then the entire set of differential equations (I-2) can be written in matrix notation as

$$CT + P + M\frac{dT}{dt} = -R \qquad \text{(I-22)}$$

where

C - matrix of conductance, including radiative conductances
T - vector whose elements are the nodal temperatures
M - diagonal matrix of the thermal masses
P - vector whose elements are the power inputs
R - vector of the radiation powers which are the constant terms obtained in the linearization process.

The solution to Equation (I-22) is

$$T = F\,E + G(t) \qquad \text{(I-23)}$$

where

F - matrix of constants depending on the initial conditions
E - vector whose components are e^{-t/τ_k}
G - vector representing the particular integral
τ_k - time constant

The time constants τ_k are found by setting the determinant of the matrix $C - \frac{1}{\tau} M$ equal to zero

$$\left|C - \frac{1}{\tau} M\right| = 0 \ . \tag{I-24}$$

The finite-difference equation corresponding to Equation (I-22) is

$$hC\ [(1 - \alpha)\ T(t) + \alpha T(t + h)] + \int_{t}^{t+h} P\ dt$$

$$+ M\ [T(t + h) - T(t)] = -hR \tag{I-25}$$

The solution to Equation (I-25) is

$$T = F\ B + H\ (t) \ . \tag{I-26}$$

where

F - the same matrix introduced in Equation (I-23)

B - vector with components $(\beta_k)^n$

H - vector representing the particular sum.

The quantities β_k are found by solving the equation

$$\left|C - \frac{1 - \beta}{h\ (1 - \alpha + \alpha\beta)} M\right| = 0 \tag{I-27}$$

Comparison of Equations (I-27) and (I-24) shows that

$$\frac{1}{\tau_k} = \frac{1 - \beta_k}{h\ (1 - \alpha + \alpha\beta_k)} \tag{I-28}$$

or

$$\beta_k = \frac{1 - (1 - \alpha)\ \frac{h}{\tau_k}}{1 + \alpha\ \frac{h}{\tau_k}} \tag{I-29}$$

If the quantities $\frac{h}{\tau_k}$ vary over a wide range, then it may be seen from Figure (I-1) that a value of α of about 0.87 minimizes the maximum percentage discrepancy between e^{-nh/τ_k} and $(\beta_k)^n$ over all values of $\frac{h}{\tau_k}$. If the quantities $\frac{h}{\tau_k}$ vary over a small range, however, a smaller value

of α gives the minimum error. Figure (I-3) shows the optimum value of α as a function of the maximum $\frac{h}{\tau_k}$. In practice, one often finds the optimum value of α by numerical experimentation.

3. Selection of the Time Increment

It is shown in Fig. (I-1) that the error introduced by the quadrature in time is reduced by making $\frac{h}{\tau}$ small. However, the time increment h must not be made too small because if a small error ε is made at each step in solving the difference equations for $T(t + h)$, this error may be highly magnified in succeeding steps. To show this most simply, we revert to the case of a single lumped mass. After we introduce the error ε, Equation (I-19) becomes

$$\begin{aligned} T(h) &= T_o\beta + \varepsilon \\ T(2h) &= T_o\beta^2 + (1 + \beta)\varepsilon \\ T(nh) &\doteq T_o\beta^n + \frac{\varepsilon}{1 - \beta} \end{aligned} \qquad \text{(I-30)}$$

We now substitute for β from Equation (I-20) and find

$$T(nh) = T_o\beta^n + (\frac{\tau}{h} + \alpha)\varepsilon \qquad \text{(I-31)}$$

It is seen from Equation (I-31) that a correlated error will be magnified by the factor $(\frac{\tau}{h} + \alpha)$ which will be large if $\frac{h}{\tau}$ is small. A generalization of the argument shows that magnification factors $(\frac{\tau_k}{h} + \alpha)$ occur in multizone problems.

B. Solution of Integral Form of Heat-Balance Equations

For values of the integration factor α greater than zero, Equation (I-14) represents a set of implicit non-linear simultaneous equations. At each time increment, the simultaneous heat-balance equations are solved by a Gauss-Seidel procedure using the Newton-Raphson Iteration Method to solve for the individual nodal temperatures.

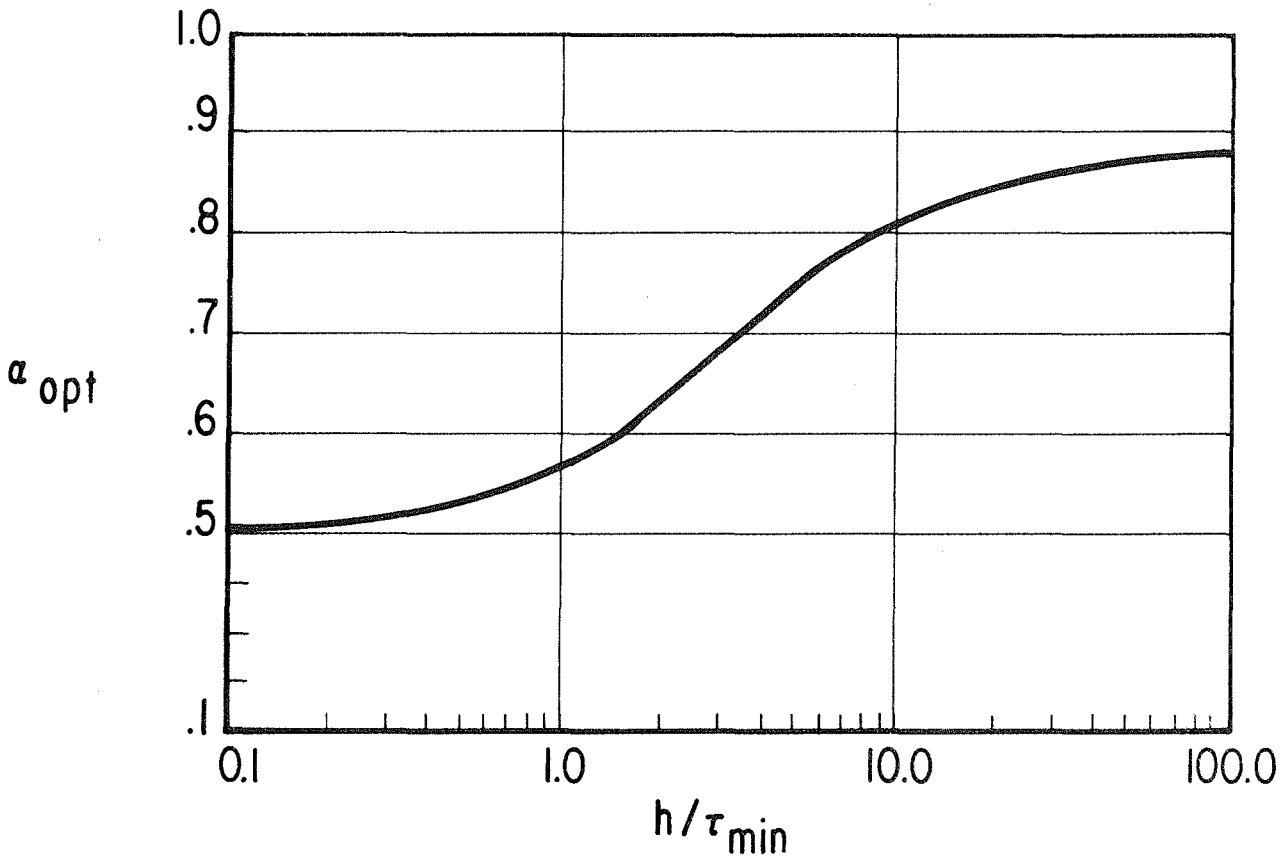

FIGURE I-3 THE OPTIMUM VALUE OF THE INTEGRATION PARAMETER AS A FUNCTION OF THE RATIO OF TIME INCREMENT TO SMALLEST TIME CONSTANT

The ordinary differential equations (I-1) can be solved only when starting temperatures $T_i(0)$ are given. In certain equations, however, the quantity M_i may be zero and the starting temperature unknown. In that case, the corresponding value of $T_i(0)$ must be calculated so that Equation (I-2) is satisfied initially as well as at all succeeding times. The program automatically carries out this calculation before proceeding with the main computation. During the iterative solution for the initial temperature of nodes with zero thermal mass, the sum of the residual errors is printed out after every 50 passes through the set of equations.

While the Gauss-Seidel procedure used to solve the difference Equation (I-14) is well known, it will be briefly described here for the sake of completeness.

To begin the process, the values of $T_i(t)$ are used as a starting approximation to $T_i(t + h)$. New approximations are obtained using the Newton-Raphson Iteration Method to solve:

$$A\, T_i(t + h) + B\, T_i^4(t + h) + C = F\,(T_i) = 0 \qquad \text{(I-32)}$$

where

$$A = M_i + h\, \alpha\, C_{ii} \qquad \text{(I-33a)}$$

$$B = h\, \alpha\, A_{ii}\, \sigma \qquad \text{(I-33b)}$$

$$\begin{aligned} C = {} & h \sum_{j \neq i} C_{ij}\, [(1 - \alpha)\, T_j(t) + \alpha T_j(t + h)] \\ & + h \sum_{j \neq i} A_{ij}\, \sigma\, [(1 - \alpha)\, T_j^4(t) + \alpha T_j^4(t + h)] \\ & + h\, C_{ii}\, (1 - \alpha)\, T_i(t) + h\, A_{ii}\, \sigma\, (1 - \alpha)\, T_i^4(t) \\ & - M_i\, T_i(t) + \int_t^{t + h} P_i(t)\, dt \end{aligned} \qquad \text{(I-33c)}$$

According to the Newton-Raphson procedure, the new value T_i $(t + h)$ is found from:

$$T_i(t + h) - \frac{F\ (T_i)}{F'\ (T_i)} \rightarrow T_i\ (t + h) \qquad \text{(I-34)}$$

where

$$F'\ (T_i) = A + 4\ BT_i^{\ 3}\ (t + h) \qquad \text{(I-35)}$$

This process continues until the solution to Equation (I-32) converges to within 10^{-5}. If the solution to Equation (I-32) is not found within 50 iterations, an error message is printed out:

CHECK YOUR DATA FOR EQUATION NO. i

and the solution is terminated.

When the root to Equation (I-32), $T_i^{\ *}\ (t + h)$, has been found, the old value of $T_i\ (t + h)$ is replaced by:

$$T_i'\ (t + h) = T_i(t + h) + \rho\ [T_i^{\ *}(t + h) - T_i(t + h)] \qquad \text{(I-36)}$$

where ρ is a relaxation factor, and the next equation is set up and solved. The relaxation factor ρ is used to accelerate the solution of the simultaneous equations. At the end of one pass through the set of simultaneous equations (say iteration n), a residual error term is calculated:

$$\varepsilon_n = \sum_i \left| T_i'\ (t + h) - T_i(t + h) \right| . \qquad \text{(I-37)}$$

This error term is compared with some tolerance value specified on the data control cards; if the residual error is larger than the tolerance, the process is repeated.

A further check is made at the end of each pass through the set of heat-balance equations to determine if the solution is convergent.

The residual error at iteration step n is compared with that at the previous time step. If the difference $\varepsilon_n - \varepsilon_{n-1}$ is positive, the method is considered divergent, and the solution is terminated, and the next control card is processed.

In principle, an optimum value of relaxation factor ρ exists for each problem. However, this value is generally not known ahead of time; in practice, one simply makes use of the fact that an optimum exists, and the best value of ρ is found by numerical experiments.

V. ENERGY BALANCES

At each time step in the program, an overall energy balance is made to allow an evaluation of the accuracy of the solution.

From the integral form of Equation (I-6), a quantity $E_s(t)$ called the System Energy Imbalance is defined:

$$E_s(t) = \sum_i M_i T_i(0) - \sum_i M_i T_i(t) - \sum_i \int_0^t P_i(t)\, dt - \sum_i \int_0^t A_i \sigma T_i^4\, dt - \sum_i \int_0^t C_i T_i\, dt \quad . \tag{I-38}$$

The current value of E_s is found from the value at the previous time step and the two-point integration formula (I-13):

$$E_s(t+h) = E_s(t) + \sum_i M_i [T_i(t) - T_i(t+h)] - \sum_i \int_t^{t+h} P_i(t)\, dt - \sum_i \int_t^{t+h} A_i \sigma T_i^4(t)\, dt - \sum_i \int_t^{t+h} C_i T_i(t)\, dt \quad . \tag{I-39}$$

If the computation were perfectly accurate, E_s should be zero at all times. In practice, of course, one requires that E_s be small. Other quantities, such as:

STORED INTERNAL ENERGY:

$$E_p = \sum_i M_i T_i(t) \qquad \text{(I-40)}$$

TOTAL ENERGY INTO SYSTEM:

$$E_{in} = \sum_i \int_0^t P_i \, dt \quad , \qquad \text{(I-41)}$$

are also printed in order to provide numbers that can be compared with E_s. The quantity E_p also serves to indicate when a system has reached the end of a transient, and E_{in} is to be used to check that the input power is correctly computed.

VI. SAMPLE PROBLEMS

A sample problem is presented to illustrate the procedure for coding the input data for ADLGTA. For the purpose of this illustration, the finite-difference thermal models are formulated using the Zone Method of Strong and Emslie.* The conventional nodal or lumped parameter finite-difference technique can also be used to formulate problems for solution with ADLGTA.

Consider the thermal model of a tubular support shown in the following figure. The support of length, ℓ, and cross-sectional area, A, is positioned between a high-temperature source at 520R and a sink at 37R. The temperature distribution is steady in time and varies spacially only in the longitudinal direction. The inner surface is

---

* P. F. Strong and A. G. Emslie, "The Method of Zones for the Calculation of Temperature Distribution," ASME Paper 65-WA/HT-47.

adiabatic; heat is radiated from the outer surface, to a zero temperature environment; and the support is subdivided into three zones of equal length, ℓ. ε is the total hemispherical emittance of the outer surface of the tubular support.

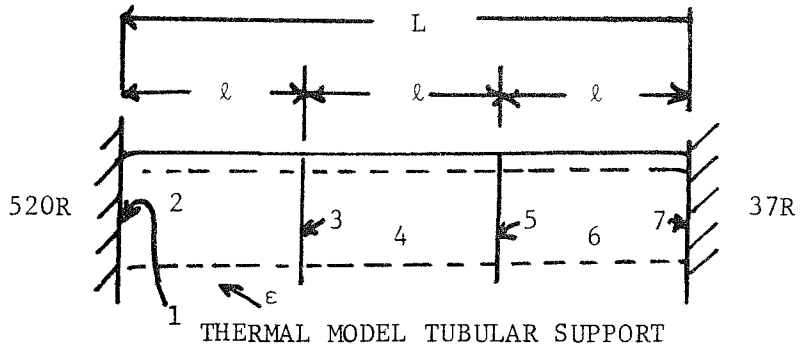

THERMAL MODEL TUBULAR SUPPORT

The temperature subscripts noted in the above figure represent the mean zone temperatures (T_2, T_4, and T_6) and the temperature of the zone boundaries (T_1, T_3, T_5 and T_7).

The following equations, which describe the heat flow and the boundary conditions, can be written according to the Zone Method:

$$\frac{dT_1}{dt} = 0;\ T_1 = 520 \qquad \text{(I-42)}$$

$$\frac{KA}{\ell}(12T_2 - 6T_1 - 6T_3) + \pi D\ell\varepsilon\sigma T_2^4 = 0 \qquad \text{(I-43)}$$

$$\frac{KA}{\ell}(6T_2 - 4T_3 - 2T_1) + \frac{KA}{\ell}(6T_4 - 4T_3 - 2T_5) = 0 \qquad \text{(I-44)}$$

$$\frac{KA}{\ell}(12T_4 - 6T_3 - 6T_5) + \pi D\ell\varepsilon\sigma T_4^4 = 0 \qquad \text{(I-45)}$$

$$\frac{KA}{\ell}(6T_6 - 4T_5 - 2T_3) + \frac{KA}{\ell}(6T_6 - 4T_5 - 2T_7) = 0 \qquad \text{(I-46)}$$

$$\frac{KA}{\ell}(12T_6 - 6T_5 - 6T_7) + \pi D\ell\varepsilon\sigma T_6^4 = 0 \qquad \text{(I-47)}$$

$$\frac{dT_7}{dt} = 0;\ T_7 = 37 \qquad \text{(I-48)}$$

Equations (I-43), (I-45) and (I-47) are the heat-balance equations for the mean zone temperatures; Equations (I-44) and (I-46) are joining equations necessary to describe the fluxes at the boundaries. The temperatures of boundaries 1 and 7 are constant and are specified in the statement of the problem.

For the sample problem, we assume $KA/\ell = 0.02$ Btu/hr °R and $\pi D\ell\varepsilon = 0.04$ ft^2. The data for the above equations, in the form required by the program, are given in Table I-2.

The data on the first cards (A_i, C_i) for the sets describing the equations were determined by considering the following equation, which describes the net flux out of the system:

$$Q_{OUT} = 0.02 \left(6T_2 - 4T_1 - 2T_3\right) + 0.04 \left(\sigma T_2^4 + \sigma T_4^4 + \sigma T_6^4\right)$$

$$+ 0.02 \left(6T_6 - 4T_7 - 2T_5\right)$$

The output for the sample problem is shown in Table I-3.

VII. OUTPUT DATA

Table I-3 shows the output data for the sample problem discussed in the preceding Section. The bulk of the output consists of the time histories of the various temperatures. One page is printed off-line for each time interval specified on the control card. It consists of three lines of heading followed by pairs of index numbers and temperatures up to the highest number specified by the control card.

The first heading line is simply the alphanumeric heading information supplied on the heading card of input. The second line gives the contents of the last control card read. The third line shows the values of time, E_p, E_S, and E_{in} as defined in Equations (I-40), (I-38), and (I-41), respectively, as well as the total number of iterations used in solving the systems of equations since the last off-line print.

TABLE I-2

INPUT DATA FOR SAMPLE PROBLEM

Card column

```
    5                   25                  45      50    55    60
                                                    5     9     7
SAMPLE PROBLEM
  1   0.0                   -0.08                   1     1
 -1   1.0                   520.0                   1    99
  2   0.04                  0.12                    2     1
  2   0.04                  0.24                    2     2
  1   0.0                   -0.12                   2     3
  3   0.0                   -0.12                   2     4
 -2   0.0                   0.0                     2    99
  3   0.0                   -0.04                   3     1
  2   0.0                   0.12                    3     2
  3   0.0                   -0.08                   3     3
  1   0.0                   -0.04                   3     4
  4   0.0                   0.12                    3     5
  3   0.0                   -0.08                   3     6
  5   0.0                   -0.04                   3     7
 -3   0.0                   0.0                     3    99
  4   0.04                  0.0                     4     1
  4   0.04                  0.24                    4     2
  3   0.0                   -0.12                   4     3
  5   0.0                   -0.12                   4     4
 -4   0.0                   0.0                     4    99
  5   0.0                   -0.04                   5     1
  4   0.0                   0.12                    5     2
  5   0.0                   -0.08                   5     3
  3   0.0                   -0.04                   5     4
  6   0.0                   0.12                    5     5
  5   0.0                   -0.08                   5     6
  7   0.0                   -0.04                   5     7
 -5   0.0                   0.0                     5    99
  6   0.04                  0.12                    6     1
  6   0.04                  0.24                    6     2
  5   0.0                   -0.12                   6     3
  7   0.0                   -0.12                   6     4
 -6   0.0                   0.0                     6    99
  7   0.0                   -0.08                   7     1
 -7   1.0                   37.0                    7    99

1.5      0.9E-02  1.0          1   10  1.0          300.0      7  1.0    1
                                                          9     6
                                                                8
```

TABLE I-3

OUTPUT DATA FOR SAMPLE PROBLEM

```
   SAMPLE PROBLEM
TEMPERATURE MEASURED IN DEGREES RANKINE,POWER IN BTU/HR
REL= 1.50  TOL= 9.0E-03  DT=     1.0  WF=   1  PF=  10  TIMX=      1.0  TB=  300.0  SIZE=   7  ALPHA= 1.00
 T1 =     1.00   EP = 5.57000000E+02   ES =-7.6120<E-05  EIN = 0.            NT=     1
   1  520.0000    2  411.7004    3  319.8040    4  246.4164    5  175.1346    6  100.0312    7   37.0000
AVERAGE TIME FOR ONE PASS THROUGH ENTIRE SET OF EQUATIONS IS     .01600 SECONDS
TIME PER REL TOL CARD =     .06000 SECONDS
          ELAPSED TIME IN TTA SOLUTION =          .064SECONDS
          TOTAL ELAPSED TIME IN TTA SOLUTION =    1.481 SECONDS
                              CHECKOUT =          .144SECONDS
                              SOLUTION =          .064SECONDS
```

Before the solution to the problem is printed, information about the input data is recorded. The off-line print consists of:

1. The heading;
2. The total average power for each equation (unless zero);
3. The equation number and sum of the elements of any rows whose sum is over tolerance. As shown in Equations (I-7) and (I-8), S_R is used to denote the sum of radiation terms and S_C is used to denote the sum of conduction terms;
4. A line of print which gives the number of equations read in, N_E, the number of row sum failures, N_R and N_C, for radiation and conduction, respectively, the number N_P, of periodic powers with incorrect average level, and P_T, the total average power to the system;
5. The column number and the sum of the elements of any columns whose sum is over tolerance. As shown in Equations (I-9) and (I-10), ${}_CS_R$ is used to denote the sum of radiation terms, and ${}_CS_C$ is used to denote the sum of conduction terms; and
6. A line of print giving N_{CSC} and N_{CSR}, which are the numbers of column sum failures for conduction and radiation, respectively.

ADLGTA uses logical unit numbers 5, 6, 7, 8 and 9. Logical units 5 and 6 are the system input and output units, respectively. The file output on unit 6 contains the computed solution. Logical units 7, 8 and 9 are used as scratch tapes; the final form of the data describing the problem solved by ADLGTA is ordinarily contained in the file of logical unit 9.

APPENDIX II

SAMPLE LISTING OF COMPUTER MODEL OF PROBE LOCATION 3 FOR MODE 3 OPERATION IN LUNAR ENVIRONMENT

This Appendix contains a complete computer listing of a typical computer model of the lunar heat flow probe in the lunar environment. The following tabulation indicates the descriptions appropriate to the eight computer models that were developed as a part of the subject work:

Experiment Location	Conductivity Experiment
1	Mode 2
2	Mode 2
3	Mode 2
4	Mode 2
1	Mode 3
2	Mode 3
3	Mode 3
4	Mode 3

The model shown was developed for Mode 3 operation at location 3 of the probe assuming an initial temperature of 225°K, and a lunar medium conductivity of k = 0.0017 w/cm-°K and density - specific heat product of ρc = 1.339 w-sec/°K. The identification numbers of the major components in the model are listed in Table II-1.

Table II-2 is a listing of the input data describing the model. The format of the input data has been discussed in Appendix I.

The units for the input data are:

Radiative couplings:	A_{ij} = cm^2
Conductive couplings:	C_{ij} = w/°K
Power:	P_i = w
Thermal mass:	M_i = w-min/°K.

TABLE II-1

IDENTIFICATION NUMBERS OF
MAJOR COMPONENTS IN THERMAL MODEL

Components	Identification Number	Refer to
Gradient Sensor	13	Figure 7
Ring Sensor	50	Figure 8
Heater	19	Figure 7
Probe Details	Remaining Nodes Between 1-121	Figure 6
Drill Casing	Zone: 141, 181, ..., 701 Boundaries: 123, 163, ..., 723	Figure 11 and Table II
Lunar Medium	Remaining Nodes Between 122-732	Figures 11 and 12 and Table I

TABLE II-2

COMPUTER LISTING OF EXPERIMENT LOCATION 3

FOR MODE 3 OPERATION IN THE LUNAR ENVIRONMENT

```
LOC 3 MODE 3  K=.0017   T=225K  RHOC=1.339  LUNAR MEDIUM
   1          0.000000000           0.000000000     1    1
   3          0.000000000            .028440000     1    2
   1         -1.695060300           -.018960000     1    3
   5          0.000000000           -.009480000     1    4
 501   1.695060300                                  1    5
   3                          0.06188               1    9
   1                         -0.04125               1   10
   5                          -0.02063              1   11
  99                          0.01056               1   12
   1                         -0.00839               1   13
  12                         -0.00352               1   14
 115                          0.00203               1   15
 116                         -0.00068               1   16
  -1                                                1   99
   2   0.0                                          2    1
   3                          0.13554               2    2
   2  -0.334                  -0.08217              2    3
   4                          -0.05337              2    4
  13   0.112                                        2    5
  24   0.013                                        2    6
  29   0.010                                        2    7
  72   0.009                                        2    8
  99   0.19                                         2    9
  -2                                                2   99
   3                                                3    1
   3                          0.48210               3    2
   1                         -0.02844               3    3
   2                         -0.16123               3    4
   4                         -0.26399               3    5
   5                         -0.02844               3    6
   3                          0.12376               3    7
   1                         -0.06188               3    8
   5                        -0.06188                3    9
  -3   0.05106                                      3   99
   4   0.0                                          4    1
   3                          0.28968               4    2
   4         -6.308845170            -.210420000    4    3
   2          0.000000000            -.079060000    4    4
 461   5.164410117                                  4    5
 501   1.164744                                     4    6
  -4                                                4   99
   5                                                5    1
   3                          0.02844               5    2
   5  -1.10236                -0.03648              5    3
   1                          -0.00948              5    4
   6                           0.02628              5    5
  19                          -0.00876              5    6
  10   1.10236                                      5    7
   3                          0.06188               5    8
   5                         -0.04125               5    9
   1                         -0.02063               5   10
  -5                                                5   99
   6                                                6    1
   6                          1.28706               6    2
   5                         -0.02628               6    3
  19                         -0.02628               6    4
   8                         -0.58391               6    5
  35                         -0.65059               6    6
  -6   0.01178                                      6   99
   7                                                7    1
  34                          0.01788               7    2
   7                         -0.01192               7    3
  33                         -0.00596               7    4
  18                          0.00264               7    5
   7                         -0.00176               7    6
  17                         -0.00088               7    7
  -7                                                7   99
   8                                                8    1
   6                          0.56724               8    2
   8  -0.10294               -0.40777              8    3
  35                         -0.19674               8    4
  10                          0.05124               8    5
  12                         -0.01397               8    6
  12   0.10294                                      8    7
  -8                                                8   99
   9   0.0                                          9    1
  34                          1.20654               9    2
   9         -3.440338440            -.813060000    9    3
  35          0.000000000            -.393480000    9    4
 461   3.440338444                                  9    5
  -9                                                9   99
  10                                               10    1
  10   1.19893                0.07512              10    2
   8                         -0.04668              10    3
  12                         -0.02844              10    4
  12  -0.09357                                      10    5
   5  -1.10236                                      10    6
 -10   0.00452                                      10   99
  12                                               12    1
  13                          0.39902              12    2
  12  -0.10651                -0.26601              12    3
  14                          -0.13301              12    4
  10   0.09357                                      12    6
   8   0.10294                                      12    7
  99                                    0.01056     12    8
  12                                   -0.00704     12    9
   1                         -0.00352               12   10
 110                          0.00168               12   11
  12                         -0.00112               12   12
  24                         -0.00056               12   13
  10                          0.02388               12   14
  12                         -0.01447               12   15
   8                         -0.00941               12   16
 -12                                                12   99
  13                                                13    1
  13   0.66913                0.79804              13    2
  12                         -0.39902              13    3
  14                         -0.39902              13    4
  19  -0.66913                                      13    5
  13   0.191                                        13    6
   2  -0.112                                        13    7
  24  -0.092                                        13    8
  26  -0.001                                        13    9
  29  -0.024                                        13   10
  72  -0.022                                        13   11
 -13   0.05833                                      13   99
  14                                                14    1
  13                          0.39902              14    2
  14  -0.02873                -0.45597              14    3
```

```
 12                          -0.13301                    14    4
 24                           0.28495                    14    5
 26                          -0.09499                    14    6
 32  0.02573                                             14    7
-14                                                      14   99
 17                                                      17    1
 37                           0.01788                    17    2
 17                          -0.01192                    17    3
 38                          -0.00596                    17    4
 18                           0.00264                    17    5
 17                          -0.00176                    17    6
  7                          -0.00088                    17    7
-17                                                      17   99
 18  0.0                                                 18    1
 18  7.96270                  0.00528                    18    2
  7                          -0.00264                    18    3
 19  -3.78118                                            18    4
421  -4.14152n                                           18    5
 17                          -0.00264                    18    6
-18  0.01691                                             18   99
 19                                                      19    1
  6                          -0.02628                    19    6
  5                           0.00876                    19    7
 20                          -0.02628                    19    8
 21                           0.00876                    19    9
 19                           0.03504                    19   10
 19  11.78349                                            19   11
 13  -n.66913                                            19   12
 18 -3.78118                                             19   13
421  -7.3n3180                                           19   14
  0                                -0.5                  19   15
-19  0.01418                                             19   99
 20                                                      20    1
 20                           1.28706                    20    2
 19                          -0.02628                    20    3
 21                          -0.02628                    20    4
 32                          -0.58391                    20    5
 36                          -0.65059                    20    6
-20  0.01178                                             20   99
 21                                                      21    1
 20                           0.02628                    21    2
 21                          -0.02812                    21    3
 19                          -0.00876                    21    4
 27                           0.01590                    21    5
 28                          -0.00530                    21    6
 21                               -0.5                   21    7
 24                                0.5                   21    8
-21                                                      21   99
 22  0.0                                                 22    1
 37                           1.20654                    22    2
 22        -3.4403384440                 -.8130600000    22    3
 36         0.0000000000                 -.3934A0000     22    4
381   3.44033A44                                        22    5
-22                                                      22   99
 24                                                      24    1
 24                                0.5699                24    2
 14                               -0.28495               24    3
 26                                -0.28495              24    4
 24  1.81981                                             24    5
  2  -0.013                                              24    6
 13  -0.042                                              24    7
 29  -0.039                                              24    8
 72  -0.036                                              24    9
 27  -1.69781                                            24   10
 24  -0.0020                                             24   11
 24                                     1.0              24   12
 32                               -0.5                   24   13
 21                                -0.5                  24   14
 12                           0.00056                    24   15
110                          -0.0016A                    24   16
 24                           0.00112                    24   17
 88         0.0000000000                  .000A898B9     24   1A
 9A         0.0000000000                 -.002A638B9     24   19
 24         0.0000000000                  .001774000     24   20
-24   0.0845                                            24   99
 26                                                      26    1
 24                           0.28495                    26    2
 26 -1.361                   -0.18996                    26    3
 14                          -0.09499                    26    4
 13  0.001                                               26    5
 24   0.002                                              26    6
 29  0.003                                               26    7
 72  0.339                                               26    8
 87  0.114                                               26    9
 65  0.002                                               26   10
 26                          -0.00136                    26   11
 88                           0.00136                    26   12
-26                                                      26   99
 27  0.0                                                 27    1
 27  4.67404                  0.03180                    27    2
 21                          -0.01590                    27    3
 28                          -0.01590                    27    4
 24  -1.69781                                            27    5
381  -2.978230                                           27    6
-27  0.00716                                             27   99
 28                                                      28    1
 27                           0.01590                    28    2
 28                          -0.01352                    28    3
 21                          -0.00530                    28    4
 29                           0.00438                    28    5
 75                          -0.00146                    28    6
-28                                                      28   99
 29  0.0                                                 29    1
 29  3.84437                  0.00876                    29    2
 28                          -0.00438                    29    3
 75                          -0.00438                    29    4
 29  1.972                                               29    5
  2 -0.010                                               29    6
 13 -0.024                                               29    7
 24  -0.019                                              29    8
 26 -0.901                                               29    9
 72 -0.928                                               29   10
 87 -0.067                                               29   11
 65 -0.001                                               29   12
381  -2.048998                                           29   13
 29   0.83                                               29   14
 98 -0.83                                                29   16
341  -1.787372                                           29   17
-29  0.00372                                             29   99
 32                                                      32    1
 20                           0.56724                    32    2
 32  -0.02573                -0.37050                    32    3
 36                          -0.19674                    32    4
 14  0.02573                                             32    5
 32                                    -0.5              32    6
 24                                0.5                   32    7
-32  0.00815                                             32   99
 33                                                      33    1
 34                           0.01788                    33    2
 33         -.4102685510                  -.0119200000    33    3
  7          0.0000000000                 -.0059600000    33    4
501   0.410269                                          33    5
```

```
-33                                                                  33   99
 34                                                                  34    1
 34                          2.34912                                 34    2
 33                         -0.01788                                 34    3
  7                         -0.01788                                 34    4
  9                         -1.18998                                 34    5
 35                         -1.12338                                 34    6
-34  0.00803                                                         34   99
 35                                                                  35    1
  6                          0.66726                                 35    2
  8                         -0.21341                                 35    3
 34                          1.10682                                 35    4
  9                         -0.37692                                 35    5
 35                         -1.18375                                 35    6
-35                                                                  35   99
 36                                                                  36    1
 20                          0.66726                                 36    2
 32                         -0.21341                                 36    3
 37                          1.10682                                 36    4
 22                         -0.37692                                 36    5
 36                         -1.18375                                 36    6
-36                                                                  36   99
 37                                                                  37    1
 37                          2.34912                                 37    2
 17                         -0.01788                                 37    3
 38                         -0.01788                                 37    4
 22                         -1.18998                                 37    5
 36                         -1.12338                                 37    6
-37  0.00803                                                         37   99
 38                                                                  38    1
 37                          0.01788                                 38    2
 38         -.4102685 10                  -.011920000               38    3
 17          0.000000000                  -.005960000               38    4
381  0.410269                                                        38    5
-38                                                                  38   99
 50  0.0                                                             50    1
181 -0.248818                                                        50    2
 56 -1.39446                                                         50    3
 51   -0.1857                 0.0                                    50    4
 61   -2.1662                 0.0                                    50    5
 51                          -0.0032466                              50    6
 50                           0.0021644                              50    7
 52                           0.0010822                              50    8
 50  6.98178                                                         50    9
221 -2.89724                                                         50   10
 50                           0.01                                   50   11
 52                          -0.01                                   50   12
-50    0.02442                0.0                                    50   99
 51    0.0                    0.0                                    51    1
 51    4.2589                                                        51    2
 50   -0.1857                                                        51    3
 61   -4.0732                                                        51    4
 51                           0.0064932                              51    5
 50                          -0.0032466                              51    6
 52                          -0.0032466                              51    7
-51  0.009421                                                        51   99
 52    0.0                    0.0                                    52    1
 51                           0.0032466                              52    2
 52                          -0.0021644                              52    3
 50                          -0.0010822                              52    4
 53                           0.0179580                              52    5
 52                          -0.0119720                              52    6
 54                          -0.0059860                              52    7
 41                           0.0053640                              52    8
 52                          -0.0035760                              52    9
 55                          -0.0017880                              52   10
 56                           0.0034908                              52   11
 52                          -0.0023272                              52   12
 55                          -0.0011636                              52   13
 53                           0.00432                                52   14
 52                          -0.00288                                52   15
 54                          -0.00144                                52   16
 52                          -0.01                                   52   17
 50                           0.01                                   52   18
-52    0.0                    0.0                                    52   99
 53    0.0                    0.0                                    53    1
 53  8.89453                                                         53    2
181 -8.89453                                                         53    3
 53                           0.0359160                              53    4
 52                          -0.0179580                              53    5
 54                          -0.0179580                              53    6
 53                           0.00864                                53    7
 52                          -0.00432                                53    8
 54                          -0.00432                                53    9
 53              7.039                                               53   16
 53             -5.026                                               53   17
 57              -.032                                               53   18
 59              -.596                                               53   19
 61              -.849                                               53   20
 64              -.285                                               53   21
 69              -.050                                               53   22
 73              -.161                                               53   23
-53  0.04492                                                         53   99
 54    0.0                    0.0                                    54    1
 53                           0.0179580                              54    2
 54                          -0.0119720                              54    3
 52                          -0.0059860                              54    4
 59                           0.0141000                              54    5
 56                          -0.0094000                              54    6
 60                          -0.0047000                              54    7
 53                           0.00432                                54    8
 54                          -0.00288                                54    9
 52                          -0.00144                                54   10
 54                          -0.000682                               54   11
 73                           0.000682                               54   12
-54    0.0                    0.0                                    54   99
 55    0.0                    0.0                                    55    1
 56                           0.0034908                              55    2
 55                          -0.0023272                              55    3
 52                          -0.0011636                              55    4
 57                           0.0088600                              55    5
 55                          -0.0059040                              55    6
 58                          -0.0029520                              55    7
 61                           0.0053640                              55    8
 55                          -0.0035760                              55    9
 52                          -0.0017880                              55   10
-55    0.0                    0.0                                    55   99
 56    0.0                    0.0                                    56    1
 56  4.39036                                                         56    2
181 -0.248730                                                        56    3
 50 -1.38466                                                         56    4
 56                           0.0069816                              56    5
 55                          -0.0034908                              56    6
 52                          -0.0034908                              56    7
221 -2.68717                                                         56    8
-56    0.00424                0.0                                    56   99
 57    0.0                    0.0                                    57    1
 57  8.11404                                                         57    2
261 -5.043070                                                        57    3
 57                           0.017712                               57    4
 55                          -0.008856                               57    5
 58                          -0.008856                               57    6
```

```
221  -3.022970                                                    57   7
 57                6.636                                         57  16
 53                -.032                                         57  17
 57               -4.739                                         57  18
 61                -.888                                         57  19
 62                -.928                                         57  20
 67                -.049                                         57  21
-57     0.020778                  0.0                           57  99
 58     0.0                       0.0                           58   1
 62                                0.00257982                    58   2
 58                               -0.00171988                    58   3
 74                               -0.00085994                    58   4
 57                                0.00886600                    58   5
 58                               -0.00590400                    58   6
 55                               -0.00295200                    58   7
-58     0.0                       0.0                           58  99
 59     0.0                       0.0                           59   1
 59          3.774343290          0.000000000                   59   2
141  -3.774343                                                    59   3
 59                                0.028200                      59   4
 54                               -0.014100                      59   5
 60                               -0.014100                      59   6
 59                2.939                                         59  16
 53                -.596                                         59  17
 59               -1.658                                         59  18
 64                -.424                                         59  19
 73                -.261                                         59  20
-59     0.0066347                 0.0                           59  99
 60     0.0                       0.0                           60   1
 59                                0.01410000                    60   2
 60                               -0.00940000                    60   3
 54                               -0.00470000                    60   4
 64                                0.00871536                    60   5
 60                               -0.00581024                    60   6
 74                               -0.00290512                    60   7
-60     0.0                       0.0                           60  99
 61     0.0                       0.0                           61   1
 61     6.2394                                                  61   2
 50    -2.1662                                                  61   3
 51    -4.0732                                                  61   4
 41                                0.010728                      61   5
 52                               -0.005364                      61   6
 55                               -0.005364                      61   7
 61                5.720                                         61  16
 53                -.889                                         61  17
 57                -.888                                         61  18
 61               -3.817                                         61  19
 62                -.086                                         61  20
 68                -.040                                         61  21
-61     0.009386                  0.0                           61  99
 62     0.0                       0.0                           62   1
 62          7.689086250          0.000000000                   62   2
301  -3.961526?5                                                  62   3
 62                                0.00515964                    62   4
 58                               -0.00257982                    62   5
 74                               -0.00257982                    62   6
261  -3.737566                                                    62   7
 62                7.332                                         62  16
 57                -.928                                         62  17
 61                -.086                                         62  18
 62               -5.093                                         62  19
 67                -.999                                         62  20
 66                -.052                                         62  21
 72                -.174                                         62  22
-62     0.0032686                 0.0                           62  99
 63     0.0                       0.0                           63   1
 63          7.689086250          0.000000000                   63   2
341  -3.529060                                                    63   3
 63                                0.00515964                    63   4
 74                               -0.00257982                    63   5
 75                               -0.00257982                    63   6
301  -4.180026                                                    63   7
 63                7.318                                         63  16
 62                -.999                                         63  17
 63               -5.129                                         63  18
 65                -.093                                         63  19
 72               -1.137                                         63  20
-63     0.0032686                 0.0                           63  99
 64     0.0                       0.0                           64   1
 64                                0.01743072                    64   2
 60                               -0.00871536                    64   3
 76                               -0.00871536                    64   4
 64          3.369946020          0.000000000                   64   5
141  -3.349946                                                    64   6
 64                2.686                                         64  16
 53                -.285                                         64  17
 59                -.424                                         64  18
 64               -1.143                                         64  19
 73                -.804                                         64  20
-64     0.0032686                 0.0                           64  99
 65     0.0                       0.0                           65   1
 65                                0.00193272                    65   2
 86                               -0.00096636                    65   3
 77                               -0.00096636                    65   4
 65  0.189                                                       65  10
 26 -0.009                                                       65  11
 29 -0.001                                                       65  12
 87 -0.184                                                       65  13
 65                 .093                                         65  16
 63                -.093                                         65  17
 65          0.000000000             .013198848                 65  18
 86          0.000000000            -.006599424                 65  19
 77          0.000000000            -.006599424                 65  20
-65  0.006594                                                    65  99
 66     0.0                       0.0                           66   1
 66                                0.00193272                    66   2
 77                               -0.00096636                    66   3
 78                               -0.00096636                    66   4
 66          0.000000000             .013198848                 66   5
 77          0.000000000            -.006599424                 66   6
 78          0.000000000            -.006599424                 66   7
 66                 .052                                         66  16
 62                -.052                                         66  17
-66  0.006594                                                    66  99
 67     0.0                       0.0                           67   1
 67                                0.00212718                    67   2
 79                               -0.00106359                    67   3
 78                               -0.00106359                    67   4
 67          0.000000000             .014436240                 67   5
 78          0.000000000            -.007218120                 67   6
 79          0.000000000            -.007218120                 67   7
 67                 .049                                         67  16
 57                -.049                                         67  17
-67  0.006540                                                    67  99
 68     0.0                       0.0                           68   1
 68                                0.00246876                    68   2
 80                               -0.00123438                    68   3
 79                               -0.00123438                    68   4
 68          0.000000000             .016807908                 68   5
 79          0.000000000            -.008403954                 68   6
 80          0.000000000            -.008403954                 68   7
 68                 .040                                         68  16
```

```
 61                -.040                                          68  17
-68  0.00465                                                      68  99
 69    0.0                                                        69   1
                                  0.0                             69   2
                                  0.00201324                      69   3
                                 -0.00100662                      69   4
                                 -0.00100662                      69   5
 69          0.000000000            .013714428                   69   6
 80          0.000000000           -.006857214                   69   7
 81          0.000000000           -.006857214                   69  16
 69                  .080                                        69  17
 53                -.050                                         69  99
-69  0.00571                                                      70   1
 70    0.0                                                        70   2
                                  0.0                             70   3
                                  0.004763742                     70   4
 81                              -0.0023818?1                     70   5
 82                              -0.0023818?1                     70   6
 70          0.000000000            .032481540                   70   7
 81          0.000000000           -.016240770                   70  99
 82          0.000000000           -.016240770                   71   1
-70  0.00242                                                      71   2
 71    0.0                                                        71   3
                                  0.0                             71   4
 71                               0.0052A4776                     71   5
 82                              -0.00264238A                     71   6
 83                              -0.00264238A                     71   7
 71          0.000000000            .0359874A4                   71  99
 82          0.000000000           -.017993742                   72   1
 83          0.000000000           -.017993742                   72   2
-71  0.00218                                                      72   3
 72                                                              72   4
 72  1.339                0.07604                                72   5
 87                      -0.02733                                72   6
 75                      -0.04871                                72   7
  2 -0.009                                                       72   8
 13 -0.029                                                       72   9
 24 -0.036                                                       72  10
 26 -0.339                                                       72  16
 29 -0.928                                                       72  17
 87 -0.008                                                       72  18
 72            1.350                                             72  19
 62            -.174                                             72  99
 63           -1.137                                             73   1
 72            -.039                                             73   2
-72  0.00815                                                      73   3
 73    0.0                                                       73   4
                                  0.0                             73   5
 73                               0.03282                         73   6
 76                              -0.02117                         73   7
 91                              -0.01165                         73   8
 73                               0.000682                        73   9
 54                              -0.000682                        73  10
 73                               0.00187                         73  16
 85                              -0.00187                         73  17
 73            1.297                                             73  18
 53            -.161                                             73  19
 59            -.261                                             73  20
 64            -.804                                             73  99
 73            -.071                                             74   1
-73  0.00599                                                      74   2
 74    0.0                                                       74   3
                                  0.0                             74   4
 62                               0.002579?82                     74   5
 74                              -0.00171988                      74   6
 58                              -0.00085994                      74   7
 63                               0.002579?82                     74  99
 74                              -0.00171988                      75   1
 75                              -0.00085994                      75   2
-74    0.0                                                       75   3
                                  0.0                             75   4
 75  0.0                                                         75   5
 29                   0.00438                                    75   6
 75        -2.796677?10              -.042760000                 75   7
 28          0.000000000             -.001460000                 75   8
341  2.796678                                                    75   9
 72                   0.05406                                    75  10
 87                  -0.01422                                    75  99
 63                   0.00257982                                 76   1
 75                  -0.00171988                                 76   2
 74                  -0.00085994                                 76   3
-75                                                             76   4
 76    0.0                                                       76   5
                                  0.0                             76   6
 76        -3.369946020              0.000000000                 76   7
141  3.369946                                                    76   8
 73                       0.02358                                76   9
 76                      -0.01741                                76  10
 91                      -0.00617                                76  11
 64                       0.00871536                             76  12
 76                      -0.00581024                             76  99
 60                      -0.00290512                             77   1
111                       0.00138                               77   2
 76                      -0.00092                                77   3
114                  -0.00046                                   77   4
-76    0.0                                                       77   5
                                  0.0                             77   6
 77    0.0                                                       77   7
                                  0.0                             77   8
 65                               0.00096636                      77   9
 77                              -0.00064424                      77  10
 86                              -0.00032212                      77  11
 66                               0.00096636                      77  12
 77                              -0.00064424                      77  13
 78                              -0.00032212                      77  99
 65          0.000000000            .006599424                   78   1
 77          0.000000000           -.004399616                   78   2
 86          0.000000000           -.002199808                   78   3
 66          0.000000000            .006599424                   78   4
 77          0.000000000           -.004399616                   78   5
 78          0.000000000           -.002199808                   78   6
-77    0.0                                                       78   7
                                  0.0                             78   8
 78    0.0                                                       78   9
                                  0.0                             78  10
 66                               0.00096636                      78  11
 78                              -0.00064424                      78  12
 77                              -0.00032212                      78  13
 67                               0.00106359                      78  99
 78                              -0.00070906                      79   1
 79                              -0.00035453                      79   2
 66          0.000000000            .006599424                   79   3
 78          0.000000000           -.004399616                   79   4
 77          0.000000000           -.002199808                   79   5
 67          0.000000000            .007218120                   79   6
 78          0.000000000           -.004812080                   79   7
 79          0.000000000           -.002406040                   79   8
-78    0.0                                                       79   9
                                  0.0                             79  10
 79    0.0                                                       79  11
                                  0.0                             79  12
 67                               0.00106359                      79  13
 79                              -0.00070906                      79  99
 78                              -0.00035453                      80   1
 68                               0.00123438                      80   2
 79                              -0.00082292                      80   3
 86                              -0.00041146                      80   4
 67          0.000000000            .007218120                   80   5
 79          0.000000000           -.004812080                   80   6
 78          0.000000000           -.002406040                   80   7
 68          0.000000000            .000803984                   80   8
 79          0.000000000           -.005602636                   80   9
 80          0.000000000           -.002801318                   80  10
-79    0.0                                                       80  11
                                  0.0                             80  12
 80    0.0                                                       80  13
                                  0.0                             80  99
                                                                  81   1
```

```
 68                                0.00123438      80    2
 80                               -0.00082292      80    3
 79                               -0.00041146      80    4
 69                                0.00100662      80    5
 80                               -0.00067108      80    6
 81                               -0.00033554      80    7
 68          0.0000000000           .00840395      80    8
 80          0.0000000000          -.00560263      80    9
 79          0.0000000000          -.00280131      80   10
 69          0.0000000000           .00685721      80   11
 80          0.0000000000          -.00457147      80   12
 81          0.0000000000          -.00228574      80   13
-80    0.0                         0.0           80   99
 81    0.0                         0.0           81    1
 69                                0.00100662      81    2
 81                               -0.00067108      81    3
 80                               -0.00033554      81    4
 70                                0.00238187      81    5
 81                               -0.00158791      81    6
 82                               -0.00079395      81    7
 69          0.0000000000           .00685721      81    8
 81          0.0000000000          -.00457147      81    9
 80          0.0000000000          -.00228574      81   10
 70          0.0000000000           .01624077      81   11
 81          0.0000000000          -.01082718      81   12
 82          0.0000000000          -.00541359      81   13
-81    0.0                         0.0           81   99
 82    0.0                         0.0           82    1
 70                                0.00238187      82    2
 82                               -0.00158791      82    3
 81                               -0.00079395      82    4
 71                                0.00264238      82    5
 82                               -0.00176159      82    6
 83                               -0.00088079      82    7
 70          0.0000000000           .01624077      82    8
 82          0.0000000000          -.01082718      82    9
 81          0.0000000000          -.00541359      82   10
 71          0.0000000000           .01799374      82   11
 82          0.0000000000          -.01199582      82   12
 83          0.0000000000          -.00599791      82   13
-82    0.0                         0.0           82   99
 83    0.0                         0.0           83    1
 71                                0.00264238      83    2
 83                               -0.00176159      83    3
 82                               -0.00088079      83    4
 84                                0.00264238      83    5
 83                               -0.00176159      83    6
 85                               -0.00088079      83    7
 71          0.0000000000           .01799374      83    8
 83          0.0000000000          -.01199582      83    9
 82          0.0000000000          -.00599791      83   10
 84          0.0000000000           .01799374      83   11
 83          0.0000000000          -.01199582      83   12
 85          0.0000000000          -.00599791      83   13
-83    0.0                         0.0           83   99
 84    0.0                         0.0           84    1
 84                                0.00528477      84    2
 83                               -0.00264238      84    3
 85                               -0.00264238      84    4
 84  3.25%                                        84    5
 91 -3.25%                                        84    6
 84          0.0000000000           .03598748      84    7
 83          0.0000000000          -.01799374      84    8
 85          0.0000000000          -.01799374      84    9
 84                          1.0                  84   10
 91                         -1.0                  84   11
-84   0.00218                                    84   99
 85    0.0                         0.0           85    1
 84                                0.00264238      85    2
 85                               -0.00176159      85    3
 83                               -0.00088079      85    4
 84          0.0000000000           .01799374      85    5
 85          0.0000000000          -.01199582      85    6
 83          0.0000000000          -.00599791      85    7
112                               0.00042         85    8
 85                              -0.00028         85    9
113                              -0.00014         85   10
112                               0.00522         85   11
 85                              -0.00348         85   12
113                              -0.00174         85   13
 85                              -0.00187         85   15
 73                         0.00187               85   15
-85    0.0                         0.0           85   99
 86    0.0                         0.0           86    1
 87                                0.00264238      86    2
 84                               -0.00176159      86    3
 88                               -0.00088079      86    4
 65                                0.00099636      86    5
 86                               -0.00064424      86    6
 77                               -0.00032212      86    7
 87          0.0000000000           .01799374      86    8
 86          0.0000000000          -.01199582      86    9
 88          0.0000000000          -.00599791      86   10
 65          0.0000000000           .00699424      86   11
 86          0.0000000000          -.00439961      86   12
 77          0.0000000000          -.00219981      86   13
-86    0.0                         0.0           86   99
 87    0.0                         0.0           87    1
 87                                0.00528477      87    2
 86                               -0.00264238      87    3
 88                               -0.00264238      87    4
 87          0.0000000000           .03598748      87    5
 88          0.0000000000          -.01799374      87    6
 86          0.0000000000          -.01799374      87    7
 72                         -0.02198               87    8
 87                          0.01311               87    9
 75                          0.00887               87   10
 87  0.37200                                      87   15
 26 -0.114                                        87   16
 29 -0.067                                        87   17
 72 -0.009                                        87   18
 65 -0.184                                        87   19
-87   0.00218                                    87   99
 88    0.0                         0.0           88    1
 87                                0.00264238      88    2
 88                               -0.00176159      88    3
 86                               -0.00088079      88    4
 98          0.0000000000           .00246389      88    5
 88          0.0000000000          -.00177400      88    6
 24          0.0000000000          -.00088989      88    7
 87          0.0000000000           .01799374      88    8
 88          0.0000000000          -.01199582      88    9
 86          0.0000000000          -.00599791      88   10
 88                         -0.00136               88   11
 26                          0.00136               88   12
-88    0.0                         0.0           88   99
 91                                               91    1
 73                          0.00924              91    2
 91                         -0.00548              91    3
 76                         -0.00376              91    4
 91 -3.25%                                        91    5
 84  3.25%                                        91    6
```

```
 91                      -1.0                                91   7
 84                       1.0                                91   8
-91                                                         91  99
 98                                                         98   1
 24          0.000000000             -.002663889            98   2
 98           .830000000              .005327777            98   3
 88          0.000000000             -.002663889            98   4
 29  -0.83                                                  98   5
-98  0.00174                                                98  99
 99                                                         99   1
  1                      -0.01056                           99   2
 12                           -0.01056                      99   3
 99                            0.02112                      99   4
  2  -0.19                                                  99   5
 99   0.19                                                  99   6
-99   0.00101                                               99  99
100  0.0                                                   100   1
-100   1.0                                                 100  99
110                                                        110   1
110                      0.00336                           110   2
 12                     -0.00168                           110   3
 24                     -0.00168                           110   4
-110  0.00476                                              110  99
111                                                        111   1
111                           0.00276                      111   2
 76                           -0.00138                     111   3
114                     -0.00138                           111   4
111 28.01592                                               111   5
100 -21.98599                                              111   6
112  -6.03                                                 111   7
-111   0.0306                                              111  99
112                                                        112   1
112                           0.00084                      112   2
 85                          -0.00042                      112   3
113                          -0.00042                      112   4
112                           0.01044                      112   5
 85                          -0.00522                      112   6
113                          -0.00522                      112   7
112   6.03                                                 112   8
111  -6.03                                                 112   9
-112   0.01603                                             112  99
113                                                        113   1
112                           0.00042                      113   2
113                          -0.00028                      113   3
 85                          -0.00014                      113   4
112                           0.00522                      113   5
113                          -0.00348                      113   6
 85                          -0.00174                      113   7
-113                                                       113  99
114                                                        114   1
111                      0.00138                           114   2
114                     -0.00092                           114   3
 76                     -0.00046                           114   4
-114                                                       114  99
115                                                        115   1
115         5.787387450             0.000000000            115   5
501 -5.34219945                                            115   8
115                      0.00406                           115   9
  1                     -0.00203                           115  10
116                     -0.00203                           115  11
541  -0.444198                                             115  12
-115  0.01925                                              115  99
116                                                        116   1
115                      0.00203                           116   2
  1                     -0.00068                           116   3
116                      -0.01207                          116   4
118         0.000000000              .01608000            116   7
119         0.000000000             -.00536000            116   8
116        -1.695060300             0.000000000           116   9
501  1.695060630                                           116  10
-116                                                       116  99
118                                                        118   1
118                      0.03216                           118   2
116                     -0.01608                           118   3
119                     -0.01608                           118   4
118        27.652447350             0.000000000           118   5
541  -7.514417035                                          118   6
581  -9.589400                                             118   7
621  -9.589400                                             118   8
661  -0.948937                                             118   9
-118  0.24730                                              118  99
119                                                        119   1
118                      0.01608                           119   2
119                     -0.01364                           119   3
116                     -0.00536                           119   4
120                      0.00438                           119   5
121                     -0.00146                           119   6
-119                                                       119  99
120                                                        120   1
120                      0.00876                           120   2
119                     -0.00438                           120   3
121                     -0.00438                           120   4
120         3.846370080             0.000000000           120   5
661  -3.846370608                                          120   6
-120  0.00372                                              120  99
121                                                        121   1
120                      0.00438                           121   2
121                     -0.00292                           121   3
119                     -0.00146                           121   4
-121                                                       121  99
122         0.000000000              .00077886            122   1
162         0.000000000              .03527590            122   2
162         0.000000000             -.01175863            122   3
122         0.000000000             -.02429613            122   4
  0      2000.000000000              .17512206            122   6
  0         0.000000000              .17524394            122   7
  0        36.100000000              .17524394            122   8
  0        72.200000000              .17524312            122   9
  0       108.300000000              .17523287            122  10
  0       144.400000000              .17520412            122  11
  0       180.500000000              .17515971            122  12
  0       216.600000000              .17510707            122  13
  0       252.700000000              .17505238            122  14
  0       288.800000000              .17499946            122  15
  0       324.900000000              .17495029            122  16
  0       361.000000000              .17490572            122  17
  0       361.000000000              .17524394            122  18
  0      2000.000000000              .17524394            122  19
-122        0.000000000             0.000000000           122  99
123         0.000000000             0.000000000           123   1
141         0.000000000              .03899998            123   2
123         0.000000000             -.02599998            123   3
163         0.000000000             -.01299999            123   4
-123        0.000000000             0.000000000           123  99
124         0.000000000              .00176607            124   1
144         0.000000000              .08064579            124   2
164         0.000000000             -.02681931            124   3
124         0.000000000             -.05552993            124   4
  0      2000.000000000              .30710016            124   6
  0         0.000000000              .39736609            124   7
  0        36.100000000              .39736609            124   8
  0        72.200000000              .39736448            124   9
```

0	108.300000000	.397343269	124	10
0	144.400000000	.397282055	124	11
0	180.500000000	.397185789	124	12
0	216.600000000	.397070315	124	13
0	252.700000000	.396949293	124	14
0	288.800000000	.396831408	124	15
0	324.900000000	.396721310	124	16
0	361.000000000	.396621075	124	17
0	361.000000000	.397366092	124	18
0	2000.000000000	.397366092	124	19
-124	0.000000000	0.000000000	124	99
126	0.000000000	.003964558	126	1
146	0.000000000	.184367895	126	2
166	0.000000000	-.061455965	126	3
126	0.000000000	-.126876487	126	4
0	2000.000000000	.891478934	126	6
0	0.000000000	.892026215	126	7
0	36.100000000	.892026215	126	8
0	72.200000000	.892023608	126	9
0	108.300000000	.891985009	126	10
0	144.400000000	.891866120	126	11
0	180.500000000	.891671400	126	12
0	216.600000000	.891431371	126	13
0	252.700000000	.891174823	126	14
0	288.800000000	.890921158	126	15
0	324.900000000	.890681415	126	16
0	361.000000000	.890460939	126	17
0	361.000000000	.892026215	126	18
0	2000.000000000	.892026215	126	19
-126	0.000000000	0.000000000	126	99
128	0.000000000	.008713965	128	1
148	0.000000000	.421491557	128	2
168	0.000000000	-.140497186	128	3
128	0.000000000	-.289708326	128	4
0	2000.000000000	1.959453597	128	6
0	0.000000000	1.960641585	128	7
0	36.100000000	1.960641584	128	8
0	72.200000000	1.960638853	128	9
0	108.300000000	1.960586542	128	10
0	144.400000000	1.960399750	128	11
0	180.500000000	1.960064437	128	12
0	216.600000000	1.959624717	128	13
0	252.700000000	1.959133402	128	14
0	288.800000000	1.958630944	128	15
0	324.900000000	1.958143161	128	16
0	361.000000000	1.957686546	128	17
0	361.000000000	1.960641585	128	18
0	2000.000000000	1.960641585	128	19
-128	0.000000000	0.000000000	128	99
130	0.000000000	.018394058	130	1
150	0.000000000	.963590394	130	2
170	0.000000000	-.321196798	130	3
130	0.000000000	-.660787654	130	4
0	2000.000000000	4.137327934	130	6
0	0.000000000	4.138466674	130	7
0	36.100000000	4.138466674	130	8
0	72.200000000	4.138465615	130	9
0	108.300000000	4.138429464	130	10
0	144.400000000	4.138450223	130	11
0	180.500000000	4.138054518	130	12
0	216.600000000	4.137468384	130	13
0	252.700000000	4.136722606	130	14
0	288.800000000	4.135911373	130	15
0	324.900000000	4.135075714	130	16
0	361.000000000	4.134251032	130	17
0	361.000000000	4.138466674	130	18
0	2000.000000000	4.138466674	130	19
-130	0.000000000	0.000000000	130	99
132	0.000000000	.036346261	132	1
152	0.000000000	2.202906397	132	2
172	0.000000000	-.734302132	132	3
132	0.000000000	-1.504970526	132	4
0	2000.000000000	8.181403274	132	6
0	0.000000000	8.182415798	132	7
0	36.100000000	8.182415798	132	8
0	72.200000000	8.182415754	132	9
0	108.300000000	8.182410353	132	10
0	144.400000000	8.182355594	132	11
0	180.500000000	8.182164860	132	12
0	216.600000000	8.181773605	132	13
0	252.700000000	8.181171208	132	14
0	288.800000000	8.180386975	132	15
0	324.900000000	8.179467093	132	16
0	361.000000000	8.178458972	132	17
0	361.000000000	8.182415798	132	18
0	2000.000000000	8.182415798	132	19
-132	0.000000000	0.000000000	132	99
141	0.000000000	0.000000000	141	1
142	0.000000000	.231068853	141	2
141	0.000000000	-.146196429	141	3
143	0.000000000	-.084872424	141	4
141	-10.514325000	0.000000000	141	5
99	3.774343000	0.000000000	141	6
64	3.369946000	0.000000000	141	7
76	3.369946000	0.000000000	141	8
141	0.000000000	-.077999965	141	9
163	0.000000000	.038999982	141	10
123	0.000000000	.038999982	141	11
-141	-.0386		141	99
142	0.000000000	0.000000000	142	1
142	0.000000000	.650996764	142	2
141	0.000000000	-.250786729	142	3
143	0.000000000	-.329658231	142	4
162	0.000000000	-.039279902	142	5
122	0.000000000	-.039279902	142	6
-142	.263009043	0.000000000	142	99
143	0.000000000	0.000000000	143	1
142	0.000000000	.349376106	143	2
143	0.000000000	-.390982236	143	3
141	0.000000000	-.104590299	143	4
144	0.000000000	.231068853	143	5
145	0.000000000	-.084872424	143	6
-143	0.000000000	0.000000000	143	99
144	0.000000000	0.000000000	144	1
144	0.000000000	.741736545	144	2
143	0.000000000	-.250786729	144	3
145	0.000000000	-.329658231	144	4
164	0.000000000	-.080645793	144	5
124	0.000000000	-.080645793	144	6
-144	.601276545	0.000000000	144	99
145	0.000000000	0.000000000	145	1
144	0.000000000	.349376106	145	2
145	0.000000000	-.390982236	145	3
143	0.000000000	-.104590299	145	4
146	0.000000000	.231068853	145	5
147	0.000000000	-.084872424	145	6
-145	0.000000000	0.000000000	145	99
146	0.000000000	0.000000000	146	1
146	0.000000000	.949180749	146	2
145	0.000000000	-.250786729	146	3
147	0.000000000	-.329658231	146	4
166	0.000000000	-.184367895	146	5

126	0.000000000	-.184367895	146	6
-146	1.374604766	0.000000000	146	99
147	0.000000000	0.000000000	147	1
146	0.000000000	.349376106	147	2
147	0.000000000	-.390982236	147	3
145	0.000000000	-.104590299	147	4
148	0.000000000	.231068853	147	5
149	0.000000000	-.084872624	147	6
-147	0.000000000	0.000000000	147	99
148	0.000000000	0.000000000	148	1
148	0.000000000	1.423428073	148	2
147	0.000000000	-.250786729	148	3
149	0.000000000	-.329658231	148	4
168	0.000000000	-.421491557	148	5
128	0.000000000	-.421491557	148	6
-148	3.142544437	0.000000000	148	99
149	0.000000000	0.000000000	149	1
148	0.000000000	.349376106	149	2
149	0.000000000	-.390982236	149	3
147	0.000000000	-.104590299	149	4
150	0.000000000	.231068853	149	5
151	0.000000000	-.084872624	149	6
-149	0.000000000	0.000000000	149	99
150	0.000000000	0.000000000	150	1
150	0.000000000	2.507625746	150	2
149	0.000000000	-.250786729	150	3
151	0.000000000	-.329658231	150	4
170	0.000000000	-.963590394	150	5
130	0.000000000	-.963590394	150	6
-150	7.184309110	0.000000000	150	99
151	0.000000000	0.000000000	151	1
150	0.000000000	.349376106	151	2
151	0.000000000	-.390982236	151	3
149	0.000000000	-.104590299	151	4
152	0.000000000	.231068853	151	5
153	0.000000000	-.084872624	151	6
-151	0.000000000	0.000000000	151	99
152	0.000000000	0.000000000	152	1
152	0.000000000	4.986257753	152	2
151	0.000000000	-.250786729	152	3
153	0.000000000	-.329658231	152	4
172	0.000000000	-2.202906397	152	5
132	0.000000000	-2.202906397	152	6
-152	16.42436517	0.000000000	152	99
153	0.000000000	.014947090	153	1
152	0.000000000	.349376106	153	2
151	0.000000000	-.104590299	153	3
153	0.000000000	-.259732896	153	4
0	2000.000000000	3.362841068	153	6
0	0.000000000	3.363098037	153	7
0	36.100000000	3.363098037	153	8
0	72.200000000	3.363098035	153	9
0	108.300000000	3.363097454	153	10
0	144.400000000	3.363098049	153	11
0	180.500000000	3.363052264	153	12
0	216.600000000	3.362964084	153	13
0	252.700000000	3.362812249	153	14
0	288.800000000	3.362597273	153	15
0	324.900000000	3.362328082	153	16
0	361.000000000	3.362017186	153	17
0	361.000000000	3.363098037	153	18
0	2000.000000000	3.363098037	153	19
-153	0.000000000	0.000000000	153	99
162	0.000000000	0.000000000	162	1
142	0.000000000	.035275902	162	2
122	0.000000000	-.011758634	162	3
162	0.000000000	-.047034537	162	4
182	0.000000000	.035275902	162	5
202	0.000000000	-.011758634	162	6
-162	0.000000000	0.000000000	162	99
163	0.000000000	0.000000000	163	1
141	0.000000000	.038999982	163	2
163	0.000000000	-.025999988	163	3
123	0.000000000	-.012999994	163	4
181	0.000000000	.038999982	163	5
163	0.000000000	-.025999988	163	6
203	0.000000000	-.012999994	163	7
-163	0.000000000	0.000000000	163	99
164	0.000000000	0.000000000	164	1
144	0.000000000	.080645793	164	2
124	0.000000000	-.026881931	164	3
164	0.000000000	-.107527723	164	4
184	0.000000000	.080645793	164	5
204	0.000000000	-.026881931	164	6
-164	0.000000000	0.000000000	164	99
166	0.000000000	0.000000000	166	1
146	0.000000000	.184367895	166	2
126	0.000000000	-.061455965	166	3
166	0.000000000	-.245823860	166	4
186	0.000000000	.184367895	166	5
206	0.000000000	-.061455965	166	6
-166	0.000000000	0.000000000	166	99
168	0.000000000	0.000000000	168	1
148	0.000000000	.421491557	168	2
128	0.000000000	-.140497186	168	3
168	0.000000000	-.561988742	168	4
188	0.000000000	.421491557	168	5
208	0.000000000	-.140497186	168	6
-168	0.000000000	0.000000000	168	99
170	0.000000000	0.000000000	170	1
150	0.000000000	.963590394	170	2
130	0.000000000	-.321196798	170	3
170	0.000000000	-1.284787191	170	4
190	0.000000000	.963590394	170	5
210	0.000000000	-.321196798	170	6
-170	0.000000000	0.000000000	170	99
172	0.000000000	0.000000000	172	1
152	0.000000000	2.202906397	172	2
132	0.000000000	-.734302132	172	3
172	0.000000000	-2.937208529	172	4
192	0.000000000	2.202906397	172	5
212	0.000000000	-.734302132	172	6
-172	0.000000000	0.000000000	172	99
181	0.000000000	0.000000000	181	1
182	0.000000000	.231068853	181	2
161	0.000000000	-.146196429	181	3
183	0.000000000	-.084872624	181	4
181	-9.411440000	0.000000000	181	5
50	.268180000	0.000000000	181	6
93	8.894530000	0.000000000	181	7
56	.248736000	0.000000000	181	8
181	0.000000000	-.077999965	181	9
203	0.000000000	.038999982	181	10
163	0.000000000	.038999982	181	11
-181	-.0346		181	99
182	0.000000000	0.000000000	182	1
182	0.000000000	.650996764	182	2
181	0.000000000	-.250786729	182	3
183	0.000000000	-.329658231	182	4
202	0.000000000	-.035275902	182	5
162	0.000000000	-.035275902	182	6
-182	.263009043	0.000000000	182	99

183	0.000000000	0.000000000	183	1
182	0.000000000	.3493761n6	183	2
183	0.000000000	-.3909R2236	183	3
181	0.000000000	-.104590299	183	4
184	0.000000000	.2310A8853	183	5
185	0.000000000	-.084872424	183	6
-183	0.000000000	0.000000000	183	99
184	0.000000000	0.000000000	184	1
184	0.000000000	.7617365l5	184	2
183	0.000000000	-.2507R6729	184	3
185	0.000000000	-.329658231	184	4
204	0.000000000	-.080665793	184	5
164	0.000000000	-.080665703	184	6
-184	.6012765a5	0.000000000	184	99
185	0.000000000	0.000000000	185	1
184	0.000000000	.3493761n6	185	2
185	0.000000000	-.3909R2236	185	3
183	0.000000000	-.104590299	185	4
186	0.000000000	.2310A8853	185	5
187	0.000000000	-.084872424	185	6
-185	0.000000000	0.000000000	185	99
186	0.000000000	0.000000000	186	1
186	0.000000000	.9491R0749	186	2
185	0.000000000	-.2507R6729	186	3
187	0.000000000	-.329658231	186	4
206	0.000000000	-.184367895	186	5
166	0.000000000	-.184367895	186	6
-186	1.374604766	0.000000000	186	99
187	0.000000000	0.000000000	187	1
186	0.000000000	.3493761n6	187	2
187	0.000000000	-.3909R2236	187	3
185	0.000000000	-.104590299	187	4
188	0.000000000	.2310A8853	187	5
189	0.000000000	-.084872424	187	6
-187	0.000000000	0.000000000	187	99
188	0.000000000	0.000000000	188	1
188	0.000000000	1.423428073	188	2
187	0.000000000	-.2507R6729	188	3
189	0.000000000	-.329658231	188	4
208	0.000000000	-.421491567	188	5
168	0.000000000	-.421491567	188	6
-188	3.142544437	0.000000000	188	99
189	0.000000000	0.000000000	189	1
188	0.000000000	.3493761n6	189	2
189	0.000000000	-.3909R2236	189	3
187	0.000000000	-.104590299	189	4
190	0.000000000	.2310A8853	189	5
191	0.000000000	-.084872424	189	6
-189	0.000000000	0.000000000	189	99
190	0.000000000	0.000000000	190	1
190	0.000000000	2.507625746	190	2
189	0.000000000	-.2507R6729	190	3
191	0.000000000	-.329658231	190	4
210	0.000000000	-.963590394	190	5
170	0.000000000	-.963590394	190	6
-190	7.184309110	0.000000000	190	99
191	0.000000000	0.000000000	191	1
190	0.000000000	.3493761n6	191	2
191	0.000000000	-.3909R2236	191	3
189	0.000000000	-.104590299	191	4
192	0.000000000	.2310A8853	191	5
193	0.000000000	-.084872424	191	6
-191	0.000000000	0.000000000	191	99
192	0.000000000	0.000000000	192	1
192	0.000000000	4.9R4257763	192	2
191	0.000000000	-.2507R6729	192	3
193	0.000000000	-.329658231	192	4
212	0.000000000	-2.202906397	192	5
172	0.000000000	-2.202906397	192	6
-192	16.42436516?7	0.000000000	192	99
193	0.000000000	.015869327	193	1
192	0.000000000	.3493761n6	193	2
191	0.000000000	-.104590299	193	3
193	0.000000000	-.260655133	193	4
0	2000.000000000	3.570164046	193	6
0	0.000000000	3.570601567	193	7
0	36.100000000	3.570601567	193	8
0	72.200000000	3.570601569	193	9
0	108.300000000	3.570599255	193	10
0	144.400000000	3.570575828	193	11
0	180.500000000	3.570493845	193	12
0	216.600000000	3.570325141	193	13
0	252.700000000	3.570064805	193	14
0	288.800000000	3.569725306	193	15
0	324.900000000	3.569326556	193	16
0	361.000000000	3.568889089	193	17
0	361.000000000	3.570601567	193	18
0	2000.000000000	3.570601567	193	19
-193	0.000000000	0.000000000	193	99
202	0.000000000	0.000000000	202	1
182	0.000000000	.035275902	202	2
162	0.000000000	-.011758634	202	3
202	0.000000000	-.047034537	202	4
222	0.000000000	.035275902	202	5
242	0.000000000	-.011758634	202	6
-202	0.000000000	0.000000000	202	99
203	0.000000000	0.000000000	203	1
181	0.000000000	.038999982	203	2
203	0.000000000	-.025999988	203	3
163	0.000000000	-.012999994	203	4
221	0.000000000	.038999982	203	5
203	0.000000000	-.025999988	203	6
243	0.000000000	-.012999994	203	7
-203	0.000000000	0.000000000	203	99
204	0.000000000	0.000000000	204	1
184	0.000000000	.080665793	204	2
164	0.000000000	-.026881931	204	3
204	0.000000000	-.107527723	204	4
224	0.000000000	.080665793	204	5
244	0.000000000	-.026881931	204	6
-204	0.000000000	0.000000000	204	99
206	0.000000000	0.000000000	206	1
186	0.000000000	.184367895	206	2
166	0.000000000	-.061455965	206	3
206	0.000000000	-.245823860	206	4
226	0.000000000	.184367895	206	5
246	0.000000000	-.061455965	206	6
-206	0.000000000	0.000000000	206	99
208	0.000000000	0.000000000	208	1
188	0.000000000	.421491587	208	2
168	0.000000000	-.140497186	208	3
208	0.000000000	-.561988742	208	4
228	0.000000000	.421491587	208	5
248	0.000000000	-.140497186	208	6
-208	0.000000000	0.000000000	208	99
210	0.000000000	0.000000000	210	1
190	0.000000000	.963590394	210	2
170	0.000000000	-.321196798	210	3
210	0.000000000	-1.284787191	210	4
230	0.000000000	.963590394	210	5
250	0.000000000	-.321196798	210	6
-210	0.000000000	0.000000000	210	99

212	0.000000000	0.000000000	212	1
192	0.000000000	2.202906397	212	2
172	0.000000000	-.734302132	212	3
212	0.000000000	-2.937208529	212	4
232	0.000000000	2.202906397	212	5
252	0.000000000	-.734302132	212	6
-212	0.000000000	0.000000000	212	99
221	0.000000000	0.000000000	221	1
222	0.000000000	.231068853	221	2
221	0.000000000	-.144194429	221	3
223	0.000000000	-.084872424	221	4
221	-8.6073R0000	0.000000000	221	5
50	2.897240000	0.000000000	221	6
56	2.687170000	0.000000000	221	7
57	3.022970000	0.000000000	221	8
221	0.000000000	-.077999965	221	9
243	0.000000000	.038999982	221	10
203	0.000000000	.038999982	221	11
-221	-.0356		221	99
222	0.000000000	0.000000000	222	1
222	0.000000000	.650996744	222	2
221	0.000000000	-.250786729	222	3
223	0.000000000	-.329658231	222	4
242	0.000000000	-.035275902	222	5
202	0.000000000	-.035275902	222	6
-222	.263009043	0.000000000	222	99
223	0.000000000	0.000000000	223	1
222	0.000000000	.349376106	223	2
223	0.000000000	-.390982236	223	3
221	0.000000000	-.104590299	223	4
224	0.000000000	.231068853	223	5
225	0.000000000	-.084872424	223	6
-223	0.000000000	0.000000000	223	99
224	0.000000000	0.000000000	224	1
224	0.000000000	.741736545	224	2
223	0.000000000	-.250786729	224	3
225	0.000000000	-.329658231	224	4
244	0.000000000	-.080645793	224	5
204	0.000000000	-.080645793	224	6
-224	.001276545	0.000000000	224	99
225	0.000000000	0.000000000	225	1
224	0.000000000	.349376106	225	2
225	0.000000000	-.390982236	225	3
223	0.000000000	-.104590299	225	4
226	0.000000000	.231068853	225	5
227	0.000000000	-.084872424	225	6
-225	0.000000000	0.000000000	225	99
226	0.000000000	0.000000000	226	1
226	0.000000000	.949180749	226	2
225	0.000000000	-.250786729	226	3
227	0.000000000	-.329658231	226	4
246	0.000000000	-.184367865	226	5
206	0.000000000	-.184367865	226	6
-226	1.374604746	0.000000000	226	99
227	0.000000000	0.000000000	227	1
226	0.000000000	.349376106	227	2
227	0.000000000	-.390982236	227	3
225	0.000000000	-.104590299	227	4
228	0.000000000	.231068853	227	5
229	0.000000000	-.084872424	227	6
-227	0.000000000	0.000000000	227	99
228	0.000000000	0.000000000	228	1
228	0.000000000	1.423428073	228	2
227	0.000000000	-.250786729	228	3
229	0.000000000	-.329658231	228	4
248	0.000000000	-.421491557	228	5
208	0.000000000	-.421491557	228	6
-228	3.142544437	0.000000000	228	99
229	0.000000000	0.000000000	229	1
228	0.000000000	.349376106	229	2
229	0.000000000	-.390982236	229	3
227	0.000000000	-.104590299	229	4
230	0.000000000	.231068853	229	5
231	0.000000000	-.084872424	229	6
-229	0.000000000	0.000000000	229	99
230	0.000000000	0.000000000	230	1
230	0.000000000	2.507625746	230	2
229	0.000000000	-.250786729	230	3
231	0.000000000	-.329658231	230	4
250	0.000000000	-.963590394	230	5
210	0.000000000	-.963590394	230	6
-230	7.184309110	0.000000000	230	99
231	0.000000000	0.000000000	231	1
230	0.000000000	.349376106	231	2
231	0.000000000	-.390982236	231	3
229	0.000000000	-.104590299	231	4
232	0.000000000	.231068853	231	5
233	0.000000000	-.084872424	231	6
-231	0.000000000	0.000000000	231	99
232	0.000000000	0.000000000	232	1
232	0.000000000	4.986257753	232	2
231	0.000000000	-.250786729	232	3
233	0.000000000	-.329658231	232	4
252	0.000000000	-2.202906397	232	5
212	0.000000000	-2.202906397	232	6
-232	16.424365167	0.000000000	232	99
233	0.000000000	.016799164	233	1
232	0.000000000	.349376106	233	2
231	0.000000000	-.104590299	233	3
233	0.000000000	-.261584971	233	4
0	2000.000000000	3.779119376	233	6
0	0.000000000	3.779815189	233	7
0	36.100000000	3.779815189	233	8
0	72.200000000	3.779815088	233	9
0	108.300000000	3.779807728	233	10
0	144.400000000	3.779752162	233	11
0	180.500000000	3.779591586	233	12
0	216.600000000	3.779301705	233	13
0	252.700000000	3.778894455	233	14
0	288.800000000	3.778399472	233	15
0	324.900000000	3.777849158	233	16
0	361.000000000	3.777271499	233	17
0	361.000000000	3.779815189	233	18
0	2000.000000000	3.779815189	233	19
-233	0.000000000	0.000000000	233	99
242	0.000000000	0.000000000	242	1
222	0.000000000	.035275902	242	2
202	0.000000000	-.011758634	242	3
242	0.000000000	-.047034537	242	4
262	0.000000000	.035275902	242	5
282	0.000000000	-.011758634	242	6
-242	0.000000000	0.000000000	242	99
243	0.000000000	0.000000000	243	1
221	0.000000000	.038999982	243	2
243	0.000000000	-.025999988	243	3
203	0.000000000	-.012999994	243	4
261	0.000000000	.038999982	243	5
243	0.000000000	-.025999988	243	6
283	0.000000000	-.012999994	243	7
-243	0.000000000	0.000000000	243	99
244	0.000000000	0.000000000	244	1
224	0.000000000	.080645793	244	2

204	0.000000000	-.026881931	244	3
244	0.000000000	-.107527723	244	4
264	0.000000000	.080645793	244	5
284	0.000000000	-.026881931	244	6
-244	0.000000000	0.000000000	244	99
246	0.000000000	0.000000000	246	1
226	0.000000000	.184367895	246	2
206	0.000000000	-.061455965	246	3
246	0.000000000	-.245823860	246	4
266	0.000000000	.184367895	246	5
286	0.000000000	-.061455965	246	6
-246	0.000000000	0.000000000	246	99
248	0.000000000	0.000000000	248	1
228	0.000000000	.421491557	248	2
208	0.000000000	-.140497186	248	3
248	0.000000000	-.561988742	248	4
268	0.000000000	.421491557	248	5
288	0.000000000	-.140497186	248	6
-248	0.000000000	0.000000000	248	99
250	0.000000000	0.000000000	250	1
230	0.000000000	.963590394	250	2
210	0.000000000	-.321196798	250	3
250	0.000000000	-1.284787191	250	4
270	0.000000000	.963590394	250	5
290	0.000000000	-.321196798	250	6
-250	0.000000000	0.000000000	250	99
252	0.000000000	0.000000000	252	1
232	0.000000000	2.202906397	252	2
212	0.000000000	-.734302132	252	3
252	0.000000000	-2.937208529	252	4
272	0.000000000	2.202906397	252	5
292	0.000000000	-.734302132	252	6
-252	0.000000000	0.000000000	252	99
261	0.000000000	0.000000000	261	1
262	0.000000000	.231088853	261	2
261	0.000000000	-.146196429	261	3
263	0.000000000	-.084872424	261	4
261	-8.820636000	0.000000000	261	5
57	5.093070000	0.000000000	261	6
62	3.727566000	0.000000000	261	7
261	0.000000000	-.077999985	261	8
283	0.000000000	.038999982	261	9
243	0.000000000	.038999982	261	10
-261	-.03946		261	99
262	0.000000000	0.000000000	262	1
262	0.000000000	.650996744	262	2
261	0.000000000	-.250786729	262	3
263	0.000000000	-.329658231	262	4
282	0.000000000	-.035275902	262	5
242	0.000000000	-.035275902	262	6
-262	.263009043	0.000000000	262	99
263	0.000000000	0.000000000	263	1
262	0.000000000	.349376106	263	2
263	0.000000000	-.390982236	263	3
261	0.000000000	-.104590299	263	4
264	0.000000000	.231088853	263	5
265	0.000000000	-.084872424	263	6
-263	0.000000000	0.000000000	263	99
264	0.000000000	0.000000000	264	1
264	0.000000000	.741736545	264	2
263	0.000000000	-.250786729	264	3
265	0.000000000	-.329658231	264	4
284	0.000000000	-.080645793	264	5
244	0.000000000	-.080645793	264	6
-264	.601276545	0.000000000	264	99
265	0.000000000	0.000000000	265	1
264	0.000000000	.349376106	265	2
265	0.000000000	-.390982236	265	3
263	0.000000000	-.104590299	265	4
266	0.000000000	.231088853	265	5
267	0.000000000	-.084872424	265	6
-265	0.000000000	0.000000000	265	99
266	0.000000000	0.000000000	266	1
266	0.000000000	.949180749	266	2
265	0.000000000	-.250786729	266	3
267	0.000000000	-.329658231	266	4
286	0.000000000	-.184367895	266	5
246	0.000000000	-.184367895	266	6
-266	1.374604766	0.000000000	266	99
267	0.000000000	0.000000000	267	1
266	0.000000000	.349376106	267	2
267	0.000000000	-.390982236	267	3
265	0.000000000	-.104590299	267	4
268	0.000000000	.231088853	267	5
269	0.000000000	-.084872424	267	6
-267	0.000000000	0.000000000	267	99
268	0.000000000	0.000000000	268	1
268	0.000000000	1.423428073	268	2
267	0.000000000	-.250786729	268	3
269	0.000000000	-.329658231	268	4
288	0.000000000	-.421491557	268	5
248	0.000000000	-.421491557	268	6
-268	3.142544437	0.000000000	268	99
269	0.000000000	0.000000000	269	1
268	0.000000000	.349376106	269	2
269	0.000000000	-.390982236	269	3
267	0.000000000	-.104590299	269	4
270	0.000000000	.231088853	269	5
271	0.000000000	-.084872424	269	6
-269	0.000000000	0.000000000	269	99
270	0.000000000	0.000000000	270	1
270	0.000000000	2.507625746	270	2
269	0.000000000	-.250786729	270	3
271	0.000000000	-.329658231	270	4
290	0.000000000	-.963590394	270	5
250	0.000000000	-.963590394	270	6
-270	7.184309110	0.000000000	270	99
271	0.000000000	0.000000000	271	1
270	0.000000000	.349376106	271	2
271	0.000000000	-.390982236	271	3
269	0.000000000	-.104590299	271	4
272	0.000000000	.231088853	271	5
273	0.000000000	-.084872424	271	6
-271	0.000000000	0.000000000	271	99
272	0.000000000	0.000000000	272	1
272	0.000000000	4.986257793	272	2
271	0.000000000	-.250786729	272	3
273	0.000000000	-.329658231	272	4
292	0.000000000	-2.202906397	272	5
252	0.000000000	-2.202906397	272	6
-272	16.424365167	0.000000000	272	99
273	0.000000000	.017694991	273	1
272	0.000000000	.349376106	273	2
271	0.000000000	-.104590299	273	3
273	0.000000000	-.262480798	273	4
0	2000.000000000	3.980347648	273	6
0	0.000000000	3.981376430	273	7
0	36.100000000	3.981376430	273	8
0	72.200000000	3.981376024	273	9
0	108.300000000	3.981356878	273	10
0	144.400000000	3.981244365	273	11
0	180.500000000	3.980967728	273	12

0	216.600000000	3.980519587	273	13
0	252.700000000	3.979936955	273	14
0	288.800000000	3.979268933	273	15
0	324.900000000	3.978559348	273	16
0	361.000000000	3.977841438	273	17
0	361.000000000	3.981376438	273	18
0	3000.000000000	3.981376438	273	19
-273	0.000000000	0.000000000	273	99
282	0.000000000	0.000000000	282	1
262	0.000000000	.035275902	282	2
242	0.000000000	-.011758634	282	3
282	0.000000000	-.047034537	282	4
302	0.000000000	.035275902	282	5
322	0.000000000	-.011758634	282	6
-282	0.000000000	0.000000000	282	99
283	0.000000000	0.000000000	283	1
301	0.000000000	.038999982	283	2
283	0.000000000	-.025999988	283	3
323	0.000000000	-.012999994	283	4
261	0.000000000	.038999982	283	5
283	0.000000000	-.025999988	283	6
243	0.000000000	-.012999994	283	7
-283	0.000000000	0.000000000	283	99
284	0.000000000	0.000000000	284	1
264	0.000000000	.080645793	284	2
244	0.000000000	-.026881931	284	3
284	0.000000000	-.107527723	284	4
304	0.000000000	.080645793	284	5
324	0.000000000	-.026881931	284	6
-284	0.000000000	0.000000000	284	99
286	0.000000000	0.000000000	286	1
266	0.000000000	.184367895	286	2
246	0.000000000	-.061455965	286	3
286	0.000000000	-.245823860	286	4
306	0.000000000	.184367895	286	5
326	0.000000000	-.061455965	286	6
-286	0.000000000	0.000000000	286	99
288	0.000000000	0.000000000	288	1
268	0.000000000	.421491557	288	2
248	0.000000000	-.140497186	288	3
288	0.000000000	-.561988742	288	4
308	0.000000000	.421491557	288	5
328	0.000000000	-.140497186	288	6
-288	0.000000000	0.000000000	288	99
290	0.000000000	0.000000000	290	1
270	0.000000000	.963590394	290	2
250	0.000000000	-.321196798	290	3
290	0.000000000	-1.284787191	290	4
310	0.000000000	.963590394	290	5
330	0.000000000	-.321196798	290	6
-290	0.000000000	0.000000000	290	99
292	0.000000000	0.000000000	292	1
272	0.000000000	2.202906397	292	2
252	0.000000000	-.734302132	292	3
292	0.000000000	-2.937208529	292	4
312	0.000000000	2.202906397	292	5
332	0.000000000	-.734302132	292	6
-292	0.000000000	0.000000000	292	99
301	0.000000000	0.000000000	301	1
302	0.000000000	.231068853	301	2
301	0.000000000	-.146196429	301	3
303	0.000000000	-.084872424	301	4
301	-8.111546250	0.000000000	301	5
62	3.961520250	0.000000000	301	6
63	4.150026000	0.000000000	301	7
301	0.000000000	-.077999965	301	8
323	0.000000000	.038999982	301	9
283	0.000000000	.038999982	301	10
-301	-.0356		301	99
302	0.000000000	0.000000000	302	1
302	0.000000000	.650996744	302	2
301	0.000000000	-.250786729	302	3
303	0.000000000	-.329658231	302	4
322	0.000000000	-.035275902	302	5
282	0.000000000	-.035275902	302	6
-302	.263009043	0.000000000	302	99
303	0.000000000	0.000000000	303	1
302	0.000000000	.349376106	303	2
303	0.000000000	-.390982236	303	3
301	0.000000000	-.104590299	303	4
304	0.000000000	.231068853	303	5
305	0.000000000	-.084872424	303	6
-303	0.000000000	0.000000000	303	99
304	0.000000000	0.000000000	304	1
304	0.000000000	.741736545	304	2
303	0.000000000	-.250786729	304	3
305	0.000000000	-.329658231	304	4
324	0.000000000	-.080645793	304	5
284	0.000000000	-.080645793	304	6
-304	.601276545	0.000000000	304	99
305	0.000000000	0.000000000	305	1
304	0.000000000	.349376106	305	2
305	0.000000000	-.390982236	305	3
303	0.000000000	-.104590299	305	4
306	0.000000000	.231068853	305	5
307	0.000000000	-.084872424	305	6
-305	0.000000000	0.000000000	305	99
306	0.000000000	0.000000000	306	1
306	0.000000000	.949180749	306	2
305	0.000000000	-.250786729	306	3
307	0.000000000	-.329658231	306	4
326	0.000000000	-.184367895	306	5
286	0.000000000	-.184367895	306	6
-306	1.374604766	0.000000000	306	99
307	0.000000000	0.000000000	307	1
306	0.000000000	.349376106	307	2
307	0.000000000	-.390982236	307	3
305	0.000000000	-.104590299	307	4
308	0.000000000	.231068853	307	5
309	0.000000000	-.084872424	307	6
-307	0.000000000	0.000000000	307	99
308	0.000000000	0.000000000	308	1
308	0.000000000	1.423428073	308	2
307	0.000000000	-.250786729	308	3
309	0.000000000	-.329658231	308	4
328	0.000000000	-.421491557	308	5
288	0.000000000	-.421491557	308	6
-308	3.142544437	0.000000000	308	99
309	0.000000000	0.000000000	309	1
308	0.000000000	.349376106	309	2
309	0.000000000	-.390982236	309	3
307	0.000000000	-.104590299	309	4
310	0.000000000	.231068853	309	5
311	0.000000000	-.084872424	309	6
-309	0.000000000	0.000000000	309	99
310	0.000000000	0.000000000	310	1
310	0.000000000	2.507625746	310	2
309	0.000000000	-.250786729	310	3
311	0.000000000	-.329658231	310	4
330	0.000000000	-.963590394	310	5
290	0.000000000	-.963590394	310	6
-310	7.184309110	0.000000000	310	99

311	0.000000000	0.000000000	311	1
310	0.000000000	.349376106	311	2
311	0.000000000	-.390982236	311	3
309	0.000000000	-.104590299	311	4
312	0.000000000	.231068853	311	5
313	0.000000000	-.084872424	311	6
-311	0.000000000	0.000000000	311	99
312	0.000000000	0.000000000	312	1
312	0.000000000	4.986257753	312	2
311	0.000000000	-.2507A6729	312	3
313	0.000000000	-.329458231	312	4
332	0.000000000	-2.202906397	312	5
292	0.000000000	-2.202906397	312	6
-312	16.424365167	0.000000000	312	99
313	0.000000000	.0185002A6	313	1
312	0.000000000	.349376106	313	2
311	0.000000000	-.104590299	313	3
313	0.000000000	-.2632A6093	313	4
0	2000.000000000	4.161161339	313	6
0	0.000000000	4.162567892	313	7
0	36.100000000	4.162567892	313	8
0	72.200000000	4.162566647	313	9
0	108.300000000	4.162526331	313	10
0	144.400000000	4.162332303	313	11
0	180.500000000	4.161911934	313	12
0	216.600000000	4.1612A6611	313	13
0	252.700000000	4.160521775	313	14
0	288.800000000	4.1596A4249	313	15
0	324.900000000	4.158826126	313	16
0	361.000000000	4.1579A2944	313	17
0	361.000000000	4.162567892	313	18
0	2000.000000000	4.162567892	313	19
-313	0.000000000	0.000000000	313	99
322	0.000000000	0.000000000	322	1
302	0.000000000	.035275902	322	2
282	0.000000000	-.011758634	322	3
322	0.000000000	-.047034537	322	4
342	0.000000000	.035275902	322	5
362	0.000000000	-.011758634	322	6
-322	0.000000000	0.000000000	322	99
323	0.000000000	0.000000000	323	1
301	0.000000000	.038999982	323	2
323	0.000000000	-.025999988	323	3
283	0.000000000	-.012999994	323	4
341	0.000000000	.038999982	323	5
323	0.000000000	-.025999988	323	6
363	0.000000000	-.012999994	323	7
-323	0.000000000	0.000000000	323	99
324	0.000000000	0.000000000	324	1
304	0.000000000	.080645793	324	2
284	0.000000000	-.026881931	324	3
324	0.000000000	-.107527723	324	4
344	0.000000000	.080645793	324	5
364	0.000000000	-.026881931	324	6
-324	0.000000000	0.000000000	324	99
326	0.000000000	0.000000000	326	1
306	0.000000000	.184367895	326	2
286	0.000000000	-.061455965	326	3
326	0.000000000	-.245823860	326	4
346	0.000000000	.184367895	326	5
366	0.000000000	-.061455965	326	6
-326	0.000000000	0.000000000	326	99
328	0.000000000	0.000000000	328	1
308	0.000000000	.421491557	328	2
288	0.000000000	-.140497186	328	3
328	0.000000000	-.561988742	328	4
348	0.000000000	.421491557	328	5
368	0.000000000	-.140497186	328	6
-328	0.000000000	0.000000000	328	99
330	0.000000000	0.000000000	330	1
310	0.000000000	.963590394	330	2
290	0.000000000	-.321196798	330	3
330	0.000000000	-1.284787191	330	4
350	0.000000000	.963590394	330	5
370	0.000000000	-.321196798	330	6
-330	0.000000000	0.000000000	330	99
332	0.000000000	0.000000000	332	1
312	0.000000000	2.202906397	332	2
292	0.000000000	-.734302132	332	3
332	0.000000000	-2.937208529	332	4
352	0.000000000	2.202906397	332	5
372	0.000000000	-.734302132	332	6
-332	0.000000000	0.000000000	332	99
341	0.000000000	0.000000000	341	1
342	0.000000000	.231068853	341	2
341	0.000000000	-.146196429	341	3
343	0.000000000	-.084872424	341	4
341	-8.123110000	0.000000000	341	5
29	1.787372000	0.000000000	341	6
63	3.539060000	0.000000000	341	7
75	2.796678000	0.000000000	341	8
341	0.000000000	-.077999965	341	9
363	0.000000000	.038999982	341	10
323	0.000000000	.038999982	341	11
-341	-.0346		341	99
342	0.000000000	0.000000000	342	1
342	0.000000000	.650996764	342	2
341	0.000000000	-.250786729	342	3
343	0.000000000	-.329658231	342	4
362	0.000000000	-.035275902	342	5
322	0.000000000	-.035275902	342	6
-342	.263009043	0.000000000	342	99
343	0.000000000	0.000000000	343	1
342	0.000000000	.349376106	343	2
343	0.000000000	-.390982236	343	3
341	0.000000000	-.104590299	343	4
344	0.000000000	.231068853	343	5
345	0.000000000	-.084872424	343	6
-343	0.000000000	0.000000000	343	99
344	0.000000000	0.000000000	344	1
344	0.000000000	.741736545	344	2
343	0.000000000	-.250786729	344	3
345	0.000000000	-.329658231	344	4
364	0.000000000	-.080645793	344	5
324	0.000000000	-.080645793	344	6
-344	.601276548	0.000000000	344	99
345	0.000000000	0.000000000	345	1
344	0.000000000	.349376106	345	2
345	0.000000000	-.390982236	345	3
343	0.000000000	-.104590299	345	4
346	0.000000000	.231068853	345	5
347	0.000000000	-.084872424	345	6
-345	0.000000000	0.000000000	345	99
346	0.000000000	0.000000000	346	1
346	0.000000000	.949180749	346	2
345	0.000000000	-.250786729	346	3
347	0.000000000	-.329658231	346	4
366	0.000000000	-.184367895	346	5
326	0.000000000	-.184367895	346	6
-346	1.374604766	0.000000000	346	99
347	0.000000000	0.000000000	347	1
346	0.000000000	.349376106	347	2

347	0.000000000	-.390982236	347	3
345	0.000000000	-.104590299	347	4
348	0.000000000	.231068853	347	5
349	0.000000000	-.084872424	347	6
-347	0.000000000	0.000000000	347	99
348	0.000000000	0.000000000	348	1
348	0.000000000	1.423428073	348	2
347	0.000000000	-.250786729	348	3
349	0.000000000	-.329658231	348	4
368	0.000000000	-.421491557	348	5
328	0.000000000	-.421491557	348	6
-348	3.142544437	0.000000000	348	99
349	0.000000000	0.000000000	349	1
348	0.000000000	.349376106	349	2
349	0.000000000	-.390982236	349	3
347	0.000000000	-.104590299	349	4
350	0.000000000	.231068853	349	5
351	0.000000000	-.084872424	349	6
-349	0.000000000	0.000000000	349	99
350	0.000000000	0.000000000	350	1
350	0.000000000	2.507825746	350	2
349	0.000000000	-.250786729	350	3
351	0.000000000	-.329658231	350	4
370	0.000000000	-.963590394	350	5
330	0.000000000	-.963590394	350	6
-350	7.184309110	0.000000000	350	99
351	0.000000000	0.000000000	351	1
350	0.000000000	.349376106	351	2
351	0.000000000	-.390982236	351	3
349	0.000000000	-.104590299	351	4
352	0.000000000	.231068853	351	5
353	0.000000000	-.084872424	351	6
-351	0.000000000	0.000000000	351	99
352	0.000000000	0.000000000	352	1
352	0.000000000	4.986257763	352	2
351	0.000000000	-.250786729	352	3
353	0.000000000	-.329658231	352	4
372	0.000000000	-2.202906397	352	5
332	0.000000000	-2.202906397	352	6
-352	16.424361147	0.000000000	352	99
353	0.000000000	.019147837	353	1
352	0.000000000	.349376106	353	2
351	0.000000000	-.104590299	353	3
353	0.000000000	-.263933644	353	4
0	2000.000000000	4.306498853	353	6
0	0.000000000	4.308267035	353	7
0	36.100000000	4.308267035	353	8
0	72.200000000	4.308264206	353	9
0	108.300000000	4.308195652	353	10
0	144.400000000	4.307909915	353	11
0	180.500000000	4.307344954	353	12
0	216.600000000	4.306554683	353	13
0	252.700000000	4.305629747	353	14
0	288.800000000	4.304650079	353	15
0	324.900000000	4.303672239	353	16
0	361.000000000	4.302731731	353	17
0	361.000000000	4.308267035	353	18
0	2000.000000000	4.308267035	353	19
-353	0.000000000	0.000000000	353	99
362	0.000000000	0.000000000	362	1
342	0.000000000	.035275902	362	2
322	0.000000000	-.011758634	362	3
362	0.000000000	-.047034537	362	4
382	0.000000000	.035275902	362	5
402	0.000000000	-.011758634	362	6
-362	0.000000000	0.000000000	362	99
363	0.000000000	0.000000000	363	1
341	0.000000000	.038999982	363	2
363	0.000000000	-.025999988	363	3
323	0.000000000	-.012999994	363	4
381	0.000000000	.038999982	363	5
363	0.000000000	-.025999988	363	6
403	0.000000000	-.012999994	363	7
-363	0.000000000	0.000000000	363	99
364	0.000000000	0.000000000	364	1
344	0.000000000	.080645793	364	2
324	0.000000000	-.026881931	364	3
364	0.000000000	-.107527723	364	4
384	0.000000000	.080645793	364	5
404	0.000000000	-.026881931	364	6
-364	0.000000000	0.000000000	364	99
366	0.000000000	0.000000000	366	1
346	0.000000000	.184367895	366	2
326	0.000000000	-.061455965	366	3
366	0.000000000	-.245823860	366	4
386	0.000000000	.184367895	366	5
406	0.000000000	-.061455965	366	6
-366	0.000000000	0.000000000	366	99
368	0.000000000	0.000000000	368	1
348	0.000000000	.421491557	368	2
328	0.000000000	-.140497186	368	3
368	0.000000000	-.561988742	368	4
388	0.000000000	.421491557	368	5
408	0.000000000	-.140497186	368	6
-368	0.000000000	0.000000000	368	99
370	0.000000000	0.000000000	370	1
350	0.000000000	.963590394	370	2
330	0.000000000	-.321196798	370	3
370	0.000000000	-1.284787191	370	4
390	0.000000000	.963590394	370	5
410	0.000000000	-.321196798	370	6
-370	0.000000000	0.000000000	370	99
372	0.000000000	0.000000000	372	1
352	0.000000000	2.202906397	372	2
332	0.000000000	-.734302132	372	3
372	0.000000000	-2.937208529	372	4
392	0.000000000	2.202906397	372	5
412	0.000000000	-.734302132	372	6
-372	0.000000000	0.000000000	372	99
381	0.000000000	0.000000000	381	1
382	0.000000000	.231068853	381	2
381	0.000000000	-.146196429	381	3
383	0.000000000	-.084872424	381	4
381	-8.887835440	0.000000000	381	5
22	3.440338440	0.000000000	381	6
27	2.978230000	0.000000000	381	7
29	2.058998000	0.000000000	381	8
38	.410269000	0.000000000	381	9
381	0.000000000	-.077999965	381	10
403	0.000000000	.038999982	381	11
363	0.000000000	.038999982	381	12
-381	-.0396		381	99
382	0.000000000	0.000000000	382	1
382	0.000000000	.650996764	382	2
381	0.000000000	-.250786729	382	3
383	0.000000000	-.329658231	382	4
402	0.000000000	-.035275902	382	5
362	0.000000000	-.035275902	382	6
-382	.263009043	0.000000000	382	99
383	0.000000000	0.000000000	383	1
382	0.000000000	.349376106	383	2
383	0.000000000	-.390982236	383	3

381	0.000000000	-.104590299	383	4
384	0.000000000	.231068853	383	5
385	0.000000000	-.084872424	383	6
-383	0.000000000	0.000000000	383	99
384	0.000000000	0.000000000	384	1
384	0.000000000	.741736545	384	2
383	0.000000000	-.250786729	384	3
385	0.000000000	-.329658231	384	4
404	0.000000000	-.080645793	384	5
364	0.000000000	-.080645793	384	6
-384	.6012765&5	0.000000000	384	99
385	0.000000000	0.000000000	385	1
384	0.000000000	.349376106	385	2
385	0.000000000	-.390982236	385	3
383	0.000000000	-.104590299	385	4
386	0.000000000	.231068853	385	5
387	0.000000000	-.084872424	385	6
-385	0.000000000	0.000000000	385	99
386	0.000000000	0.000000000	386	1
386	0.000000000	.949180749	386	2
385	0.000000000	-.250786729	386	3
387	0.000000000	-.329658231	386	4
406	0.000000000	-.184367895	386	5
366	0.000000000	-.184367895	386	6
-386	1.374604766	0.000000000	386	99
387	0.000000000	0.000000000	387	1
386	0.000000000	.349376106	387	2
387	0.000000000	-.390982236	387	3
385	0.000000000	-.104590299	387	4
388	0.000000000	.231068853	387	5
389	0.000000000	-.084872424	387	6
-387	0.000000000	0.000000000	387	99
388	0.000000000	0.000000000	388	1
388	0.000000000	1.423428073	388	2
387	0.000000000	-.250786729	388	3
389	0.000000000	-.329658231	388	4
408	0.000000000	-.421491557	388	5
368	0.000000000	-.421491557	388	6
-388	3.142544417	0.000000000	388	99
389	0.000000000	0.000000000	389	1
388	0.000000000	.349376106	389	2
389	0.000000000	-.390982236	389	3
387	0.000000000	-.104590299	389	4
390	0.000000000	.231068853	389	5
391	0.000000000	-.084872424	389	6
-389	0.000000000	0.000000000	389	99
390	0.000000000	0.000000000	390	1
390	0.000000000	2.507625746	390	2
389	0.000000000	-.250786729	390	3
391	0.000000000	-.329658231	390	4
410	0.000000000	-.963590394	390	5
370	0.000000000	-.963590394	390	6
-390	7.184309110	0.000000000	390	99
391	0.000000000	0.000000000	391	1
390	0.000000000	.349376106	391	2
391	0.000000000	-.390982236	391	3
389	0.000000000	-.104590299	391	4
392	0.000000000	.231068853	391	5
393	0.000000000	-.084872424	391	6
-391	0.000000000	0.000000000	391	99
392	0.000000000	0.000000000	392	1
392	0.000000000	4.986257753	392	2
391	0.000000000	-.250786729	392	3
393	0.000000000	-.329658231	392	4
412	0.000000000	-2.202906397	392	5
372	0.000000000	-2.202906397	392	6
-392	16.424365167	0.000000000	392	99
393	0.000000000	.019570605	393	1
392	0.000000000	.349376106	393	2
391	0.000000000	-.104590299	393	3
393	0.000000000	-.264356412	393	4
0	7000.000000000	4.401356640	393	6
0	0.000000000	4.403389991	393	7
0	36.100000000	4.403389990	393	8
0	72.200000000	4.403385591	393	9
0	108.300000000	4.403291124	393	10
0	144.400000000	4.402931080	393	11
0	180.500000000	4.402257529	393	12
0	216.600000000	4.401349749	393	13
0	252.700000000	4.400315253	393	14
0	288.800000000	4.399241389	393	15
0	324.900000000	4.398186443	393	16
0	361.000000000	4.397184923	393	17
0	361.000000000	4.403389991	393	18
0	2000.000000000	4.403389991	393	19
-393	0.000000000	0.000000000	393	99
402	0.000000000	0.000000000	402	1
382	0.000000000	.035275902	402	2
362	0.000000000	-.011758634	402	3
402	0.000000000	-.047034537	402	4
422	0.000000000	.035275902	402	5
442	0.000000000	-.011758634	402	6
-402	0.000000000	0.000000000	402	99
403	0.000000000	0.000000000	403	1
381	0.000000000	.038999982	403	2
403	0.000000000	-.025999988	403	3
363	0.000000000	-.012999994	403	4
421	0.000000000	.038999982	403	5
403	0.000000000	-.025999988	403	6
443	0.000000000	-.012999994	403	7
-403	0.000000000	0.000000000	403	99
404	0.000000000	0.000000000	404	1
384	0.000000000	.080645793	404	2
364	0.000000000	-.026881931	404	3
404	0.000000000	-.107527723	404	4
424	0.000000000	.080645793	404	5
444	0.000000000	-.026881931	404	6
-404	0.000000000	0.000000000	404	99
406	0.000000000	0.000000000	406	1
386	0.000000000	.184367895	406	2
366	0.000000000	-.061455965	406	3
406	0.000000000	-.245823860	406	4
426	0.000000000	.184367895	406	5
446	0.000000000	-.061455965	406	6
-406	0.000000000	0.000000000	406	99
408	0.000000000	0.000000000	408	1
388	0.000000000	.421491557	408	2
368	0.000000000	-.140497186	408	3
408	0.000000000	-.561988742	408	4
428	0.000000000	.421491557	408	5
448	0.000000000	-.140497186	408	6
-408	0.000000000	0.000000000	408	99
410	0.000000000	0.000000000	410	1
390	0.000000000	.963590394	410	2
370	0.000000000	-.321196798	410	3
410	0.000000000	-1.284787191	410	4
430	0.000000000	.963590394	410	5
450	0.000000000	-.321196798	410	6
-410	0.000000000	0.000000000	410	99
412	0.000000000	0.000000000	412	1
392	0.000000000	2.202906397	412	2
372	0.000000000	-.734302132	412	3

412	0.000000000	-2.937208529	412	4
432	0.000000000	2.202906397	412	5
452	0.000000000	-.734302132	412	6
-412	0.000000000	0.000000000	412	99
421	0.000000000	0.000000000	421	1
422	0.000000000	.231068853	421	2
421	0.000000000	-.146196429	421	3
423	0.000000000	-.084872424	421	4
421	-11.484700000	0.000000000	421	5
18	4.181520000	0.000000000	421	6
19	7.303180000	0.000000000	421	7
421	0.000000000	-.077999965	421	8
443	0.000000000	.038999982	421	9
403	0.000000000	.038999982	421	10
-421	-.0346		421	99
422	0.000000000	0.000000000	422	1
422	0.000000000	.650996764	422	2
421	0.000000000	-.250786729	422	3
423	0.000000000	-.329658231	422	4
442	0.000000000	-.035275902	422	5
402	0.000000000	-.035275902	422	6
-422	.263009043	0.000000000	422	99
423	0.000000000	0.000000000	423	1
422	0.000000000	.349376106	423	2
423	0.000000000	-.390982236	423	3
421	0.000000000	-.104590299	423	4
424	0.000000000	.231068853	423	5
425	0.000000000	-.084872424	423	6
-423	0.000000000	0.000000000	423	99
424	0.000000000	0.000000000	424	1
424	0.000000000	.741736545	424	2
423	0.000000000	-.250786729	424	3
425	0.000000000	-.329658231	424	4
444	0.000000000	-.080645793	424	5
404	0.000000000	-.080645793	424	6
-424	.601276545	0.000000000	424	99
425	0.000000000	0.000000000	425	1
424	0.000000000	.349376106	425	2
425	0.000000000	-.390982236	425	3
423	0.000000000	-.104590299	425	4
426	0.000000000	.231068853	425	5
427	0.000000000	-.084872424	425	6
-425	0.000000000	0.000000000	425	99
426	0.000000000	0.000000000	426	1
426	0.000000000	.949180749	426	2
425	0.000000000	-.250786729	426	3
427	0.000000000	-.329658231	426	4
446	0.000000000	-.184367895	426	5
406	0.000000000	-.184367895	426	6
-426	1.374604766	0.000000000	426	99
427	0.000000000	0.000000000	427	1
426	0.000000000	.349376106	427	2
427	0.000000000	-.390982236	427	3
425	0.000000000	-.104590299	427	4
428	0.000000000	.231068853	427	5
429	0.000000000	-.084872424	427	6
-427	0.000000000	0.000000000	427	99
428	0.000000000	0.000000000	428	1
428	0.000000000	1.423428073	428	2
427	0.000000000	-.250786729	428	3
429	0.000000000	-.329658231	428	4
448	0.000000000	-.421491557	428	5
408	0.000000000	-.421491557	428	6
-428	3.142544437	0.000000000	428	99
429	0.000000000	0.000000000	429	1
428	0.000000000	.349376106	429	2
429	0.000000000	-.390982236	429	3
427	0.000000000	-.104590299	429	4
430	0.000000000	.231068853	429	5
431	0.000000000	-.084872424	429	6
-429	0.000000000	0.000000000	429	99
430	0.000000000	0.000000000	430	1
430	0.000000000	2.507625746	430	2
429	0.000000000	-.250786729	430	3
431	0.000000000	-.329658231	430	4
450	0.000000000	-.963590394	430	5
410	0.000000000	-.963590394	430	6
-430	7.184309110	0.000000000	430	99
431	0.000000000	0.000000000	431	1
430	0.000000000	.349376106	431	2
431	0.000000000	-.390982236	431	3
429	0.000000000	-.104590299	431	4
432	0.000000000	.231068853	431	5
433	0.000000000	-.084872424	431	6
-431	0.000000000	0.000000000	431	99
432	0.000000000	0.000000000	432	1
432	0.000000000	4.986257753	432	2
431	0.000000000	-.250786729	432	3
433	0.000000000	-.329658231	432	4
452	0.000000000	-2.202906397	432	5
412	0.000000000	-2.202906397	432	6
-432	16.424365167	0.000000000	432	99
433	0.000000000	.019717875	433	1
432	0.000000000	.349376106	433	2
431	0.000000000	-.104590299	433	3
433	0.000000000	-.264503682	433	4
0	2000.000000000	4.434394556	433	6
0	0.000000000	4.436925795	433	7
0	36.100000000	4.436525794	433	8
0	72.200000000	4.436520641	433	9
0	108.30000000	4.436415566	433	10
0	144.40000000	4.436026765	433	11
0	180.50000000	4.435312772	433	12
0	216.60000000	4.434362385	433	13
0	252.70000000	4.433288962	433	14
0	288.80000000	4.432182176	433	15
0	324.90000000	4.431100729	433	16
0	361.00000000	4.430078525	433	17
0	361.00000000	4.436525795	433	18
0	2000.000000000	4.436525795	433	19
-433	0.000000000	0.000000000	433	99
442	0.000000000	0.000000000	442	1
422	0.000000000	.035275902	442	2
402	0.000000000	-.011758634	442	3
442	0.000000000	-.047034537	442	4
462	0.000000000	.035275902	442	5
482	0.000000000	-.011758634	442	6
-442	0.000000000	0.000000000	442	99
443	0.000000000	0.000000000	443	1
421	0.000000000	.038999982	443	2
443	0.000000000	-.025999988	443	3
403	0.000000000	-.012999994	443	4
461	0.000000000	.038999982	443	5
443	0.000000000	-.025999988	443	6
483	0.000000000	-.012999994	443	7
-443	0.000000000	0.000000000	443	99
444	0.000000000	0.000000000	444	1
424	0.000000000	.080645793	444	2
404	0.000000000	-.026881931	444	3
444	0.000000000	-.107527723	444	4
464	0.000000000	.080645793	444	5
484	0.000000000	-.026881931	444	6

-444	0.000000000	0.000000000	444	99
446	0.000000000	0.000000000	446	1
426	0.000000000	.184367895	446	2
406	0.000000000	-.061455965	446	3
446	0.000000000	-.245823860	446	4
466	0.000000000	.184367895	446	5
486	0.000000000	-.061455965	446	6
-446	0.000000000	0.000000000	446	99
448	0.000000000	0.000000000	448	1
428	0.000000000	.421491557	448	2
408	0.000000000	-.140497186	448	3
448	0.000000000	-.561988742	448	4
468	0.000000000	.421491557	448	5
488	0.000000000	-.140497186	448	6
-448	0.000000000	0.000000000	448	99
450	0.000000000	0.000000000	450	1
430	0.000000000	.963590394	450	2
410	0.000000000	-.321196798	450	3
450	0.000000000	-1.284787191	450	4
470	0.000000000	.963590394	450	5
490	0.000000000	-.321196798	450	6
-450	0.000000000	0.000000000	450	99
452	0.000000000	0.000000000	452	1
432	0.000000000	2.202906397	452	2
412	0.000000000	-.734302132	452	3
452	0.000000000	-2.937208529	452	4
472	0.000000000	2.202906397	452	5
492	0.000000000	-.734302132	452	6
-452	0.000000000	0.000000000	452	99
461	0.000000000	0.000000000	461	1
462	0.000000000	.231068853	461	2
461	0.000000000	-.146196429	461	3
463	0.000000000	-.084872424	461	4
461	-8.594439610	0.000000000	461	5
4	5.154101170	0.000000000	461	6
9	3.440338440	0.000000000	461	7
461	0.000000000	-.077999965	461	8
483	0.000000000	.038999982	461	9
443	0.000000000	.038999982	461	10
-461	-.0386		461	99
462	0.000000000	0.000000000	462	1
462	0.000000000	.650996744	462	2
461	0.000000000	-.250786729	462	3
463	0.000000000	-.329658231	462	4
482	0.000000000	-.035275902	462	5
442	0.000000000	-.035275902	462	6
-462	.263009043	0.000000000	462	99
463	0.000000000	0.000000000	463	1
462	0.000000000	.349376106	463	2
463	0.000000000	-.390982236	463	3
461	0.000000000	-.104590299	463	4
464	0.000000000	.231068853	463	5
465	0.000000000	-.084872424	463	6
-463	0.000000000	0.000000000	463	99
464	0.000000000	0.000000000	464	1
464	0.000000000	.741736545	464	2
463	0.000000000	-.250786729	464	3
465	0.000000000	-.329658231	464	4
484	0.000000000	-.080645793	464	5
444	0.000000000	-.080645793	464	6
-464	.601276545	0.000000000	464	99
465	0.000000000	0.000000000	465	1
464	0.000000000	.349376106	465	2
465	0.000000000	-.390982236	465	3
463	0.000000000	-.104590299	465	4
466	0.000000000	.231068853	465	5
467	0.000000000	-.084872424	465	6
-465	0.000000000	0.000000000	465	99
466	0.000000000	0.000000000	466	1
466	0.000000000	.949180749	466	2
465	0.000000000	-.250786729	466	3
467	0.000000000	-.329658231	466	4
486	0.000000000	-.184367895	466	5
446	0.000000000	-.184367895	466	6
-466	1.374604766	0.000000000	466	99
467	0.000000000	0.000000000	467	1
466	0.000000000	.349376106	467	2
467	0.000000000	-.390982236	467	3
465	0.000000000	-.104590299	467	4
468	0.000000000	.231068853	467	5
469	0.000000000	-.084872424	467	6
-467	0.000000000	0.000000000	467	99
468	0.000000000	0.000000000	468	1
468	0.000000000	1.423428073	468	2
467	0.000000000	-.250786729	468	3
469	0.000000000	-.329658231	468	4
488	0.000000000	-.421491557	468	5
448	0.000000000	-.421491557	468	6
-468	3.142544437	0.000000000	468	99
469	0.000000000	0.000000000	469	1
468	0.000000000	.349376106	469	2
469	0.000000000	-.390982236	469	3
467	0.000000000	-.104590299	469	4
470	0.000000000	.231068853	469	5
471	0.000000000	-.084872424	469	6
-469	0.000000000	0.000000000	469	99
470	0.000000000	0.000000000	470	1
470	0.000000000	2.507625746	470	2
469	0.000000000	-.250786729	470	3
471	0.000000000	-.329658231	470	4
490	0.000000000	-.963590394	470	5
450	0.000000000	-.963590394	470	6
-470	7.184369110	0.000000000	470	99
471	0.000000000	0.000000000	471	1
470	0.000000000	.349376106	471	2
471	0.000000000	-.390982236	471	3
469	0.000000000	-.104590299	471	4
472	0.000000000	.231068853	471	5
473	0.000000000	-.084872424	471	6
-471	0.000000000	0.000000000	471	99
472	0.000000000	0.000000000	472	1
472	0.000000000	4.986257753	472	2
471	0.000000000	-.250786729	472	3
473	0.000000000	-.329658231	472	4
492	0.000000000	-2.202906397	472	5
452	0.000000000	-2.202906397	472	6
-472	16.424365167	0.000000000	472	99
473	0.000000000	.019570605	473	1
472	0.000000000	.349376106	473	2
471	0.000000000	-.104590299	473	3
473	0.000000000	-.264356412	473	4
0	2000.000000000	4.401356640	473	6
0	0.000000000	4.403389991	473	7
0	36.100000000	4.403389990	473	8
0	72.200000000	4.403385591	473	9
0	108.300000000	4.403291124	473	10
0	144.400000000	4.402931080	473	11
0	180.500000000	4.402257929	473	12
0	216.600000000	4.401349749	473	13
0	252.700000000	4.400315293	473	14
0	288.800000000	4.399241369	473	15
0	324.900000000	4.398186443	473	16

0	361.000000000	4.397184923	473	17
0	361.000000000	4.403389991	473	18
0	2000.000000000	4.403389991	473	19
-473	0.000000000	0.000000000	473	99
482	0.000000000	0.000000000	482	1
462	0.000000000	.035275902	482	2
442	0.000000000	-.011758634	482	3
482	0.000000000	-.047034537	482	4
502	0.000000000	.035275902	482	5
522	0.000000000	-.011758634	482	6
-482	0.000000000	0.000000000	482	99
483	0.000000000	0.000000000	483	1
461	0.000000000	.038999982	483	2
483	0.000000000	-.025999988	483	3
443	0.000000000	-.012999994	483	4
501	0.000000000	.038999982	483	5
483	0.000000000	-.025999988	483	6
523	0.000000000	-.012999994	483	8
-483	0.000000000	0.000000000	483	99
484	0.000000000	0.000000000	484	1
464	0.000000000	.080645793	484	2
444	0.000000000	-.026881931	484	3
484	0.000000000	-.107527723	484	4
504	0.000000000	.080645793	484	5
524	0.000000000	-.026881931	484	6
-484	0.000000000	0.000000000	484	99
486	0.000000000	0.000000000	486	1
466	0.000000000	.184367895	486	2
446	0.000000000	-.061455965	486	3
486	0.000000000	-.245823860	486	4
506	0.000000000	.184367895	486	5
526	0.000000000	-.061455965	486	6
-486	0.000000000	0.000000000	486	99
488	0.000000000	0.000000000	488	1
468	0.000000000	.421491557	488	2
448	0.000000000	-.140497186	488	3
488	0.000000000	-.561988742	488	4
508	0.000000000	.421491557	488	5
528	0.000000000	-.140497186	488	6
-488	0.000000000	0.000000000	488	99
490	0.000000000	0.000000000	490	1
470	0.000000000	.963590394	490	2
450	0.000000000	-.321196798	490	3
490	0.000000000	-1.284787191	490	4
510	0.000000000	.963590394	490	5
530	0.000000000	-.321196798	490	6
-490	0.000000000	0.000000000	490	99
492	0.000000000	0.000000000	492	1
472	0.000000000	2.202906397	492	2
452	0.000000000	-.734302132	492	3
492	0.000000000	-2.937208529	492	4
512	0.000000000	2.202906397	492	5
532	0.000000000	-.734302132	492	6
-492	0.000000000	0.000000000	492	99
501	0.000000000	0.000000000	501	1
502	0.000000000	.231068853	501	2
501	0.000000000	-.146196429	501	3
503	0.000000000	-.084872424	501	4
501	-10.297326050	0.000000000	501	5
1	1.695060300	0.000000000	501	6
4	1.154744000	0.000000000	501	7
33	.410269000	0.000000000	501	8
115	5.342192450	0.000000000	501	9
116	1.695060300	0.000000000	501	10
501	0.000000000	-.077999965	501	11
523	0.000000000	.038999982	501	12
483	0.000000000	.038999982	501	13
-501	-.0356		501	99
502	0.000000000	0.000000000	502	1
502	0.000000000	.650996764	502	2
501	0.000000000	-.250786729	502	3
503	0.000000000	-.329658231	502	4
522	0.000000000	-.035275902	502	5
482	0.000000000	-.035275902	502	6
-502	.263009043	0.000000000	502	99
503	0.000000000	0.000000000	503	1
502	0.000000000	.349376106	503	2
503	0.000000000	-.390982236	503	3
501	0.000000000	-.104590299	503	4
504	0.000000000	.231068853	503	5
505	0.000000000	-.084872424	503	6
-503	0.000000000	0.000000000	503	99
504	0.000000000	0.000000000	504	1
504	0.000000000	.741736545	504	2
503	0.000000000	-.250786729	504	3
505	0.000000000	-.329658231	504	4
524	0.000000000	-.080645793	504	5
484	0.000000000	-.080645793	504	6
-504	.601276545	0.000000000	504	99
505	0.000000000	0.000000000	505	1
504	0.000000000	.349376106	505	2
505	0.000000000	-.390982236	505	3
503	0.000000000	-.104590299	505	4
506	0.000000000	.231068853	505	5
507	0.000000000	-.084872424	505	6
-505	0.000000000	0.000000000	505	99
506	0.000000000	0.000000000	506	1
506	0.000000000	.949180749	506	2
505	0.000000000	-.250786729	506	3
507	0.000000000	-.329658231	506	4
526	0.000000000	-.184367895	506	5
486	0.000000000	-.184367895	506	6
-506	1.374604766	0.000000000	506	99
507	0.000000000	0.000000000	507	1
506	0.000000000	.349376106	507	2
507	0.000000000	-.390982236	507	3
505	0.000000000	-.104590299	507	4
508	0.000000000	.231068853	507	5
509	0.000000000	-.084872424	507	6
-507	0.000000000	0.000000000	507	99
508	0.000000000	0.000000000	508	1
508	0.000000000	1.423428073	508	2
507	0.000000000	-.250786729	508	3
509	0.000000000	-.329658231	508	4
528	0.000000000	-.421491557	508	5
488	0.000000000	-.421491557	508	6
-508	3.142544437	0.000000000	508	99
509	0.000000000	0.000000000	509	1
508	0.000000000	.349376106	509	2
509	0.000000000	-.390982236	509	3
507	0.000000000	-.104590299	509	4
510	0.000000000	.231068853	509	5
511	0.000000000	-.084872424	509	6
-509	0.000000000	0.000000000	509	99
510	0.000000000	0.000000000	510	1
510	0.060000000	2.507625746	510	2
509	0.000000000	-.250786729	510	3
511	0.000000000	-.329658231	510	4
530	0.000000000	-.963590394	510	5
490	0.000000000	-.963590394	510	6
-510	7.184309110	0.000000000	510	99
511	0.000000000	0.000000000	511	1

510	0.000000000	.349376106	511	2
511	0.000000000	-.390982236	511	3
509	0.000000000	-.104590299	511	4
512	0.000000000	.231068853	511	5
513	0.000000000	-.084872424	511	6
-511	0.000000000	0.000000000	511	99
512	0.000000000	0.000000000	512	1
512	0.000000000	4.986257753	512	2
511	0.000000000	-.250786729	512	3
513	0.000000000	-.329658231	512	4
532	0.000000000	-2.202906397	512	5
492	0.000000000	-2.202906397	512	6
-512	16.424365167	0.000000000	512	99
513	0.000000000	.019167837	513	1
512	0.000000000	.349376106	513	2
511	0.000000000	-.104590299	513	3
513	0.000000000	-.263933644	513	4
0	>000.000000000	4.306498853	513	6
0	0.000000000	4.308267035	513	7
0	36.100000000	4.308267035	513	8
0	72.200000000	4.308264296	513	9
0	108.300000000	4.308195652	513	10
0	144.400000000	4.307909915	513	11
0	180.500000000	4.307144964	513	12
0	216.600000000	4.306554683	513	13
0	252.700000000	4.305629767	513	14
0	288.800000000	4.304650079	513	15
0	324.900000000	4.303672239	513	16
0	361.000000000	4.302731731	513	17
0	361.000000000	4.308267035	513	18
0	>000.000000000	4.308267035	513	19
-513	0.000000000	0.000000000	513	99
522	0.000000000	0.000000000	522	1
502	0.000000000	.035275902	522	2
482	0.000000000	-.011758634	522	3
522	0.000000000	-.047034537	522	4
542	0.000000000	.035275902	522	5
562	0.000000000	-.011758634	522	6
-522	0.000000000	0.000000000	522	99
523	0.000000000	0.000000000	523	1
501	0.000000000	.038999982	523	2
523	0.000000000	-.025999988	523	3
483	0.000000000	-.012999994	523	4
541	0.000000000	.038999982	523	5
523	0.000000000	-.025999988	523	6
563	0.000000000	-.012999994	523	7
-523	0.000000000	0.000000000	523	99
524	0.000000000	0.000000000	524	1
504	0.000000000	.080645793	524	2
484	0.000000000	-.026881931	524	3
524	0.000000000	-.107527723	524	4
544	0.000000000	.080645793	524	5
564	0.000000000	-.026881931	524	6
-524	0.000000000	0.000000000	524	99
526	0.000000000	0.000000000	526	1
506	0.000000000	.184367895	526	2
486	0.000000000	-.061455965	526	3
526	0.000000000	-.245823860	526	4
546	0.000000000	.184367895	526	5
566	0.000000000	-.061455965	526	6
-526	0.000000000	0.000000000	526	99
528	0.000000000	0.000000000	528	1
508	0.000000000	.421491557	528	2
488	0.000000000	-.140497186	528	3
528	0.000000000	-.561988742	528	4
548	0.000000000	.421491557	528	5
568	0.000000000	-.140497186	528	6
-528	0.000000000	0.000000000	528	99
530	0.000000000	0.000000000	530	1
510	0.000000000	.963590394	530	2
490	0.000000000	-.321196798	530	3
530	0.000000000	-1.284787191	530	4
550	0.000000000	.963590394	530	5
570	0.000000000	-.321196798	530	6
-530	0.000000000	0.000000000	530	99
532	0.000000000	0.000000000	532	1
512	0.000000000	2.202906397	532	2
492	0.000000000	-.734302132	532	3
532	0.000000000	-2.937208529	532	4
552	0.000000000	2.202906397	532	5
572	0.000000000	-.734302132	532	6
-532	0.000000000	0.000000000	532	99
541	0.000000000	0.000000000	541	1
542	0.000000000	.231068853	541	2
541	0.000000000	-.146196429	541	3
543	0.000000000	-.084872424	541	4
541	-7.959905350	0.000000000	541	5
115	.445195000	0.000000000	541	6
118	7.514710350	0.000000000	541	7
541	0.000000000	-.077999965	541	8
563	0.000000000	.038999982	541	9
523	0.000000000	.038999982	541	10
-541	-.0346		541	99
542	0.000000000	0.000000000	542	1
542	0.000000000	.650996764	542	2
541	0.000000000	-.250786729	542	3
543	0.000000000	-.329658231	542	4
562	0.000000000	-.035275902	542	5
522	0.000000000	-.035275902	542	6
-542	.263009043	0.000000000	542	99
543	0.000000000	0.000000000	543	1
542	0.000000000	.349376106	543	2
543	0.000000000	-.390982236	543	3
541	0.000000000	-.104590299	543	4
544	0.000000000	.231068853	543	5
545	0.000000000	-.084872424	543	6
-543	0.000000000	0.000000000	543	99
544	0.000000000	0.000000000	544	1
544	0.000000000	.741736545	544	2
543	0.000000000	-.250786729	544	3
545	0.000000000	-.329658231	544	4
564	0.000000000	-.080645793	544	5
524	0.000000000	-.080645793	544	6
-544	.601276545	0.000000000	544	99
545	0.000000000	0.000000000	545	1
544	0.000000000	.349376106	545	2
545	0.000000000	-.390982236	545	3
543	0.000000000	-.104590299	545	4
546	0.000000000	.231068853	545	5
547	0.000000000	-.084872424	545	6
-545	0.000000000	0.000000000	545	99
546	0.000000000	0.000000000	546	1
546	0.000000000	.949180749	546	2
545	0.000000000	-.250786729	546	3
547	0.000000000	-.329658231	546	4
566	0.000000000	-.184367895	546	5
526	0.000000000	-.184367895	546	6
-546	1.374604766	0.000000000	546	99
547	0.000000000	0.000000000	547	1
546	0.000000000	.349376106	547	2
547	0.000000000	-.390982236	547	3
545	0.000000000	-.104590299	547	4

548	0.000000000	.231068853	547	5
549	0.000000000	-.084872424	547	6
-547	0.000000000	0.000000000	547	99
548	0.000000000	0.000000000	548	1
548	0.000000000	1.423428073	548	2
547	0.000000000	-.250786729	548	3
549	0.000000000	-.329658231	548	4
568	0.000000000	-.421491557	548	5
528	0.000000000	-.421491557	548	6
-548	3.142544437	0.000000000	548	99
549	0.000000000	0.000000000	549	1
548	0.000000000	.349376106	549	2
549	0.000000000	-.390982236	549	3
547	0.000000000	-.104590299	549	4
550	0.000000000	.231068853	549	5
551	0.000000000	-.084872424	549	6
-549	0.000000000	0.000000000	549	99
550	0.000000000	0.000000000	550	1
550	0.000000000	2.507825746	550	2
549	0.000000000	-.250786729	550	3
551	0.000000000	-.329658231	550	4
570	0.000000000	-.963590394	550	5
530	0.000000000	-.963590394	550	6
-550	7.184309110	0.000000000	550	99
551	0.000000000	0.000000000	551	1
550	0.000000000	.349376106	551	2
551	0.000000000	-.390982236	551	3
549	0.000000000	-.104590299	551	4
552	0.000000000	.231068853	551	5
553	0.000000000	-.084872424	551	6
-551	0.000000000	0.000000000	551	99
552	0.000000000	0.000000000	552	1
552	0.000000000	4.986257753	552	2
551	0.000000000	-.250786729	552	3
553	0.000000000	-.329658231	552	4
572	0.000000000	-2.202906397	552	5
532	0.000000000	-2.202906397	552	6
-552	16.424365167	0.000000000	552	99
553	0.000000000	.018500286	553	1
552	0.000000000	.349376106	553	2
551	0.000000000	-.104590299	553	3
553	0.000000000	-.263286093	553	4
0	2000.000000000	4.161161339	553	6
0	0.000000000	4.162567892	553	7
0	36.100000000	4.162567892	553	8
0	72.200000000	4.162566647	553	9
0	108.300000000	4.162526331	553	10
0	144.400000000	4.162332303	553	11
0	180.500000000	4.161911934	553	12
0	216.600000000	4.161286611	553	13
0	252.700000000	4.160521775	553	14
0	288.800000000	4.159684249	553	15
0	324.900000000	4.158826126	553	16
0	361.000000000	4.157982964	553	17
0	361.000000000	4.162567892	553	18
0	2000.000000000	4.162567892	553	19
-553	0.000000000	0.000000000	553	99
562	0.000000000	0.000000000	562	1
542	0.000000000	.035275902	562	2
522	0.000000000	-.011758634	562	3
562	0.000000000	-.047034537	562	4
582	0.000000000	.035275902	562	5
602	0.000000000	-.011758634	562	6
-562	0.000000000	0.000000000	562	99
563	0.000000000	0.000000000	563	1
541	0.000000000	.038999982	563	2
563	0.000000000	-.025999988	563	3
523	0.000000000	-.012999994	563	4
581	0.000000000	.038999982	563	5
563	0.000000000	-.025999988	563	6
603	0.000000000	-.012999994	563	7
-563	0.000000000	0.000000000	563	99
564	0.000000000	0.000000000	564	1
544	0.000000000	.080645793	564	2
524	0.000000000	-.026881931	564	3
564	0.000000000	-.107527723	564	4
584	0.000000000	.080645793	564	5
604	0.000000000	-.026881931	564	6
-564	0.000000000	0.000000000	564	99
566	0.000000000	0.000000000	566	1
546	0.000000000	.184367895	566	2
526	0.000000000	-.061455965	566	3
566	0.000000000	-.245823860	566	4
586	0.000000000	.184367895	566	5
606	0.000000000	-.061455965	566	6
-566	0.000000000	0.000000000	566	99
568	0.000000000	0.000000000	568	1
548	0.000000000	.421491557	568	2
528	0.000000000	-.140497186	568	3
568	0.000000000	-.561988742	568	4
588	0.000000000	.421491557	568	5
608	0.000000000	-.140497186	568	6
-568	0.000000000	0.000000000	568	99
570	0.000000000	0.000000000	570	1
550	0.000000000	.963590394	570	2
530	0.000000000	-.321196798	570	3
570	0.000000000	-1.284787191	570	4
590	0.000000000	.963590394	570	5
610	0.000000000	-.321196798	570	6
-570	0.000000000	0.000000000	570	99
572	0.000000000	0.000000000	572	1
552	0.000000000	2.202906397	572	2
532	0.000000000	-.734302132	572	3
572	0.000000000	-2.937208529	572	4
592	0.000000000	2.202906397	572	5
612	0.000000000	-.734302132	572	6
-572	0.000000000	0.000000000	572	99
581	0.000000000	0.000000000	581	1
582	0.000000000	.231068853	581	2
581	0.000000000	-.146196429	581	3
583	0.000000000	-.084872424	581	4
581	-9.599400000	0.000000000	581	5
118	9.599400000	0.000000000	581	6
581	0.000000000	-.077999965	581	7
563	0.000000000	.038999982	581	8
603	0.000000000	.038999982	581	9
-581	-.0366		581	99
582	0.000000000	0.000000000	582	1
582	0.000000000	.650996764	582	2
581	0.000000000	-.250786729	582	3
583	0.000000000	-.329658231	582	4
602	0.000000000	-.035275902	582	5
562	0.000000000	-.035275902	582	6
-582	.263009043	0.000000000	582	99
583	0.000000000	0.000000000	583	1
582	0.000000000	.349376106	583	2
583	0.000000000	-.390982236	583	3
581	0.000000000	-.104590299	583	4
584	0.000000000	.231068853	583	5
585	0.000000000	-.084872424	583	6
-583	0.000000000	0.000000000	583	99
584	0.000000000	0.000000000	584	1

584	0.000000000	.741736545	584	2
583	0.000000000	-.2507A6729	584	3
585	0.000000000	-.329658231	584	4
604	0.000000000	-.080645793	584	5
564	0.000000000	-.080645793	584	6
-584	.601276545	0.000000000	584	99
585	0.000000000	0.000000000	585	1
584	0.000000000	.349376106	585	2
585	0.000000000	-.3909A2236	585	3
583	0.000000000	-.104590299	585	4
586	0.000000000	.2310A8853	585	5
587	0.000000000	-.084A72424	585	6
-585	0.000000000	0.000000000	585	99
586	0.000000000	0.000000000	586	1
586	0.000000000	.9491A0749	586	2
585	0.000000000	-.2507A6729	586	3
587	0.000000000	-.329658231	586	4
606	0.000000000	-.1843A7895	586	5
566	0.000000000	-.1843A7895	586	6
-586	1.374804766	0.000000000	586	99
587	0.000000000	0.000000000	587	1
586	0.000000000	.349376106	587	2
587	0.000000000	-.3909A2236	587	3
585	0.000000000	-.104590299	587	4
588	0.000000000	.2310A8853	587	5
589	0.000000000	-.084A72424	587	6
-587	0.000000000	0.000000000	587	99
589	0.000000000	0.000000000	588	1
588	0.000000000	1.42342A073	588	2
587	0.000000000	-.2507A6729	588	3
589	0.000000000	-.329658231	588	4
608	0.000000000	-.421491557	588	5
568	0.000000000	-.421491557	588	6
-588	3.142544437	0.000000000	588	99
589	0.000000000	0.000000000	589	1
588	0.000000000	.349376106	589	2
589	0.000000000	-.3909A2236	589	3
587	0.000000000	-.104590299	589	4
590	0.000000000	.2310A8853	589	5
591	0.000000000	-.084A72424	589	6
-589	0.000000000	0.000000000	589	99
590	0.000000000	0.000000000	590	1
590	0.000000000	2.507625746	590	2
589	0.000000000	-.2507A6729	590	3
591	0.000000000	-.329658231	590	4
610	0.000000000	-.963590394	590	5
570	0.000000000	-.963590394	590	6
-590	7.184309110	0.000000000	590	99
591	0.000000000	0.000000000	591	1
590	0.000000000	.349376106	591	2
591	0.000000000	-.3909A2236	591	3
589	0.000000000	-.104590299	591	4
592	0.000000000	.2310A8853	591	5
593	0.000000000	-.084A72424	591	6
-591	0.000000000	0.000000000	591	99
592	0.000000000	0.000000000	592	1
592	0.000000000	4.986257753	592	2
591	0.000000000	-.2507A6729	592	3
593	0.000000000	-.329658231	592	4
612	0.000000000	-2.202906397	592	5
572	0.000000000	-2.202906397	592	6
-592	16.42436516 7	0.000000000	592	99
593	0.000000000	.017694991	593	1
592	0.000000000	.349376106	593	2
591	0.000000000	-.104590299	593	3
593	0.000000000	-.2624A0798	593	4
0	2000.000000000	3.980347648	593	6
0	0.000000000	3.981376438	593	7
0	36.100000000	3.981376438	593	8
0	72.200000000	3.981376024	593	9
0	108.300000000	3.981356878	593	10
0	144.400000000	3.981244365	593	11
0	180.500000000	3.980967728	593	12
0	216.600000000	3.980519587	593	13
0	252.700000000	3.979936985	593	14
0	288.800000000	3.979288933	593	15
0	324.900000000	3.978559348	593	16
0	361.000000000	3.977841438	593	17
0	361.000000000	3.981376438	593	18
0	2000.000000000	3.981376438	593	19
-593	0.000000000	0.000000000	593	99
602	0.000000000	0.000000000	602	1
582	0.000000000	.035275962	602	2
562	0.000000000	-.011758634	602	3
602	0.000000000	-.047034537	602	4
622	0.000000000	.035275962	602	5
642	0.000000000	-.011758634	602	6
-602	0.000000000	0.000000000	602	99
603	0.000000000	0.000000000	603	1
581	0.000000000	.038999982	603	2
603	0.000000000	-.025999988	603	3
563	0.000000000	-.012999994	603	4
621	0.000000000	.038999982	603	5
603	0.000000000	-.025999988	603	6
643	0.000000000	-.012999994	603	7
-603	0.000000000	0.000000000	603	99
604	0.000000000	0.000000000	604	1
584	0.000000000	.080645793	604	2
564	0.000000000	-.026881931	604	3
604	0.000000000	-.107527723	604	4
624	0.000000000	.080645793	604	5
644	0.000000000	-.026881931	604	6
-604	0.000000000	0.000000000	604	99
606	0.000000000	0.000000000	606	1
586	0.000000000	.184367895	606	2
566	0.000000000	-.061455965	606	3
606	0.000000000	-.245823860	606	4
626	0.000000000	.184367895	606	5
646	0.000000000	-.061455965	606	6
-606	0.000000000	0.000000000	606	99
608	0.000000000	0.000000000	608	1
588	0.000000000	.421491557	608	2
568	0.000000000	-.140497186	608	3
608	0.000000000	-.561988742	608	4
628	0.000000000	.421491557	608	5
648	0.000000000	-.140497186	608	6
-608	0.000000000	0.000000000	608	99
610	0.000000000	0.000000000	610	1
590	0.000000000	.963590394	610	2
570	0.000000000	-.321196798	610	3
610	0.000000000	-1.284787191	610	4
630	0.000000000	.963590394	610	5
650	0.000000000	-.321196798	610	6
-610	0.000000000	0.000000000	610	99
612	0.000000000	0.000000000	612	1
592	0.000000000	2.202906397	612	2
572	0.000000000	-.734302132	612	3
612	0.000000000	-2.937208529	612	4
632	0.000000000	2.202906397	612	5
652	0.000000000	-.734302132	612	6
-612	0.000000000	0.000000000	612	99
621	0.000000000	0.000000000	621	1

622	0.000000000	.231068853	621	2
621	0.000000000	-.146196429	621	3
623	0.000000000	-.084872424	621	4
621	-9.599400000	0.000000000	621	5
118	9.599400000	0.000000000	621	6
621	0.000000000	-.077999965	621	7
643	0.000000000	.038999982	621	8
603	0.000000000	.038999982	621	9
-621	-.0396		621	99
622	0.000000000	0.000000000	622	1
622	0.000000000	.650996764	622	2
621	0.000000000	-.2507R6729	622	3
623	0.000000000	-.329658231	622	4
642	0.000000000	-.03527590Z	622	5
602	0.000000000	-.03527590Z	622	6
-622	.2630n9043	0.000000000	622	99
623	0.000000000	0.000000000	623	1
622	0.000000000	.349376106	623	2
623	0.000000000	-.3909R2236	623	3
621	0.000000000	-.104590299	623	4
624	0.000000000	.231068853	623	5
625	0.000000000	-.084872424	623	6
-623	0.000000000	0.000000000	623	99
624	0.000000000	0.000000000	624	1
624	0.000000000	.741736545	624	2
623	0.000000000	-.2507R6729	624	3
625	0.000000000	-.329658231	624	4
644	0.000000000	-.080645793	624	5
604	0.000000000	-.080645793	624	6
-624	.6012765a5	0.000000000	624	99
625	0.000000000	0.000000000	625	1
624	0.000000000	.349376106	625	2
625	0.000000000	-.3909R2236	625	3
623	0.000000000	-.104590299	625	4
626	0.000000000	.231068853	625	5
627	0.000000000	-.084872424	625	6
-625	0.000000000	0.000000000	625	99
626	0.000000000	0.000000000	626	1
626	0.000000000	.9491R0749	626	2
625	0.000000000	-.2507R6729	626	3
627	0.000000000	-.329658231	626	4
646	0.000000000	-.1843R7895	626	5
606	0.000000000	-.1843R7895	626	6
-626	1.3746n4766	0.000000000	626	99
627	0.000000000	0.000000000	627	1
626	0.000000000	.349376106	627	2
627	0.000000000	-.3909R2236	627	3
625	0.000000000	-.104590299	627	4
628	0.000000000	.231068853	627	5
629	0.000000000	-.084872424	627	6
-627	0.000000000	0.000000000	627	99
628	0.000000000	0.000000000	628	1
628	0.000000000	1.42342R073	628	2
627	0.000000000	-.2507R6729	628	3
629	0.000000000	-.329658231	628	4
648	0.000000000	-.42149155T	628	5
608	0.000000000	-.42149155T	628	6
-628	3.142544437	0.000000000	628	99
629	0.000000000	0.000000000	629	1
628	0.000000000	.349376106	629	2
629	0.000000000	-.3909R2236	629	3
627	0.000000000	-.104590299	629	4
630	0.000000000	.231068853	629	5
631	0.000000000	-.084872424	629	6
-629	0.000000000	0.000000000	629	99
630	0.000000000	0.000000000	630	1
630	0.000000000	2.507625746	630	2
629	0.000000000	-.2507R6729	630	3
631	0.000000000	-.329658231	630	4
650	0.000000000	-.963590394	630	5
610	0.000000000	-.963590394	630	6
-630	7.184309110	0.000000000	630	99
631	0.000000000	0.000000000	631	1
630	0.000000000	.349376106	631	2
631	0.000000000	-.3909R2236	631	3
629	0.000000000	-.104590299	631	4
632	0.000000000	.231068853	631	5
633	0.000000000	-.084872424	631	6
-631	0.000000000	0.000000000	631	99
632	0.000000000	0.000000000	632	1
632	0.000000000	4.986257753	632	2
631	0.000000000	-.2507R6729	632	3
633	0.000000000	-.329658231	632	4
652	0.000000000	-2.202906397	632	5
612	0.000000000	-2.202906397	632	6
-632	16.42436516T	0.000000000	632	99
633	0.000000000	.016799164	633	1
632	0.000000000	.349376106	633	2
631	0.000000000	-.104590299	633	3
633	0.000000000	-.261584971	633	4
0	2000.000000000	3.779119376	633	6
0	0.000000000	3.779815189	633	7
0	36.100000000	3.779815189	633	8
0	72.200000000	3.779815088	633	9
0	108.300000000	3.779807728	633	10
0	144.400000000	3.779752102	633	11
0	180.500000000	3.779591556	633	12
0	216.600000000	3.779301705	633	13
0	252.700000000	3.778804655	633	14
0	288.800000000	3.778099472	633	15
0	324.900000000	3.777849158	633	16
0	361.000000000	3.777271499	633	17
0	361.000000000	3.779815189	633	18
0	2000.000000000	3.779815189	633	19
-633	0.000000000	0.000000000	633	99
642	0.000000000	0.000000000	642	1
622	0.000000000	.035275902	642	2
602	0.000000000	-.011758634	642	3
642	0.000000000	-.047034537	642	4
662	0.000000000	.035275902	642	5
682	0.000000000	-.011758634	642	6
-642	0.000000000	0.000000000	642	99
643	0.000000000	0.000000000	643	1
621	0.000000000	.038999982	643	2
643	0.000000000	-.025999988	643	3
603	0.000000000	-.012999994	643	4
661	0.000000000	.038999982	643	5
643	0.000000000	-.025999988	643	6
683	0.000000000	-.012999994	643	7
-643	0.000000000	0.000000000	643	99
644	0.000000000	0.000000000	644	1
624	0.000000000	.080645793	644	2
604	0.000000000	-.026881931	644	3
644	0.000000000	-.107527723	644	4
664	0.000000000	.080645793	644	5
684	0.000000000	-.026881931	644	6
-644	0.000000000	0.000000000	644	99
646	0.000000000	0.000000000	646	1
626	0.000000000	.184367895	646	2
606	0.000000000	-.061455965	646	3
646	0.000000000	-.245823860	646	4
666	0.000000000	.184367895	646	5

686	0.000000000	-.061455965	646	6
-646	0.000000000	0.000000000	646	99
648	0.000000000	0.000000000	648	1
628	0.000000000	.421491557	648	2
608	0.000000000	-.140497186	648	3
648	0.000000000	-.561988742	648	4
668	0.000000000	.421491557	648	5
688	0.000000000	-.140497186	648	6
-648	0.000000000	0.000000000	648	99
650	0.000000000	0.000000000	650	1
630	0.000000000	.963590394	650	2
610	0.000000000	-.321196798	650	3
650	0.000000000	-1.284787191	650	4
670	0.000000000	.963590394	650	5
690	0.000000000	-.321196798	650	6
-650	0.000000000	0.000000000	650	99
652	0.000000000	0.000000000	652	1
632	0.000000000	2.202906397	652	2
612	0.000000000	-.734302132	652	3
652	0.000000000	-2.937208529	652	4
672	0.000000000	2.202906397	652	5
692	0.000000000	-.734302132	652	6
-652	0.000000000	0.000000000	652	99
661	0.000000000	0.000000000	661	1
662	0.000000000	.231068853	661	2
661	0.000000000	-.146196429	661	3
663	0.000000000	-.084872424	661	4
661	-4.785307080	0.000000000	661	5
118	.938937000	0.000000000	661	6
120	3.846370080	0.000000000	661	7
661	0.000000000	-.077999965	661	8
683	0.000000000	.038999982	661	9
643	0.000000000	.038999982	661	10
-661	-.0396		661	99
662	0.000000000	0.000000000	662	1
662	0.000000000	.650996744	662	2
661	0.000000000	-.250786729	662	3
663	0.000000000	-.329658231	662	4
682	0.000000000	-.035275902	662	5
642	0.000000000	-.035275902	662	6
-662	.263009043	0.000000000	662	99
663	0.000000000	0.000000000	663	1
662	0.000000000	.349376106	663	2
663	0.000000000	-.390982236	663	3
661	0.000000000	-.104590299	663	4
664	0.000000000	.231068853	663	5
665	0.000000000	-.084872424	663	6
-663	0.000000000	0.000000000	663	99
664	0.000000000	0.000000000	664	1
664	0.000000000	.741736545	664	2
663	0.000000000	-.250786729	664	3
665	0.000000000	-.329658231	664	4
684	0.000000000	-.080445793	664	5
644	0.000000000	-.080445793	664	6
-664	.601276545	0.000000000	664	99
665	0.000000000	0.000000000	665	1
664	0.000000000	.349376106	665	2
665	0.000000000	-.390982236	665	3
663	0.000000000	-.104590299	665	4
666	0.000000000	.231068853	665	5
667	0.000000000	-.084872424	665	6
-665	0.000000000	0.000000000	665	99
666	0.000000000	0.000000000	666	1
666	0.000000000	.949180749	666	2
665	0.000000000	-.250786729	666	3
667	0.000000000	-.329658231	666	4
686	0.000000000	-.184367895	666	5
646	0.000000000	-.184367895	666	6
-666	1.374604766	0.000000000	666	99
667	0.000000000	0.000000000	667	1
666	0.000000000	.349376106	667	2
667	0.000000000	-.390982236	667	3
665	0.000000000	-.104590299	667	4
668	0.000000000	.231068853	667	5
669	0.000000000	-.084872424	667	6
-667	0.000000000	0.000000000	667	99
668	0.000000000	0.000000000	668	1
668	0.000000000	1.423428073	668	2
667	0.000000000	-.250786729	668	3
669	0.000000000	-.329658231	668	4
688	0.000000000	-.421491557	668	5
648	0.000000000	-.421491557	668	6
-668	3.142544437	0.000000000	668	99
669	0.000000000	0.000000000	669	1
668	0.000000000	.349376106	669	2
669	0.000000000	-.390982236	669	3
667	0.000000000	-.104590299	669	4
670	0.000000000	.231068853	669	5
671	0.000000000	-.084872424	669	6
-669	0.000000000	0.000000000	669	99
670	0.000000000	0.000000000	670	1
670	0.000000000	2.507625746	670	2
669	0.000000000	-.250786729	670	3
671	0.000000000	-.329658231	670	4
690	0.000000000	-.963590394	670	5
650	0.000000000	-.963590394	670	6
-670	7.184309110	0.000000000	670	99
671	0.000000000	0.000000000	671	1
670	0.000000000	.349376106	671	2
671	0.000000000	-.390982236	671	3
669	0.000000000	-.104590299	671	4
672	0.000000000	.231068853	671	5
673	0.000000000	-.084872424	671	6
-671	0.000000000	0.000000000	671	99
672	0.000000000	0.000000000	672	1
672	0.000000000	4.986257753	672	2
671	0.000000000	-.250786729	672	3
673	0.000000000	-.329658231	672	4
692	0.000000000	-2.202906397	672	5
652	0.000000000	-2.202906397	672	6
-672	16.424369167	0.000000000	672	99
673	0.000000000	.015869327	673	1
672	0.000000000	.349376106	673	2
671	0.000000000	-.104590299	673	3
673	0.000000000	-.260655133	673	4
0	2000.000000000	3.570164046	673	6
0	0.000000000	3.570601567	673	7
0	36.100000000	3.570601567	673	8
0	72.200000000	3.570601549	673	9
0	108.300000000	3.570599255	673	10
0	144.400000000	3.570575828	673	11
0	180.500000000	3.570493845	673	12
0	216.600000000	3.570325141	673	13
0	252.700000000	3.570064805	673	14
0	288.800000000	3.569725306	673	15
0	324.900000000	3.569326556	673	16
0	361.000000000	3.568889089	673	17
0	361.000000000	3.570601567	673	18
0	2000.000000000	3.570601567	673	19
-673	0.000000000	0.000000000	673	99
682	0.000000000	0.000000000	682	1
662	0.000000000	.035275902	682	2

642	0.000000000	-.011758634	682	3
682	0.000000000	-.047034537	682	4
702	0.000000000	.035275902	682	5
722	0.000000000	-.011758634	682	6
-682	0.000000000	0.000000000	682	99
683	0.000000000	0.000000000	683	1
661	0.000000000	.038999982	683	2
683	0.000000000	-.025999988	683	3
643	0.000000000	-.012999994	683	4
701	0.000000000	.038999982	683	5
683	0.000000000	-.025999988	683	6
723	0.000000000	-.012999994	683	7
-683	0.000000000	0.000000000	683	99
684	0.000000000	0.000000000	684	1
664	0.000000000	.080645793	684	2
644	0.000000000	-.026881931	684	3
684	0.000000000	-.107527723	684	4
704	0.000000000	.080645793	684	5
724	0.000000000	-.026881931	684	6
-684	0.000000000	0.000000000	684	99
686	0.000000000	0.000000000	686	1
666	0.000000000	.184367895	686	2
646	0.000000000	-.061455965	686	3
686	0.000000000	-.245823860	686	4
706	0.000000000	.184367895	686	5
726	0.000000000	-.061455965	686	6
-686	0.000000000	0.000000000	686	99
688	0.000000000	0.000000000	688	1
668	0.000000000	.421491557	688	2
648	0.000000000	-.140497186	688	3
688	0.000000000	-.561988742	688	4
708	0.000000000	.421491557	688	5
728	0.000000000	-.140497186	688	6
-688	0.000000000	0.000000000	688	99
690	0.000000000	0.000000000	690	1
670	0.000000000	.963590394	690	2
650	0.000000000	-.321196798	690	3
690	0.000000000	-1.284787151	690	4
710	0.000000000	.963590394	690	5
730	0.000000000	-.321196798	690	6
-690	0.000000000	0.000000000	690	99
692	0.000000000	0.000000000	692	1
672	0.000000000	2.202906397	692	2
652	0.000000000	-.734302132	692	3
692	0.000000000	-2.937208529	692	4
712	0.000000000	2.202906397	692	5
732	0.000000000	-.734302132	692	6
-692	0.000000000	0.000000000	692	99
701	0.000000000	0.000000000	701	1
702	0.000000000	.231068853	701	2
701	0.000000000	-.146196429	701	3
703	0.000000000	-.084872424	701	4
701	0.000000000	-.077999965	701	5
723	0.000000000	.038999982	701	6
683	0.000000000	.038999982	701	7
-701	-.03586		701	99
702	0.000000000	0.000000000	702	1
702	0.000000000	.650996744	702	2
701	0.000000000	-.250786729	702	3
703	0.000000000	-.329658231	702	4
722	0.000000000	-.035275902	702	5
682	0.000000000	-.035275902	702	6
-702	.263009043	0.000000000	702	99
703	0.000000000	0.000000000	703	1
702	0.000000000	.349376106	703	2
703	0.000000000	-.390982236	703	3
701	0.000000000	-.104590299	703	4
704	0.000000000	.231068853	703	5
705	0.000000000	-.084872424	703	6
-703	0.000000000	0.000000000	703	99
704	0.000000000	0.000000000	704	1
704	0.000000000	.741736545	704	2
703	0.000000000	-.250786729	704	3
705	0.000000000	-.329658231	704	4
724	0.000000000	-.080645793	704	5
684	0.000000000	-.080645793	704	6
-704	.601276545	0.000000000	704	99
705	0.000000000	0.000000000	705	1
704	0.000000000	.349376106	705	2
705	0.000000000	-.390982236	705	3
703	0.000000000	-.104590299	705	4
706	0.000000000	.231068853	705	5
707	0.000000000	-.084872424	705	6
-705	0.000000000	0.000000000	705	99
706	0.000000000	0.000000000	706	1
706	0.000000000	.949180749	706	2
705	0.000000000	-.250786729	706	3
707	0.000000000	-.329658231	706	4
726	0.000000000	-.184367895	706	5
686	0.000000000	-.184367895	706	6
-706	1.374604766	0.000000000	706	99
707	0.000000000	0.000000000	707	1
706	0.000000000	.349376106	707	2
707	0.000000000	-.390982236	707	3
705	0.000000000	-.104590299	707	4
708	0.000000000	.231068853	707	5
709	0.000000000	-.084872424	707	6
-707	0.000000000	0.000000000	707	99
708	0.000000000	0.000000000	708	1
708	0.000000000	1.423428073	708	2
707	0.000000000	-.250786729	708	3
709	0.000000000	-.329658231	708	4
728	0.000000000	-.421491557	708	5
688	0.000000000	-.421491557	708	6
-708	3.142544437	0.000000000	708	99
709	0.000000000	0.000000000	709	1
708	0.000000000	.349376106	709	2
709	0.000000000	-.390982236	709	3
707	0.000000000	-.104590299	709	4
710	0.000000000	.231068853	709	5
711	0.000000000	-.084872424	709	6
-709	0.000000000	0.000000000	709	99
710	0.000000000	0.000000000	710	1
710	0.000000000	2.507625746	710	2
709	0.000000000	-.250786729	710	3
711	0.000000000	-.329658231	710	4
730	0.000000000	-.963590394	710	5
690	0.000000000	-.963590394	710	6
-710	7.184309110	0.000000000	710	99
711	0.000000000	0.000000000	711	1
710	0.000000000	.349376106	711	2
711	0.000000000	-.390982236	711	3
709	0.000000000	-.104590299	711	4
712	0.000000000	.231068853	711	5
713	0.000000000	-.084872424	711	6
-711	0.000000000	0.000000000	711	99
712	0.000000000	0.000000000	712	1
712	0.000000000	4.986257753	712	2
711	0.000000000	-.250786729	712	3
713	0.000000000	-.329658231	712	4
732	0.000000000	-2.202906397	712	5
692	0.000000000	-2.202906397	712	6

-712	16.424365167	0.000000000	712	99
713	0.000000000	.014947090	713	1
712	0.000000000	.3493761n6	713	2
711	0.000000000	-.104590299	713	3
713	0.000000000	-.259732896	713	4
0	2000.000000000	3.362841068	713	6
0	0.000000000	3.363n98037	713	7
0	36.100000000	3.363098037	713	8
0	72.200000000	3.363098035	713	9
0	108.300000000	3.363n97454	713	10
0	144.400000000	3.363n89049	713	11
0	180.500000000	3.363052264	713	12
0	216.600000000	3.362964084	713	13
0	252.700000000	3.362812249	713	14
0	288.800000000	3.362597273	713	15
0	324.900000000	3.362328082	713	16
0	361.000000000	3.362017186	713	17
0	361.000000000	3.363n98037	713	18
0	2000.000000000	3.363n98037	713	19
-713	0.000000000	0.000000000	713	99
722	0.000000000	.000778841	722	1
702	0.000000000	.0352759n2	722	2
682	0.000000000	-.011758634	722	3
722	0.000000000	-.024296130	722	4
0	2000.000000000	.175122058	722	6
0	0.000000000	.175243942	722	7
0	36.100000000	.175243942	722	8
0	72.200000000	.175243126	722	9
0	108.300000000	.175232870	722	10
0	144.400000000	.175204122	722	11
0	180.500000000	.175159712	722	12
0	216.600000000	.175107074	722	13
0	252.700000000	.175052381	722	14
0	288.800000000	.174999457	722	15
0	324.900000000	.174950292	722	16
0	361.000000000	.174905722	722	17
0	361.000000000	.175243942	722	18
0	2000.000000000	.175243942	722	19
-722	0.000000000	0.000000000	722	99
723	0.000000000	0.000000000	723	1
701	0.000000000	.0389999n2	723	2
723	0.000000000	-.025999998	723	3
683	0.000000000	-.012999994	723	4
-723	0.000000000	0.000000000	723	99
724	0.000000000	.001766070	724	1
704	0.000000000	.080445793	724	2
684	0.000000000	-.026881931	724	3
724	0.000000000	-.055529932	724	4
0	2000.000000000	.397100108	724	6
0	0.000000000	.397366092	724	7
0	36.100000000	.397366091	724	8
0	72.200000000	.397364486	724	9
0	108.300000000	.397343269	724	10
0	144.400000000	.397282055	724	11
0	180.500000000	.397185789	724	12
0	216.600000000	.397070315	724	13
0	252.700000000	.396949293	724	14
0	288.800000000	.396831408	724	15
0	324.900000000	.396721318	724	16
0	361.000000000	.396621075	724	17
0	361.000000000	.397366092	724	18
0	2000.000000000	.397366092	724	19
-724	0.000000000	0.000000000	724	99
726	0.000000000	.003964558	726	1
706	0.000000000	.184367895	726	2
686	0.000000000	-.061455965	726	3
726	0.000000000	-.126876487	726	4
0	2000.000000000	.891478934	726	6
0	0.000000000	.892026215	726	7
0	36.100000000	.892026215	726	8
0	72.200000000	.892023608	726	9
0	108.300000000	.891985009	726	10
0	144.400000000	.891866120	726	11
0	180.500000000	.891671400	726	12
0	216.600000000	.891431371	726	13
0	252.700000000	.891178823	726	14
0	288.800000000	.890921158	726	15
0	324.900000000	.890681415	726	16
0	361.000000000	.890460939	726	17
0	361.000000000	.892026215	726	18
0	2000.000000000	.892026215	726	19
-726	0.000000000	0.000000000	726	99
728	0.000000000	.008713955	728	1
708	0.000000000	.421491557	728	2
688	0.000000000	-.140497186	728	3
728	0.000000000	-.289708326	728	4
0	2000.000000000	1.959653597	728	6
0	0.000000000	1.960641585	728	7
0	36.100000000	1.960641584	728	8
0	72.200000000	1.960638853	728	9
0	108.300000000	1.960586542	728	10
0	144.400000000	1.960399790	728	11
0	180.500000000	1.960064497	728	12
0	216.600000000	1.959624717	728	13
0	252.700000000	1.959133402	728	14
0	288.800000000	1.958630944	728	15
0	324.900000000	1.958143161	728	16
0	361.000000000	1.957684546	728	17
0	361.000000000	1.960641585	728	18
0	2000.000000000	1.960641585	728	19
-728	0.000000000	0.000000000	728	99
730	0.000000000	.018394058	730	1
710	0.000000000	.963590394	730	2
690	0.000000000	-.321196798	730	3
730	0.000000000	-.660787854	730	4
0	2000.000000000	4.137322934	730	6
0	0.000000000	4.138666674	730	7
0	36.100000000	4.138666674	730	8
0	72.200000000	4.138665615	730	9
0	108.300000000	4.138629464	730	10
0	144.400000000	4.138450223	730	11
0	180.500000000	4.138054518	730	12
0	216.600000000	4.137458384	730	13
0	252.700000000	4.136722606	730	14
0	288.800000000	4.135911373	730	15
0	324.900000000	4.135075714	730	16
0	361.000000000	4.134251032	730	17
0	361.000000000	4.138666674	730	18
0	2000.000000000	4.138666674	730	19
-730	0.000000000	0.000000000	730	99
732	0.000000000	.036366261	732	1
712	0.000000000	2.202906397	732	2
692	0.000000000	-.734302132	732	3
732	0.000000000	-1.504970526	732	4
0	2000.000000000	8.181403274	732	6
0	0.000000000	8.182415798	732	7
0	36.100000000	8.182415798	732	8
0	72.200000000	8.182415754	732	9
0	108.300000000	8.182410353	732	10
0	144.400000000	8.182355594	732	11
0	180.500000000	8.182164860	732	12
0	216.600000000	8.181773605	732	13

```
    0        252.7000000000          8.1811712108  732   14
    0        288.8000000000          8.1803186975  732   15
    0        324.9000000000          8.1794667093  732   16
    0        361.0000000000          8.1786568972  732   17
    0        361.0000000000          8.1824115798  732   18
    0       2000.0000000000          8.1824115798  732   19
 -732          0.0000000000          0.0000000000  732   99
                                                    -0   -0
1.85   1.0E-02  30.0        1   10   90.0          225.0      732  1.0
1.85   1.0E-03   1.0        1   10   91.0                     732  1.0
1.85   1.0E-02  30.0        1   10  361.0                     732  1.0
0.00
                                                    -0    9    5   -0
                                                    -0   -0    A   -0
```

APPENDIX III

FINITE-DIFFERENCE EQUATIONS AND BOUNDARY CONDITIONS FOR THERMAL MODELS OF LUNAR MEDIUM

Figure 10 in the body of the report illustrates a typical annular element used in the finite-difference representation of the lunar medium. Shown in the figure are the coordinate system and the dimensions of the ring. According to the Method of Zones, a parabolic temperature distribution is assumed within each element. Expressions for the net heat flow from faces 1 through 4 are found in terms of the average surface temperatures, T_1 through T_4 and the mean temperature of the element, T_m:

$$Q_1 = \frac{2\pi k \ell a}{b - a}\left(6T_m - \frac{3b + 5a}{b + a}T_1 - \frac{3b + a}{b + a}T_2\right) \qquad \text{(III-1)}$$

$$Q_2 = \frac{2\pi k \ell b}{b - a}\left(6T_m - \frac{5b + 3a}{b + a}T_2 - \frac{b + 3a}{b + a}T_1\right) \qquad \text{(III-2)}$$

$$Q_3 = \frac{k\pi(b^2 - a^2)}{\ell}\left(6T_m - 4T_3 + 2T_4\right) \qquad \text{(III-3)}$$

$$Q_4 = \frac{k\pi(b^2 - a^2)}{\ell}\left(6T_m - 4T_4 + 2T_3\right) \qquad \text{(III-4)}$$

The mean temperature of each annular zone is described by:

$$Q_1 + Q_2 + Q_3 + Q_4 + \rho\ \pi\ (b^2 - a^2)\ \ell\ C\ \frac{dT_m}{dt} = 0 \qquad \text{(III-5)}$$

where ρ is the density and C is the specific heat of the lunar medium.

Thermal connection between the zones is made by way of the net heat flows at the zone surfaces. For example, the heat flow from the outer surface of an element (surface 2 in Figure 10) is equal to the negative of the heat flow from the inside surface (1) of the surrounding annular ring.

At the outer boundaries, the heat flow from the surfaces are matched with the form of solution predicted for a spherical surface heat source:

$$Q'' = \frac{k}{R^*} T\ (R^*,\ t) - \frac{k}{R^*} T_\infty + f\ (Q_o,\ R^*,\ t) \qquad \text{(III-6)}$$

where

Q'' - heat flux at boundary surface

R^* - distance from center of source

Q_o - strength of heat source

T_∞ - initial temperature of lunar medium

and

$$f\ (Q_o,\ R^*,\ t) = \frac{Q_o}{8\pi R_o R^*}\left[\text{erfc}\left(\frac{R_o - R^*}{2\sqrt{\alpha t}}\right) - \text{erfc}\left(\frac{R_o + R^*}{2\sqrt{\alpha t}}\right)\right] \qquad \text{(III-7a)}$$

$$\text{erfc}\ (z) = 1 - \frac{2}{\sqrt{\pi}} \int_o^z e^{-x^2}\, dx \qquad \text{(III-7b)}$$

Applying these equations over a boundary surface of area A_b, the total heat flow at the boundary is expressed as:

$$Q_b = A_b\ k\ T_b/R^* + P_b\ (R^*,\ t) \qquad \text{(III-8a)}$$

where

$$P_b\ (R^*,\ t) = A_b\ f\ (Q_o,\ R^*,\ t) - A_b\ k\ T_\infty/R^* \quad . \qquad \text{(III-8b)}$$

The quantity P_b represents a negative power applied to the boundary surface (See Appendix I). The value used for R^* corresponds to the radial distance from the center of the gradient sensor to the center position on the boundary surface.

APPENDIX IV

TABULATION OF PERFORMANCE PREDICTIONS IN THE LUNAR ENVIRONMENT

Table No.	Description
IV-1	Predicted Performance for Mode 2 Operation in Lunar Environment, Experiment Location 2
IV-2	Predicted Performance for Mode 2 Operation in Lunar Environment, Experiment Location 4
IV-3	Predicted Performance for Mode 3 Operation in Lunar Environment
IV-4	Temperature Decay of Ring Sensor after Heating Period in Mode 3 Experiment
IV-5	Temperature Decay of Gradient Sensor after Heating Period of Mode 3 Experiment
IV-6	Predicted Performance for Mode 3 Parametric Studies
IV-7	Influence of Interface between Probe Alignment Springs and Drill Case
IV-8	Influence on Radiation Coupling between Drill Casing and the Moon

TABLE IV-1

PREDICTED PERFORMANCE FOR MODE 2
OPERATION IN LUNAR ENVIRONMENT,
EXPERIMENT LOCATION 2

(ρc = 1.339 w-sec/cc °K)

$K = 2.1 \times 10^{-5}$ w/cm °K

Time after Start of Heating (min)	Temperature Rise of Gradient Sensor (°K) T = 205°K	T = 225°K	T = 245°K
0	0.000	0.000	0.000
15	0.084	0.079	0.076
30	0.151	0.142	0.134
45	0.204	0.191	0.179
60	0.247	0.229	0.214
91	0.311	0.286	0.266
121	0.357	0.327	0.303
151	0.394	0.360	0.332
181	0.423	0.386	0.357
241	0.468	0.426	0.393
301	0.502	0.457	0.420
361	0.529	0.481	0.443
421	0.552	0.502	0.461
481	0.572	0.519	0.477
541	0.588	0.534	0.490
601	0.603	0.547	0.502
722	0.627	0.568	0.520
842	0.646	0.586	0.535
962	0.663	0.600	0.548
1082	0.677	0.612	0.558
1202	0.689	0.623	0.567

TABLE IV-1 - Cont'd.

$K = 7.3 \times 10^{-5}$ w/cm °K

Time after Start of Heating (min)	Temperature Rise of Gradient Sensor (°K) T = 205°K	T = 225°K	T = 245°K
0	0.000	0.000	0.000
15	0.082	0.077	0.073
30	0.146	0.136	0.126
45	0.195	0.179	0.165
60	0.233	0.212	0.194
91	0.285	0.257	0.233
121	0.321	0.287	0.259
151	0.347	0.309	0.279
181	0.367	0.327	0.295
241	0.396	0.351	0.317
301	0.416	0.370	0.334
361	0.432	0.385	0.348
421	0.446	0.397	0.359
481	0.457	0.407	0.369
541	0.466	0.416	0.377
601	0.474	0.423	0.384
722	0.488	0.436	0.396
842	0.500	0.447	0.406
962	0.509	0.456	0.414
1082	0.517	0.463	0.421
1202	0.525	0.470	0.427

TABLE IV-1 - Cont'd.

$K = 1.5 \times 10^{-4}$ w/cm °K

Time after Start of Heating (min)	Temperature Rise of Gradient Sensor (°K) T = 205°K	T = 225°K	T = 245°K
0	0.000	0.000	0.000
15	0.081	0.076	0.071
30	0.144	0.133	0.122
45	0.190	0.173	0.158
60	0.226	0.203	0.184
91	0.273	0.242	0.216
121	0.303	0.267	0.237
151	0.325	0.284	0.252
181	0.340	0.297	0.264
241	0.361	0.315	0.280
301	0.376	0.328	0.292
361	0.387	0.338	0.301
421	0.395	0.346	0.308
481	0.403	0.353	0.315
541	0.409	0.358	0.320
601	0.414	0.364	0.325
722	0.423	0.373	0.333
842	0.430	0.379	0.340
962	0.436	0.385	0.345
1082	0.441	0.389	0.350
1202	0.446	0.393	0.354

TABLE IV-1 - Cont'd.

$K = 4.2 \times 10^{-4}$ w/cm °K

Time after Start of Heating (min)	Temperature Rise of Gradient Sensor (°K) T = 205°K	T = 225°K	T = 245°K
0	0.000	0.000	0.000
15	0.080	0.075	0.069
30	0.141	0.129	0.117
45	0.185	0.166	0.149
60	0.217	0.192	0.171
91	0.258	0.224	0.196
121	0.282	0.242	0.210
51	0.298	0.254	0.219
181	0.308	0.262	0.226
241	0.321	0.272	0.235
301	0.329	0.278	0.241
361	0.335	0.283	0.245
421	0.339	0.287	0.249
481	0.342	0.290	0.252
541	0.345	0.293	0.254
601	0.347	0.295	0.256
722	0.350	0.298	0.259
842	0.353	0.301	0.261
962	0.355	0.303	0.263
1082	0.357	0.304	0.265
1202	0.358	0.305	0.266

TABLE IV-2

PREDICTED PERFORMANCE FOR MODE 2
OPERATION IN LUNAR ENVIRONMENT,
EXPERIMENT LOCATION 4

(ρc = 1.339 w-sec/cc °K)

$K = 2.1 \times 10^{-5}$ w/cm °K

Time after Start of Heating (min)	Temperature Rise of Gradient Sensor (°K)		
	T = 205°K	T = 225°K	T = 245°K
0	0.000	0.000	0.000
15	0.090	0.085	0.081
30	0.163	0.153	0.144
45	0.176	0.206	0.193
60	0.268	0.248	0.232
91	0.339	0.312	0.290
121	0.392	0.360	0.333
151	0.435	0.398	0.368
181	0.470	0.430	0.398
241	0.524	0.480	0.446
301	0.568	0.521	0.484
361	0.605	0.556	0.517
421	0.636	0.586	0.546
481	0.664	0.612	0.571
541	0.688	0.636	0.593
601	0.711	0.657	0.613
722	0.749	0.694	0.648
842	0.781	0.725	0.678
962	0.810	0.753	0.704
1082	-	0.777	0.727
1202	-	-	-

TABLE IV-2 - Cont'd.

$K = 1.5 \times 10^{-4}$ w/cm °K

Time after Start of Heating (min)	Temperature Rise of Gradient Sensor (°K)		
	T = 205°K	T = 225°K	T = 245°K
0	0.000	0.000	0.000
15	0.087	0.082	0.076
30	0.155	0.143	0.132
45	0.206	0.187	0.170
60	0.245	0.219	0.198
91	0.297	0.262	0.234
121	0.330	0.289	0.256
151	0.354	0.308	0.273
181	0.372	0.323	0.286
241	0.395	0.343	0.303
301	0.412	0.357	0.317
361	0.425	0.369	0.328
421	0.435	0.378	0.337
481	0.443	0.386	0.344
541	0.450	0.393	0.351
601	0.457	0.399	0.357
722	0.467	0.410	0.367
842	0.476	0.418	0.375
962	0.483	0.425	0.382
1082	0.490	0.431	0.389
1202	0.495	0.437	0.394

TABLE IV-2 - Cont'd.

$K = 7.3 \times 10^{-5}$ w/cm °K

Time after Start of Heating (min)	Temperature Rise of Gradient Sensor (°K) T = 205°K	T = 225°K	T = 245°K
0	0.000	0.000	0.000
15	0.088	0.083	0.078
30	0.158	0.146	0.136
45	0.211	0.193	0.178
60	0.252	0.229	0.209
91	0.310	0.278	0.252
121	0.350	0.312	0.281
151	0.379	0.337	0.303
181	0.402	0.357	0.321
241	0.435	0.385	0.347
301	0.459	0.408	0.368
361	0.478	0.425	0.385
421	0.494	0.440	0.399
481	0.508	0.453	0.412
541	0.520	0.465	0.423
601	0.531	0.475	0.433
722	0.549	0.493	0.449
842	0.564	0.507	0.463
962	0.576	0.520	0.476
1082	0.588	0.531	0.486
1202	0.598	0.541	0.496

TABLE IV-2 - Cont'd.

$K = 4.2 \times 10^{-4}$ w/cm °K

Time after Start of Heating (min)	Temperature Rise of Gradient Sensor (°K) T = 205°K	T = 225°K	T = 245°K
0	0.000	0.000	0.000
15	0.086	0.080	0.074
30	0.152	0.139	0.126
45	0.200	0.179	0.161
60	0.235	0.208	0.184
91	0.280	0.242	0.211
121	0.307	0.262	0.227
151	0.325	0.275	0.237
181	0.337	0.284	0.244
241	0.351	0.295	0.253
301	0.360	0.302	0.260
361	0.366	0.308	0.265
421	0.371	0.312	0.269
481	0.374	0.315	0.272
541	0.377	0.318	0.274
601	0.380	0.321	0.277
722	0.384	0.324	0.281
842	0.387	0.327	0.283
962	0.389	0.329	0.286
1082	0.391	0.331	0.288
1202	0.393	0.333	0.289

TABLE IV-3

PREDICTED PERFORMANCE FOR
MODE 3 OPERATION IN LUNAR ENVIRONMENT

MODE 3
LOCATION 2
K= 0.0001500 W/CM-DEG K
RHO*C = 1.3390 W-SEC/CC-DEG K
TEMP LEVEL = 225.0 DEG K
DURATION = 361.0 MIN.

TIME(MIN)	TEMP(DEG K)	SLOPE(DEG K/MIN)
0.000	0.000000	0.004531
30.000	0.255900	0.012528
60.000	0.751700	0.018571
90.000	1.370200	0.021483
120.000	2.040700	0.021346
151.000	2.670300	0.020008
181.000	3.261800	0.019023
211.000	3.811700	0.017673
241.000	4.322200	0.016426
271.000	4.797300	0.015316
301.000	5.241200	0.014338
331.000	5.657600	0.013478
361.000	6.049900	0.012674

MODE 3
LOCATION 2
K= 0.0010000 W/CM-DEG K
RHO*C = 1.3390 W-SEC/CC-DEG K
TEMP LEVEL = 225.0 DEG K
DURATION = 361.0 MIN.

TIME(MIN)	TEMP(DEG K)	SLOPE(DEG K/MIN)
0.000	0.000000	0.001848
30.000	0.089100	0.004091
60.000	0.245500	0.005508
90.000	0.419600	0.005617
121.000	0.587800	0.005077
151.000	0.730000	0.004431
181.000	0.853700	0.003880
211.000	0.962800	0.003454
241.000	1.061000	0.003134
271.000	1.150900	0.002888
301.000	1.234300	0.002691
331.000	1.312400	0.002523
361.000	1.385700	0.002363

TABLE IV-3 - Cont'd.

MODE 3
LOCATION 2
K= 0.0006000 W/CM-DEG K
RHO*C = 1.3390 W-SEC/CC-DEG K
TEMP LEVEL = 225.0 DEG K
DURATION = 361.0 MIN.

TIME(MIN)	TEMP(DEG K)	SLOPE(DEG K/MIN)
0.000	0.000000	0.002165
30.000	0.108900	0.005094
60.000	0.305700	0.007051
90.000	0.532000	0.007420
121.000	0.758100	0.006925
151.000	0.955200	0.006208
181.000	1.130600	0.005541
211.000	1.287700	0.004998
241.000	1.430500	0.004571
271.000	1.562000	0.004233
301.000	1.684500	0.003960
331.000	1.799600	0.003729
361.000	1.908300	0.003516

MODE 3
LOCATION 2
K= 0.0017000 W/CM-DEG K
RHO*C = 1.3390 W-SEC/CC-DEG K
TEMP LEVEL = 225.0 DEG K
DURATION = 361.0 MIN.

TIME(MIN)	TEMP(DEG K)	SLOPE(DEG K/MIN)
0.000	0.000000	0.001656
30.000	0.077600	0.003516
60.000	0.211000	0.004633
90.000	0.355600	0.004600
121.000	0.491200	0.004034
151.000	0.602400	0.003416
181.000	0.696200	0.002908
211.000	0.776900	0.002526
241.000	0.847800	0.002241
271.000	0.911400	0.002023
301.000	0.969200	0.001846
331.000	1.022200	0.001699
361.000	1.071200	0.001566

TABLE IV-3 - Cont'd.

MODE 3
LOCATION 2
K= 0.0054000 W/CM-DEG K
RHO*C = 1.3390 W-SEC/CC-DEG K
TEMP LEVEL = 225.0 DEG K
DURATION = 361.0 MIN.

TIME(MIN)	TEMP(DEG K)	SLOPE(DEG K/MIN)
0.000	0.000000	0.001533
30.000	0.068400	0.003026
60.000	0.181600	0.003814
90.000	0.297300	0.003540
121.000	0.396900	0.002815
151.000	0.469800	0.002118
181.000	0.524000	0.001581
211.000	0.564700	0.001206
241.000	0.596400	0.000953
271.000	0.621900	0.000775
301.000	0.642900	0.000646
331.000	0.660700	0.000551
361.000	0.676000	0.000468

TABLE IV-4

TEMPERATURE DECAY OF RING SENSOR AFTER HEATING PERIOD OF MODE 3 EXPERIMENT

Experiment Location 2
ρc = 1.339 w-sec/cc °K
T = 225°K

Time after Start of Heating (min)	Time after Heater Turn-Off (min)	Thermal Conductivity of Lunar Material (w/cm °K)				
		5.4×10^{-3}	1.7×10^{-3}	1.0×10^{-3}	6.0×10^{-4}	1.5×10^{-4}
361	0	0.676*	1.071	1.386	1.908	(6.050)+
421	60	0.551	0.971	1.291	1.811	(5.931)
481	120	0.405	0.819	1.125	1.607	(5.427)
541	180	0.298	0.692	0.978	1.417	(4.874)
601	24	0.229	0.598	0.866	1.266	(4.383)
721	360	0.161	0.483	0.721	1.065	(3.669)
841	480	0.120	0.406	0.617	0.921	(3.145)
961	600	0.092	0.350	0.539	0.811	-
1081	1720	0.071	0.308	0.477	0.723	-
1201	840	0.056	0.275	0.429	0.652	-
1321	960	0.043	0.248	0.389	-	-
1441	1080	0.034	0.225	0.357	-	-

* + All values shown are temperatures in deg. K above an initial equilibrium value of 225°K. Temperatures in parentheses are outside of the ring-bridge sensitivity range.

TABLE IV-5

TEMPERATURE DECAY OF GRADIENT SENSOR AFTER HEATING PERIOD OF MODE 3 EXPERIMENT

Experiment Location 2
ρc= 1.339 w-sec/cc °K
T = 225°K

Time after Start of Heating (min)	Time after Heater Turn-Off (min)	Thermal Conductivity of Lunar Material (w/cm °K) 5.4×10^{-3}	1.7×10^{-3}	1.0×10^{-3}	6.0×10^{-4}	1.5×10^{-4}
361	0	(43.633)+	(46.702)	(49.160)	(55.324)	(65.271)
421	60	14.140*	16.798	19.029	(21.945)	(33.896)
481	120	4.848	6.878	8.686	11.1105	(21.279)
541	180	1.839	3.339	4.762	6.727	15.255
601	240	0.813	1.933	3.059	4.664	11.882
721	360	0.343	1.073	1.853	3.020	8.586
841	480	0.209	0.736	1.306	2.199	6.685
961	600	0.154	0.569	1.005	1.715	-
1081	720	0.120	0.471	0.817	1.398	-
1201	840	0.096	0.406	0.690	1.175	-
1321	960	0.078	0.358	0.600	-	-
1441	1080	0.063	0.321	0.534	-	-

* All values shown are temperatures in deg. K above an initial equilibrium value of 225°K.
\+ Temperatures in parentheses are outside of the range of the low-sensitivity gradient-bridge measurement (±20°K).

TABLE IV-6

PREDICTED PERFORMANCE FOR MODE 3 PARAMETRIC STUDIES

NOMINAL CASE

MODE 3
LOCATION 2
K= 0.0017000 W/CM-DEG K
RHO*C = 1.3390 W-SEC/CC-DEG K
TEMP LEVEL = 225.0 DEG K
DURATION = 361.0 MIN.

RING SENSOR RESPONSE

TIME(MIN)	TEMP(DEG K)	SLOPE(DEG K/MIN)
0.000	0.000000	0.001656
30.000	0.077600	0.003516
60.000	0.211000	0.004633
90.000	0.355600	0.004600
121.000	0.491200	0.004034
151.000	0.602400	0.003416
181.000	0.696200	0.002908
211.000	0.776900	0.002526
241.000	0.847800	0.002241
271.000	0.911400	0.002023
301.000	0.969200	0.001846
331.000	1.022200	0.001699
361.000	1.071200	0.001566

Change: 20% increase in thermal mass of lunar material (RHO*C)

TIME(MIN)	TEMP(DEG K)	SLOPE(DEG K/MIN)
0.000	0.000000	0.001606
30.000	0.074100	0.003333
60.000	0.200000	0.004346
90.000	0.334900	0.004266
121.000	0.459800	0.003694
151.000	0.560900	0.003100
181.000	0.645800	0.002631
211.000	0.718800	0.002289
241.000	0.783200	0.002043
271.000	0.841400	0.001858
301.000	0.894700	0.001711
331.000	0.944100	0.001591
361.000	0.990200	0.001481

TABLE IV-6 - Cont'd.

Change: 20°K decrease in temperature level

TIME(MIN)	TEMP(DEG K)	SLOPE(DEG K/MIN)
0.000	0.000000	0.002008
30.000	0.099700	0.004638
60.000	0.278300	0.006264
90.000	0.475600	0.006262
121.000	0.659700	0.005400
151.000	0.806100	0.004404
181.000	0.924000	0.003568
211.000	1.020200	0.002944
241.000	1.100700	0.002496
271.000	1.170000	0.002178
301.000	1.231400	0.001941
331.000	1.286500	0.001758
361.000	1.336900	0.001601

Change: 20°K increase in temperature level

TIME(MIN)	TEMP(DEG K)	SLOPE(DEG K/MIN)
0.000	0.000000	0.001421
30.000	0.063900	0.002838
60.000	0.170300	0.003684
90.000	0.285000	0.003683
121.000	0.394700	0.003320
151.000	0.488000	0.002926
181.000	0.570300	0.002598
211.000	0.643900	0.002338
241.000	0.710600	0.002128
271.000	0.771600	0.001951
301.000	0.827700	0.001803
331.000	0.879800	0.001674
361.000	0.928200	0.001551

Change: 20% increase in thermal conductance of drill casing

TIME(MIN)	TEMP(DEG K)	SLOPE(DEG K/MIN)
0.000	0.000000	0.001701
30.000	0.079700	0.003611
60.000	0.216700	0.004763
90.000	0.365500	0.004736
121.000	0.505200	0.004155
151.000	0.619700	0.003519
181.000	0.716400	0.002991
211.000	0.799200	0.002590
241.000	0.871800	0.002293
271.000	0.936800	0.002063
301.000	0.995600	0.001878
331.000	1.049500	0.001726
361.000	1.099200	0.001586

TABLE IV-6 - Cont'd.

Change: Experiment Location 1

TIME(MIN)	TEMP(DEG K)	SLOPE(DEG K/MIN)
0.000	0.000000	0.001478
30.000	0.071900	0.003314
60.000	0.198900	0.004473
90.000	0.340300	0.004544
121.000	0.475800	0.004048
151.000	0.587900	0.003448
181.000	0.682700	0.002933
211.000	0.763900	0.002524
241.000	0.834200	0.002216
271.000	0.896900	0.001990
301.000	0.953600	0.001808
331.000	1.005400	0.001628
361.000	1.051300	0.001431

Change: Experiment Location 3

TIME(MIN)	TEMP(DEG K)	SLOPE(DEG K/MIN)
0.000	0.000000	0.001236
30.000	0.060500	0.002796
60.000	0.167800	0.003813
90.000	0.289300	0.003949
121.000	0.408500	0.003617
151.000	0.510400	0.003176
181.000	0.599100	0.002774
211.000	0.676900	0.002449
241.000	0.746100	0.002193
271.000	0.808500	0.001990
301.000	0.865500	0.001823
331.000	0.917900	0.001681
361.000	0.966400	0.001551

Change: Experiment Location 4

TIME(MIN)	TEMP(DEG K)	SLOPE(DEG K/MIN)
0.000	0.000000	0.001360
30.000	0.064100	0.002913
60.000	0.174800	0.003874
90.000	0.296600	0.003924
121.000	0.413900	0.003543
151.000	0.513200	0.003099
181.000	0.599900	0.002720
211.000	0.676400	0.002421
241.000	0.745200	0.002188
271.000	0.807700	0.001998
301.000	0.865100	0.001841
331.000	0.918200	0.001705
361.000	0.967400	0.001575

TABLE IV-7

INFLUENCE OF INTERFACE BETWEEN PROBE ALIGNMENT SPRINGS AND DRILL CASE (SEE Text, Section V.F.2.a.)

MODE 2 EXPERIMENT WITH WELL-COUPLED INTERFACE BETWEEN SPRINGS AND DRILL CASING

LOCATION 4
K= 0.0004200 W/CM-DEG K
RHO*C = 1.3390 W-SEC/CC-DEG K
TEMP LEVEL = 225.0 DEG K

	GRADIENT SENSOR	
TIME(MIN)	TEMP(DEG K)	SLOPE(DEG K/MIN)
0.000	0.000000	0.004166
15.000	0.052000	0.002766
30.000	0.083000	0.001633
45.000	0.101000	0.001033
60.000	0.114000	0.000741
91.000	0.129000	0.000390
121.000	0.138000	0.000266
151.000	0.145000	0.000216
181.000	0.151000	0.000177
241.000	0.159000	0.000116
301.000	0.165000	0.000083
361.000	0.169000	0.000066
421.000	0.173000	0.000058
481.000	0.176000	0.000050
541.000	0.179000	0.000041
601.000	0.181000	0.000033
722.000	0.185000	0.000029
842.000	0.188000	0.000020
962.000	0.190000	0.000016
1082.000	0.192000	0.000012
1202.000	0.193000	0.000004

TABLE IV-7 - Cont'd.

MODE 3 EXPERIMENT WITH WELL-COUPLED INTERFACE

BETWEEN SPRINGS AND CASING

LOCATION 2
K= 0.0017000 W/CM-DEG K
RHO*C = 1.3390 W-SEC/CC-DEG K
TEMP LEVEL = 225.0 DEG K

RING SENSOR

TIME(MIN)	TEMP(DEG K)	SLOPE(DEG K/MIN)
0.000	0.000000	0.000908
30.000	0.042800	0.001944
60.000	0.116700	0.002619
90.000	0.200000	0.002750
121.000	0.284400	0.002624
151.000	0.360300	0.002431
181.000	0.430300	0.002253
211.000	0.495500	0.002094
241.000	0.556000	0.001943
271.000	0.612100	0.001809
301.000	0.664600	0.001693
331.000	0.713700	0.001586
361.000	0.759800	0.001486

TABLE IV-8

INFLUENCE ON RADIATION COUPLING BETWEEN DRILL CASING AND THE MOON

(SEE Text, Section IV.F.2.b)

MODE 3 EXPERIMENT WITH RADIATION COUPLING BETWEEN CASING AND MOON

MODE 3
LOCATION 2
K= 0.0054000 W/CM-DEG K
RHO*C = 1.3390 W-SEC/CC-DEG K
TEMP LEVEL = 225.0 DEG K

RING SENSOR

TIME(MIN)	TEMP(DEG K)	SLOPE(DEG K/MIN)
0.000	0.000000	0.009794
30.000	0.422800	0.018391
60.000	1.103500	0.022531
90.000	1.774700	0.020084
121.000	2.324000	0.014990
151.000	2.694500	0.010265
181.000	2.939900	0.006731
211.000	3.098400	0.004341
241.000	3.200400	0.002813
271.000	3.267200	0.001866
301.000	3.312400	0.001286
331.000	3.344400	0.000929
361.000	3.368200	0.000656

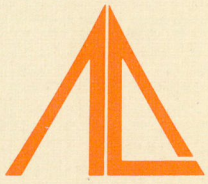

Arthur D. Little, Inc.

CAMBRIDGE,
MASSACHUSETTS

CHICAGO
SAN FRANCISCO
SANTA MONICA
WASHINGTON
ATHENS
BRUSSELS
LONDON
MEXICO CITY
PARIS
RIO DE JANEIRO
TORONTO
ZURICH